UNIVERSITÀ DEGLI STUDI DI TORINO

SCUOLA DI DOTTORATO IN SCIENZE DELLA NATURA E TECNOLOGIE INNOVATIVE

DOTTORATO IN SCIENZE AGRARIE, FORESTALI ED AGROALIMENTARI

CYCLE: XXX

INNOVATIVE THERMAL PROCESSES AND PLANTS FOR FOOD INDUSTRY

Eng. Alessandro Biglia

Supervisors:
Prof. Paolo Gay
Prof. Enrico Fabrizio

Coordinator of the Ph.D:
Prof. Aldo Ferrero

YEARS
2015; 2016; 2017

Acknowledgements

I would like to express my sincere gratitude to my Supervisors Prof. Paolo Gay at the University of Torino (DiSAFA) and Prof. Enrico Fabrizio at the Politecnico of Torino (DENERG) for the continuous support of my Ph.D period.

I would also like to thank the entire research team at the University of Torino (DiSAFA): Paolo Barge, Lorenzo Comba, Leandro Eloi Alcatrão, Davide Ricauda Aimonino, Cristina Tortia.

My sincere thanks also go to Prof. Judith Evans at the London South Bank University, for offering me the opportunity to join her research group during my research period in England.

Last but not the least, I would like to thank my family for supporting me throughout my life experience.

Alessandro Biglia

Abstract

The food industry is an integral component of the worldwide economy, transforming raw products into tradable food. The food industry is also one of the largest manufacturing sectors, resulting in significant final energy consumption that accounted for approximately 6% of the industry sector in 2014. The world demand for food is expected to increase as world population should increase from 7.1 billion in 2013 to 9.6 billion by 2050. Moreover, life standards are also expected to improve in developing countries, thus leading to a possible larger per capita consumption of food.

Food industries are complex systems that can simultaneously require thermal, cooling and electric energy. Indeed, raw materials are usually cleaned, processed at different temperatures as a function of the food processing and combined to obtain finished products.

The food industry sector is receiving increasing attention because of the opportunity to exploit innovative processing plants, the potential of increase in the energy efficiency and in the quality of final food products that lies in the plants, if correctly designed and managed. Research suggests that the adoption of smart energy monitoring systems is also important to understand how the plants operate and how they can be optimised.

Given this picture, this thesis provides original, both theoretical and applied, contributions to the design of two different types of food processing plants:

1. A plant for steam batch thermal processes in unsteady state conditions. Many food processes require high amounts of steam. Design and operation of steam plants are particularly complex when steam is required for short and intermittent periods and with a varying time schedules. The discontinuous needs of steam can be fulfilled by using a thermal energy storage. The dynamic model of plant is here proposed.
2. A plant for food freezing at very low temperature. Freezing is a valuable method to increase food shelf life and to ensure high quality standards during long-term storage. Additional benefits to frozen food quality can be achieved by freezing at very low temperatures (« -50

°C): small ice crystals formation during fast freezing reduces food cell wall rupture, preventing water and texture loss during thawing. An innovative food freezing plant, based on a reversed Brayton cycle, is here presented. A numerical model of the reversed Brayton cycle was also developed.

The thesis also provides a contribution in the data analysis of energy monitored data of domestic cold appliances and of a plant in a chocolate industry.

The potential applications of the outcomes of this work are of considerable interest since the importance of food quality and food demand are expected to grow in the next future. Moreover, results of the design tools here presented indicate measures that can be adopted to properly operate the analysed food processing plants.

Summary

1. Introduction

The research for green energy resources, the effort to guarantee food and medical treatments to the population, the international geopolitical strategies and economy have been the main topics discussed over the last twenty years and they will become increasingly important in the future.
Energy is essential to human activities, providing comfort, increasing productivity and allowing us to live the way we want too. "*...the world's Information-Communications-Technologies (ICT) ecosystem uses about 1500 TWh of electricity annually, equal to all electric generation of Japan and Germany combined – as much electricity as was used for global illumination in 1985. The ICT ecosystem now approaches 10% of world electricity generation... although charging up a single tablet or smartphone requires a negligible amount of electricity, using either to watch an hour of video weekly consumes annually more electricity than domestic cold appliances use on average in a year. And as the world continues to electrify, migrating towards one refrigerator per household, it also evolves towards several smartphones and equivalent per person...*" reported Mark P. Mills in the report: The Cloud Begins With Coal (2013). Moreover, much of the increase in energy demand will result from rapid economic growth in China and India. Indeed, those countries are expected to grow at a rate higher than any other country.
Until the second part of the 20th century, energy efficiency in the food and beverage industry was not considered as matter of concern. The policy was mainly to increase food production, without considering the food wasted and the energy lost along the food life cycle. In the 21st century, growth in global population and changing eating habits in emerging countries (e.g. there recently was a very rapid increase in the import of dairy products in China from 2014 to 2017) are projected to sharply increase food demand to feed 9 billion people by 2050. The greatest challenge faced by food and beverage industry is to meet development and sustainability goals, while increasing production. Indeed, the increasing demand for foods requires and will require identification of measures to prevent depletion of natural resources as well as reduce energy consumption and food waste, thus minimising economic costs. Besides, recent progress in the legislative

frameworks have encouraged food and beverage industry to improve energy and management policies, there remains a significant challenge ahead for the food and beverage industry to be more sustainable. Sustainability has been defined in many ways over the last years but, probably, the most used definition of sustainability is "*the development that meets the needs of the present without compromising the ability of future generations to meet their own needs*". This definition underlines the importance of environmental conservation. However, the concept of sustainability has evolved nowadays and it is used by many industries to increase competitiveness over other companies. Many organisations recognise nowadays the benefit of sustainability principles into their business strategy and future plans. Sustainability involves many aspects such as: (1) setting clear targets; (2) designing measures to produce less food waste and reduce energy consumption and (3) developing innovative food processing for enlarge economic benefits.

Responding to these goals, research activities that are of particular relevance to the food and beverage industry include: reduction of waste energy and valorisation of sub-products (from production to the end user); development of innovative food processing technologies and packaging methods; providing new tools to design food plants; reduction and optimisation of water use and development of diagnostic systems for the abatement of chemical and biological contaminants along the food chain up to the consumer.

1.1. Contents of the thesis

The provision of a secure, continuous, efficient energy supply is becoming an issue for all sectors of society and the food processing industry as a major energy user must address these issues. Energy in food industry is an important input in preparing, processing, packaging, storing and distributing of food.

Pasteurisation and sterilisation are two of the main techniques in food and beverage industries for food preservation (e.g. canned foods, vacuum packed hams, etc.). These thermal treatments reduce or destroy microbial and enzyme activities and they can be performed by batch or continuous in different kinds of plant, e.g. autoclaves or retorts, by using steam. The

focus of this study has been on discontinuous thermal processes and, in particular on their thermal supply. A new plant design tool able to simulate the unsteady operation of a steam batch process was developed and presented in the thesis.

Freezing is a well-established preservation process to extend the food storage life. There is a general view that fast freezing, and the formation of small ice crystals, offers some quality advantages in the final quality of frozen foods. Some innovative freezing processes are essentially improvements of existing methods while a new concept (adopted technology, freezing temperatures, etc.) of freezing is here presented.

Many organisations recognise nowadays the benefit of sustainability principles into their business strategy and future plans as the monitoring systems offer a better understanding of how the industry and/or the equipment work and how they can be improved. Different types of data were collected and here reported: solar heat and domestic hot water production in a chocolate industry and electricity consumption and temperatures in domestic cold appliances. This information can be used to identify problems in the operation of the technical equipment and to validate simulation models.

More in detail, the following topics are treated in the thesis:

- Modelling of steam batch processes for food thermal treatments, able to describe unsteady operative conditions.

  The proposed model demonstrates its effectiveness as a design tool to: (1) avoid plant oversizing or (2) to verify the operating conditions and the energy requirements of a given plant. Indeed, the model allows the proper trade-off between the steam boiler capacity, the steam accumulator volume, the processing tank volume and others design parameter, predicting the performance on the entire process, to be obtained.
- The design of an innovative food freezing system operating at very low temperatures, based on a modified reversed Brayton cycle. Moreover, useful charts for designing a low temperature freezing process in terms of freezing time, food production rate, type of food product, etc. were developed.

The designed freezing system is able to produce cooling energy at a temperature below −110 °C. A numerical model of the system was developed to (1) evaluate the plant performance at steady-state conditions; (2) identify which components affect the performance of the plant the most and (3) optimise the overall thermodynamic cycle. The proposed system turns out to be an alternative to liquid nitrogen in very low temperatures freezing processes. At the present, the first prototype is in its first realisation phase.

- Results from a survey of domestic cold appliances in households in England were statistically analysed and here reported.

  Data on ambient temperature, refrigerator and/or freezer temperature and electricity consumption of the cold appliance was monitored. Such data analysis may be used to target high consuming cold appliances and find whether cold appliances operate within the recommended temperature.

- A thermal model of a multi-energy system for a chocolate industry was developed within the TRNSYS® software tool and was used to study and optimise the energy performance of the system during the summer season.

  The thermal model was calibrated against measured data obtained by a monitoring system installed in the existing plant.

1.2. Outline of the thesis

The thesis has been organised as structured collection of the papers published in International Journals during the Ph.D period (Biglia et al., 2015; Biglia et al., 2016; Biglia et al., 2017a; Biglia et al., 2017b; Biglia et al., 2017c).

The subject of energy applied to food applications together with the scope of the work were reported in *Chapter 1*.

Chapter 2 first deals with the subject of energy-systems in food and beverage industry. Information about energy consumption in food industry and examples of data about how much energy is used to process some food products were presented in the first part of the chapter. The discussion on two energy management approaches that may help to understand where, when and how much energy is consumed is also presented in chapter 2.

Last section of chapter 2 is focused on the main energy converters adopted in food industry.

Chapter 3 presents three main topics related to the heating, cooling and electricity demand in food processing and storing: (1) energy modelling for steam supply in debacterisation processes and (2) innovative food freezing plant at very low temperatures and (3) energy monitoring and systems simulation.

Chapters 4, 5 and 6 are dedicated to the study of topics presented in chapter 3. First of all, literature data were deeply analysed for each topic to understand how research activities here presented may improve previously works published to date. Then, technologies and phases of certain food processes were studied from theoretical point of view and, finally, mathematical and/or numerical models were implemented.

Finally, conclusions and future works are reported in *Chapter 7*.

1.3. References

Mills MP. The Cloud Begins With Coal. An Overview of The Electricity Used By The Global Digital Ecosystem. August 2013. www.tech-pundit.com/wp-content/uploads/2013/07/Cloud_Begins_With_Coal.pdf.

Biglia A, Fabrizio E, Ferrara M, Gay P, Ricauda Aimonino D. Performance assessment of a multi-energy system for a food industry. *Energy Procedia* 82 (2015) pp. 540-545.

Biglia A, Comba L, Fabrizio E, Gay P, Ricauda Aimonino D. Case studies in food freezing at very low temperature. *Energy Procedia* 101 (2016) pp. 305-312.

Biglia A, Comba L, Fabrizio E, Gay P, Ricauda Aimonino D. Steam batch thermal processes in unsteady state conditions: Modelling and application to a case study in the food industry. *Appl Therm Eng* 118 (2017a) pp. 638-651.

Biglia A, Comba L, Fabrizio E, Gay P, Mannini A, Mussinatto A, Ricauda Aimonino D. Reversed Brayton cycle for food freezing at very low temperatures: Energy performance and optimisation. *Int J Refrig* 81 (2017b) pp. 82-95.

Biglia A, Gemmell AJ, Foster HJ, Evans JA. Temperature and energy performance of domestic cold appliances in households in England. *Int J Refrig* (2017c) in Press.

2. Energy consumption in food industry

The past decades have been marked by rapid industrialisation and economic growth worldwide, which resulted in an increasing final energy consumption (FEC). The trend of the FEC is positive and by 2014 it amounted to around 10,000 Mtoe as shown in Fig. 1 (IEA, 2017). Moreover, this value is expected to rise up in the next years due to further industrialisation of developing countries and population growth. Industry sector is responsible for 29% of the FEC, and together with transport and residential sectors around 90% of the FEC is covered (Fig. 1). The food and beverage (F&B) industry is an integral component of the worldwide economy, transforming raw products into tradable food. The F&B industry is one of the largest manufacturing sectors, resulting in significant FEC that accounted for approximately 6% of the industry sector in 2014 (Fig. 1). In USA, the food industry takes a 10% share of the GDP (Egilmez et al., 2014) and around 9.3% of the total employment (Glaser and Morrison, 2016).

The world demand for food is expected to increase as world population should increase from 7.1 billion in 2013 to 9.6 billion by 2050 (United Nations, 2017). Life standards are also expected to improve in developing countries, thus leading to a possible larger per capita consumption of food (Alexandratos and Bruinsma, 2012).

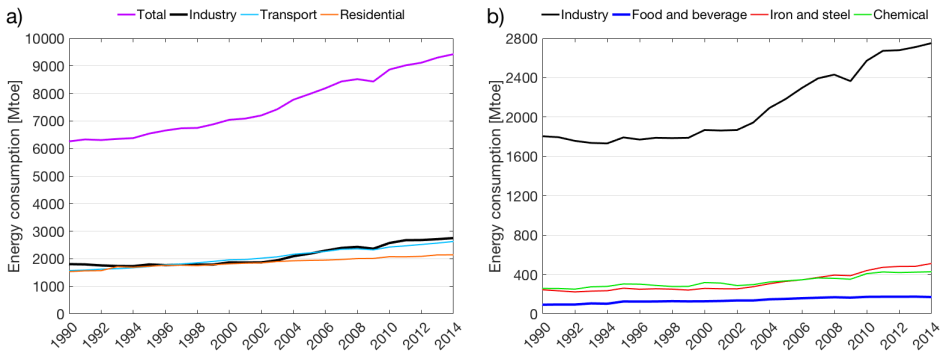

Fig. 1. Part (a) shows the worldwide final energy consumption trend and its breakdown by industry, transport and residential. Part (b) focuses on industry sector breakdown by food and beverage, iron and steel and chemical. (IEA, 2017).

Focusing on the Europe community, the F&B industry is considered one of the most significant sector as it plays a key role in the Europe economy and in foreign trade due to its diverse tradable products. The final food industry energy consumption was 28.7 Mtoe in 2014, which accounted for 10.6% of the total industry sector (Fig. 2). The European F&B industry consists of more 300,000 companies engaged in multiple sectors, providing employment to more than three million people and accounting for an annual sales volume of about 900 billion euros (Eurostat, 2015). The European F&B industry is also the largest manufacturing sector in terms of value added (1.9% of the Europe community) and gross revenue.

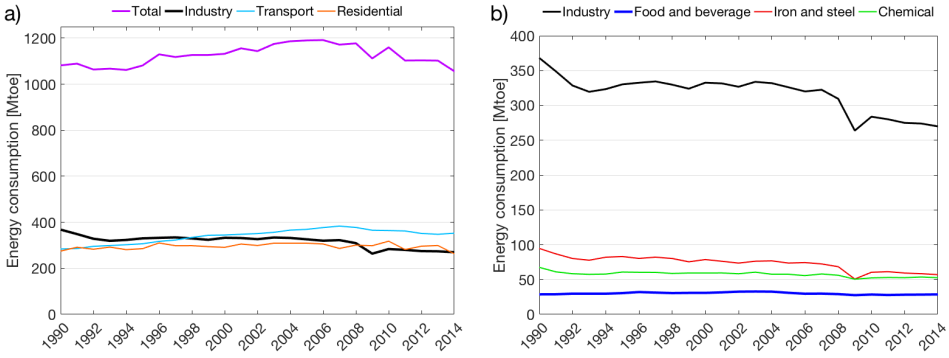

Fig. 2. Section (a) shows the Europe final energy consumption trend and its breakdown by industry, transport and residential. Section (b) focuses on industry sector breakdown by food and beverage, iron and steel and chemical. (Eurostat, 2015).

Among different types of sub-sectors in the European food industry, the meat sector is the largest one, representing 20% of total sales proceeds. This sector has the greatest number of large companies followed by the bakery industry, which is primarily based on small scale and craft production. The bakery sub-sector ranks first in terms of value added, employment and number of companies. The top 5 sub-sectors, which are meat, bakery products, dairy products, drinks and fruit and vegetables, represent 76% of the total sales proceeds. The drinks industry is one of the largest exporting sector in Europe with Italy, France, Spain, United Kingdom and Germany being the largest drink producers. The drinks industry reached 31% of the market share in 2011, followed by the meat and dairy products sectors, processed tea and coffee and oils. Unrefined

tea and coffee, together with grain, represent the largest imported products in Europe.

In Italy, the food and beverage industry, which is the third largest sector behind textile and mechanical sectors, contributes significantly to the country's economy, employing around 385,000 people and generating total sales proceeds of about 135 billion euros in 2015, with exports amounting to 36.9 billion euros. Italian food production, processing and retail are very spread among the country. The average size of food producers is typically medium-small sized in comparison with multinational companies. In particular, Italian food businesses (e.g. pasta, pizza, wine, cheese, etc.) benefit from the strong "Made in Italy" trademark reputation to enlarge sales volume. Dairy products, wine and processed meat are amongst the leading sector that contributes greatly to the Italy's food industry sales proceeds. The trend of the Italian food industry consumption in the last years is reported in Table 1 together with others European countries (Odyssee-Mure, 2016).

Table 1. Final consumption [Mtoe] of food industry in European Union (Odyssee-Mure, 2016).

	2007	**2008**	**2009**	**2010**	**2011**	**2012**	**2013**	**2014**
Europe	29.8	29.1	27.6	28.5	27.8	28.2	28.4	28.7
Austria	0.52	0.51	0.53	0.59	0.59	0.61	0.57	0.55
Belgium	1.04	1.07	1.08	1.24	1.21	1.27	1.36	1.41
Bulgaria	0.28	0.29	0.26	0.25	0.23	0.23	0.24	0.23
Croatia	0.25	0.30	0.24	0.25	0.25	0.23	0.22	0.22
Cyprus	0.04	0.04	0.04	0.04	0.03	0.03	0.03	0.04
Czech Rep.	0.67	0.60	0.55	0.55	0.56	0.55	0.54	0.55
Denmark	0.68	0.72	0.64	0.69	0.65	0.59	0.58	0.59
Estonia	0.08	0.07	0.06	0.07	0.06	0.06	0.06	0.06
Finland	0.41	0.37	0.45	0.44	0.41	0.38	0.40	0.43
France	5.35	5.26	5.38	5.46	5.48	5.44	5.34	5.41
Germany	4.88	4.80	4.77	4.99	4.92	4.98	4.94	5.00
Greece	0.64	0.66	0.62	0.58	0.60	0.54	0.47	0.52
Hungary	0.41	0.45	0.40	0.41	0.41	0.35	0.50	0.57
Ireland	0.54	0.52	0.50	0.49	0.45	0.41	0.43	0.44
Italy	3.19	3.29	3.00	2.78	2.73	2.68	2.66	2.74
Latvia	0.12	0.10	0.09	0.09	0.09	0.09	0.09	0.09

Lithuania	0.19	0.17	0.16	0.17	0.18	0.18	0.19	0.18
Luxembourg	0.02	0.02	0.02	0.02	0.02	0.02	0.02	0.03
Malta	0.01	0.01	0.01	0.01	0.01	0.01	0.01	n.a.
Netherlands	2.15	2.06	1.84	1.94	1.98	1.90	1.90	1.98
Norway	0.37	0.37	0.33	0.38	0.36	0.35	0.36	0.36
Poland	1.96	1.89	1.78	1.80	1.79	1.88	1.86	1.87
Portugal	0.56	0.54	0.52	0.55	0.46	0.44	0.45	0.44
Romania	0.73	0.69	0.53	0.56	0.57	0.57	0.54	0.56
Slovakia	0.18	0.16	0.14	0.12	0.12	0.14	0.14	0.14
Slovenia	0.08	0.08	0.07	0.07	0.07	0.06	0.06	0.07
Spain	2.28	2.20	2.14	2.21	1.82	2.07	2.18	2.28
Sweden	0.47	0.45	0.45	0.45	0.45	0.45	0.45	0.45

Since the food industry produces a wide selection of products, six main sub-sectors may be identified (Wang, 2014): 1) fruits and vegetables, 2) meat and fish, 3) grain and oilseed milling, 4) bakery products, 5) dairy products and 6) beverages. The energy consumption in F&B industries depends on a number of factors: the food processing and packaging, the size of the product, the physical and chemical properties of the product, the technology (Nunes et al., 2014; Pereira and Vicente, 2010). Food processes used in dairy establishments and meat sector are particularly energy demanding as they require for both heating and cooling. For example, dairy sector consumed $1444 \cdot 10^5$ TWh of primary energy in France, $944 \cdot 10^5$ TWh in Germany, $444 \cdot 10^5$ TWh in Netherlands and $388 \cdot 10^5$ TWh in UK (Ramirez et al., 2006a). Moreover, Table 2 provides examples of energy consumption for processing different food products (Wang, 2014; Wojdalski et al., 2013; Xu et al., 2009; Ramírez et al., 2006b).

Table 2. Energy consumption for processing different foods.

Product	Electricity consumption	Heat consumption	Unit
Beer	5.4	42.5	kWh/hl product
Cheese	335.0	586.9	kWh/t product
Dried vegetables and fruits	416.7	1250.0	kWh/t product
Fresh fish	35.8	1.7	kWh/t product
Frozen fish	168.9	1.7	kWh/t product
Frozen vegetables and fruits	205.0	500.0	kWh/t product
Milk powder	291.9	2606.9	kWh/t product
Mineral water and soft drinks	369.4	552.8	kWh/hl product
Pasta	180.0	0.6	kWh/t product
Pig	1260.0	8610.0	kWh/t product
Poultry	280.0	160.0	kWh/t dress carcass
Refined sugar	154.2	1477.8	kWh/t product
Roasted coffee	143.9	554.7	kWh/t product
Wheat starch	822.2	2444.4	kWh/t product

The food industry is dependent on energy for food processing, food preservation, food packaging and food storage. Energy is also required for non-process uses: space heating and cooling, ventilation, lighting, equipment drive, etc. Fossil fuels, with natural gas being the largest used, and/or electricity are usually adopted in heating processes that include for example baking, cooking, pasteurisation, roasting, blanching, drying, etc. Heating processes are divided into two categories: direct and indirect. Indeed, heat may be applied directly to the product or it may be applied to a medium (e.g. air, water, oil) that then transfers heat to the product. Fig. 3 shows typical temperature ranges with which thermal energy demand is supplied in the F&B industry (Fluch et al., 2017). Solar thermal energy applications are considered a viable solution for integrating renewable energies in food industry plants when low temperatures are required (Baniassadi et al., 2018).

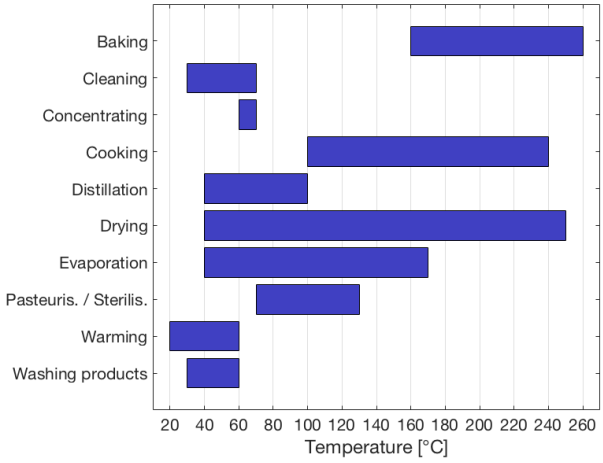

Fig. 3. Temperature ranges for typical processes in the food and beverage industry.

Electricity is the most common source of energy for cooling and mechanical (e.g. mixing, separating, etc.) systems in the F&B industry. The cooling systems are intensive electricity consumption systems. Indeed, the electricity demand for refrigerated food cold storage can overcome 70/80% of the total electricity consumption (Evans et al., 2014). Food products usually undergone a first chilling process to remove sensible heat until reaching the recommended storage temperature (0÷5 °C). Swain et al. (2008) reported as in UK, 532 GWh per year, 114 GWh per year, 59 GWh per year, 36 GWh per year, 6.5 GWh per year and 5.9 GWh per year of electricity were used for milk, meat, potatoes, vegetables, fish and fruits respectively during the first chilling process.

2.1. Modelling approaches to energy management

The F&B industry includes several food processes with which raw materials are cleaned, processed and combined to obtain finished products. Although the F&B industry cannot be considered energy intensive as heavy industries it is an important energy consumer due to its extended scale (Muller et al., 2007). Because of the introduction of International and European rules about greenhouse gases emission, it has become extremely important to enhance the food processing energy efficiency (Lin and Xie, 2016). The increasing in energy efficient in F&B industry may provide benefits for: (1) reduction in energy consumption and energy costs, (2)

reduction in greenhouse gases emission and (3) industrial competitiveness and European certification such as ISO 50001. Wang (2014) reported that roughly 60% of the energy input into the F&B industry from fuels and electricity is lost for energy plant inefficiencies.

Research is increasing into developing strategies able to reducing energy consumption in F&B industry. For example, Govindan (2018) has provided a review on sustainable supply chain management and sustainable supply chains in the food industry; Xu and Szmerekovsky (2017) have designed a system dynamic model to simulate the situation for the US food industry; Nunes et al. (2016) have characterised the production process and the energy consumption of twenty sausages processing industry in Portugal; Lin and Xie (2015) have proposed some policy suggestions on energy conservation according to the results of substitution relationship among input factors (e.g. capital, energy and labour costs) and the rebound effect in the China's food industry; Seck et al. (2013, 2015) have shown that the use of a heat recovery system based on the heat pump technology could allow to reduce CO_2 emissions in the French F&B industry.

The key to reducing energy consumption in F&B industry is understanding where, when and how much is being consumed and having the ability to act. Indeed, energy management programs of food processes include planning (short and long term), monitoring, data analysis, operation, maintenance and optimisation. Methods employed in such energy management are based on two different approaches: top-down (TD) and bottom-up (BU). The TD and BU approaches are two different methods to analyse data on a big scale and to establish a relation between large-scale model and single data. The TD approach relies on the decomposition of an industry into its detailing subsystems/processes until the definition of a set of equations (Shindo and Yanagawa, 2017; Lee and Zhong, 2014). Moreover, information required by the TD model, as energy costs, raw materials' costs, productivity, etc., may be easily collected and/or monitored. Important results of the TD approach that may impact the food industry energy management are: (1) definition of a scheme of the food industry where energy and food products flows are identified and (2) collection of energy and economic data in order to define benchmark

values by using static analysis (e.g. regression, neural networks, etc.). Based on collected data, energy and economic indicators may be defined to monitor the food industry trend. An energy indicator may provide the amount of energy inputs for processing a given consumable products:

$$I_{\mathrm{en}} = \frac{\sum_{\mathrm{i}=1}^{\mathrm{n}} E_{\mathrm{in,i}}}{\sum_{\mathrm{j}=1}^{\mathrm{m}} M_{\mathrm{p,j}}} \quad (1)$$

where $E_{\mathrm{in,i}}$ and $M_{\mathrm{p,j}}$ account for the energy inputs (e.g. fuels, electricity, etc.) expressed in kWh and the amount of consumable products expressed in kg. An economic indicator may be defined to evaluate the total cost for supply the energy per selling price of the consumable products:

$$I_{\mathrm{ec}} = \frac{\sum_{\mathrm{i}=1}^{\mathrm{n}} E_{\mathrm{in,i}} \cdot c_{\mathrm{i}}}{\sum_{\mathrm{j}=1}^{\mathrm{m}} M_{\mathrm{p,j}} \cdot p_{\mathrm{j}}} \quad (2)$$

where c_{i} and p_{j} account for the energy inputs cost expressed in € per kWh and the price of consumable products expressed in € per kg.

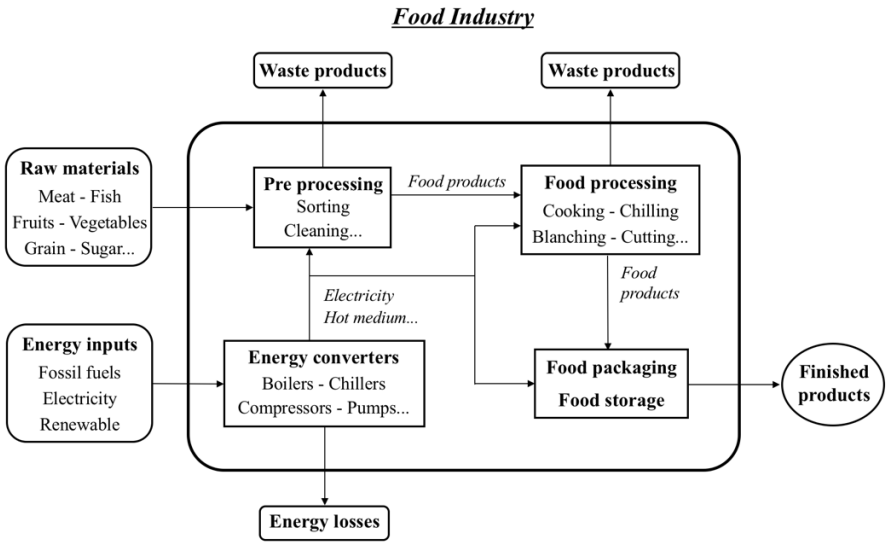

Fig. 4. Simplified scheme of a food industry.

On the contrary, the BU approach analyses the effects associated with an industry by coupling the various disaggregated subsystems/processes information (Silva et al., 2018; Zuberi and Patel, 2017). This approach aims at explicitly modelling the energy use of each food process to obtain the entire energy consumption of the facility. This might be very complex and advanced skills (e.g. thermodynamic, mechanic, etc.), human

resources, investment costs (e.g. meters) and computational time are required. Results of such methodology allow better understanding of the energy efficiency of each process. Moreover, coupling numerical simulations and monitored data might help to identify critical phases of the process.

Recent advances in computers and electronics devices can support an energy management program in order to: (1) monitor energy consumption; (2) collect big data (Wolfert et al., 2017; Lokers et al., 2016) and develop advanced tools for statistical analysis (Cristóvão et al., 2016; Lim and Antony, 2016); (3) define key performance indicators depending on several parameters such as energy consumption, energy costs, food production, etc. (Corsini et al., 2016); (4) simulate the food process and (5) define and optimise new strategies for energy efficiency enhancement (Eiholzer et al., 2017; Paudel et al., 2017; Walmsley et al., 2016).

2.2. Technology review

Important factors when analysing energy efficiency in a F&B industry plant are: (1) the type of food process (e.g. cooking, smashing, storage, etc.); (2) the adopted energy source (e.g. natural gas, biomass, electricity, etc.); (3) the size of the plant; (4) the energy costs from bills; (5) the energy demand depending on the food process scheduling (e.g. monitoring system). Energy use for food processing can be reduced by using energy efficient technology and/or by modifying the food process scheduling where possible. This section focuses on the analysis of the most common technologies in the F&B industry for heating and cooling processes: boilers and chillers respectively.

2.2.1. Boilers

Boilers are pressurised vessels in which the fluid (water or thermal oil) is heated: heat is still one of the most widespread means to reduce microbiological risk in food. Heat is also needed for other operations, as sterilization of packaged food, equipment and food plant cleaning and sanitation. The produced heat in the boiler furnace is transferred through hot flue gases to the fluid. This technology is widely used in F&B industry for providing hot water and/or superheated steam (Lee et al., 2017; Isleroglu and Kaymak-Ertekin, 2016; Xu et al., 2016; Bingol et., 2014).

Boilers may be fueled with fossil fuels or biomasses. Natural gas and fuel oil are the most common fuels as the mass flow rate of those fuels may be easily regulated in the furnace.

The boiler efficiency is the ratio between the heat exported by the fluid and the heat provided by the fuel. The efficiency of new boiler is in the range from 85% to 95% depending on the type of fuel and on the characteristics of the boiler. Losses from the boiler are due to hot flue gas, warm surfaces and blowdown with hot flue gas being the major one. The flue gas temperatures exiting the boiler are typically in the range from 80 °C to 250 °C (Barma et al., 2017).

Considering the boiler lifetime, the major costs are due to fuel costs and maintenance. Ensuring efficient operation is critical to minimise the fuel costs and to extend the boiler lifetime. Therefore, a scheduled energy management program is essential to identify energy losses and to guarantee efficient operation; it also helps to analyse how the plant may be improved taking into account technical and economic parameters.

Waste heat due to flue gas

The major quote of waste heat in a boiler is due to flue gas. The higher the temperature and/or the mass flow rate of flue gas the higher the waste heat will be. The flue gas temperature and the flue gas mass flow rate depend on the: (1) temperature of the heated fluid exiting the boiler; (2) heat exchange between flue gas and fluid to be heated and (3) combustion process.

The fluid temperature exiting the boiler is a design parameter and therefore the boiler is normally regulated to fulfil that temperature.

The heat exchange in the boiler furnace can reduce due to fouling. On the fire-side, surface has to be cleaned to remove fouling due to combustion products, this process is particularly relevant in case of fuel oil, coal and biomass. On the fluid-side, fouling can be reduced by preventive chemical fluid treatment. Otherwise, fouling might reduce the heat transfer coefficient resulting in additional fuel consumption (Euh et al., 2017).

The fuel mass flow rate is regulated with respect to the fluid temperature exiting the boiler. The regulation of the air mass flow rate depends on the type of fuel and on the fuel mass flow rate. When incomplete combustion occurs due to poor mixing between air and fuel lot of energy is not released

by the combustion and lost through the chimney. Low combustion efficiency also involves high level of pollutants' emissions. Moreover, the amount of air has to be controlled to limit mass flow rate of flue gas. Waste heat due to flue gas may be reduced by several measures as follow: (1) installation of a flue gas heat recovery system (Suntivarakorn and Treedet, 2016). The flue gas, before exiting the chimney, are channelled into a heat exchanger, usually called economizer, and the amount of heat, recovered by the fluid to be heated, depends on the flue gas temperature. Economizer has to be design to be capable of withstanding acid condensation that occurs when flue gas temperature drops below acid dew point; (2) installation of equipment for improving combustion efficiency. Boilers should be equipped with variable speed fan and with control systems to regulate the air mass flow to optimise the combustion process (Lee and Jou, 2011) and (3) maintenance scheduling, as cleaning of the furnace, of the heat transfer surface and of the chimney.

Waste heat due to convection

Convection occurs when there is a temperature difference between the boiler external surface and the ambient temperature where the boiler was installed. The amount of heat lost is directly proportional to the temperature difference. Since temperature in the boiler, chimney and distribution piping is very high to minimise the heat lost those surfaces have to be insulated. Otherwise convection losses could have a significant effect on the boiler energy balance.

Thermal insulation has to be designed in terms of thickness, thermal conductivity and resistance to high temperature. Convection losses are within 1-5% of the entire boiler energy balance.

Waste heat due blowdown

Solid particles form sediments in the boiler reduce the heat transfer coefficient between the flue gas and the fluid to be heated. Sediments also increased pressure drops. To reduce sedimentation, fluid is drained from the bottom of the boiler. Blowdown rate may be reduced by using an automatic control system and by installing a fluid treatment system.

2.2.2. Chillers

Food safety and hygiene in the dairy, meat, fisheries and other food industries have top priority nowadays. Refrigeration technologies are vital to enable the consumption of healthy and safe food, particularly in terms of nutritional, organoleptic and microbial quality. For chilled and frozen foods, quality and safety are reliant on the food being maintained at sufficiently low temperatures throughout them processing, storage and distribution to prevent growth of bacterial pathogens (van Holsteijn and Kemna, 2018; Aste et al., 2017).

Industrial chillers and/or freezers are classified as refrigeration systems that cool and/or dehumidify process fluid, typically water or air, in industrial food facilities. Standard chillers and/or freezers use vapour compression cycle to cool (Cardoso et al., 2017).

A vapour compression chiller consists of four primary components of the refrigeration cycle. They include a compressor, evaporator, condenser and an expansion valve. The chiller cycle typically utilises HFC refrigerants to achieve a refrigeration effect. Compressor is driven by an electric motor and acts as a pump for the refrigerant. Compressed refrigerant gas is sent from the compressor to a condenser unit that rejects the heat from the refrigerant to the warm region (e.g. cooling tower). The transfer of heat allows the refrigerant gas to condense into a liquid which is then sent to an expansion valve. The expansion valve restricts the flow of liquid refrigerant that causes a drop in pressure. The drop in pressure causes the warm refrigerant liquid to change phase from liquid to gas. The expansion valve is positioned so that the expanding refrigerant gas is contained within the evaporator, transferring the heat from the region or fluid (water or air) to be cooled into the refrigerant gas. The warm refrigerant gas is then sent back to the compressor to start the cycle over again and the newly chilled water in the separate loop can now be used for cooling. When very low temperatures (< -40 °C) are required in the cold region, two vapour compressor cycles can be arranged in series with a counter flow heat exchanger linking them. In the intermediate heat exchanger, the energy rejected during condensation of the refrigerant in the lower temperature cycle is used to evaporate the refrigerant in the higher-temperature cycle. The desired refrigeration effect occurs in the low temperature evaporator,

and heat rejection from the overall cycle occurs in the high-temperature condenser.

Energy efficiency measures

The energy consumption in a chiller is mainly by the compressor motor and is dependent on the mass of refrigerant to be compressed, the compressor lift (pressure difference between the evaporator and condenser) and design characteristics of the cold region system and/or of the chilled fluid (water or air) system. Therefore, savings in energy consumption of the chiller can be achieved by: (1) reducing the compressor load (mass of refrigerant that needs to be compressed), (2) reducing the compressor lift, and (3) optimising the operation based on compressor characteristics (Wei et al., 2014).

The evaporator pressure (named also suction pressure) can be maximised by operating the system to produce chilled fluid at the highest temperature acceptable for the cooling/freezing process. It would also be necessary to ensure proper insulation of the circulation piping system, thus preventing not required heat gain by the chilled fluid. In F&B industries that require the chilled fluid to be at several temperatures, instead of operating a chiller at a temperature to supply the lowest temperature required, two or more chillers should be operated at different temperature levels.

Reducing condenser pressure allows the compressor to be lowered. This can be achieved by reducing warm region temperature where the condenser heat is rejected (Kabeel et al., 2017). The most common condenser cooling fluid is water which is circulated through a cooling tower system to reject heat to the atmosphere. The mass flow rate of condenser cooling water also affects the condenser pressure.

Loss of refrigerant from the circuit would have a remarkable effect on the efficiency of the system. Selection of a refrigerant is a compromise between many factors including toxicity, flammability, environmental impact, and thermodynamic properties as well as energy efficiency (Domanski et al., 2017). Good heat transfer and lubricant properties are also important to reducing temperature lifts in the compressor. Indeed, compressor maintenance and preservation of lubricant quality are important to retain cycle efficiency.

2.3. References

Alexandratos N, Bruinsma J. World Agriculture Towards 2030/2050. Agricultural Development Economics Division, Food and Agriculture Organization of the United Nations (2012) ESA Working Paper No 12-03.

Aste N, Del Pero C, Leonforte F. Active refrigeration technologies for food preservation in humanitarian context – A review. *Sust Energ Tech Ass* 22 (2017) pp. 150-160.

Baniassadi A, Momen M, Amidpour M, Pourali O. Modeling and design of solar heat integration in process industries with heat storage. *J Clean Prod* 170 (2018) pp. 522-534.

Barma MC, Saidur R, Rahman SMA, Allouhi A, Akash BA, Sait SM. A review on boilers energy use, energy savings, and emissions reductions. *Renew Sust Energ Rev* 79 (2017) pp. 970-983.

Bingol G, Wang B, Zhang A, Pan Z, McHugh TH. Comparison of water and infrared blanching methods for processing performance and final product quality of French fries. *J Food Eng* 121 (2014) pp. 135-142.

Cardoso BJ, Lamas FB, Gaspar AR, Ribeiro JB. Refrigerants used in the Portuguese food industry: Current status. *Int J Refrig* 83 (2017) pp. 60-74.

Corsini A, Bonacina F, Feudo S, Lucchetta F, Marchegiani A. Multivariate KPI for Energy Management of Cooling Systems in Food Industry. *Energy Procedia* 101 (2016) pp. 297-304.

Cristóvão RO, Pinto VMS, Gonçalves, A, Martins RJE, Loureiro JM, Boaventura RAR Fish canning industry wastewater variability assessment using multivariate statistical methods. *Process Saf Environ* 102 (2016) pp. 263-276.

Domanski PA, Brignoli R, Brown JS, Kazakov AF, McLinden MO. Low-GWP refrigerants for medium and high-pressure applications. *Int J Refrig* 84 (2017) pp. 198-209.

Egilmez G, Kucukvar M, Tatari O, Bhutta MKS. Resources, conservation and recycling supply chain sustainability assessment of the U.S. food manufacturing sectors: a life cycle-based frontier approach. *Resour Conserv Recycl* 82 (2014) pp. 8-20.

Eiholzer T, Olsen D, Hoffmann S, Sturm B, Welling B. Integration of a solar thermal system in a medium-sized brewery using pinch analysis: Methodology and case study. *Appl Therm Eng* 113 (2017) pp. 1558-1568.

Eurostat. Key economic indicators on food and beverage sector for EU 28 in 2015.

Euh SH, Kafle S, Lee SY, Lee CG, Jo L, Sung Y et al. Establishment and validation of tar fouling mechanism in wood pellet boiler using kinetic models. *Appl Therm Eng* 127 (2017) pp. 165-175.

Evans JA, Hammond EC, Gigiel AJ, Foster AM, Reinholdt L, Fikiin K, Zilio C. Assessment of methods to reduce the energy consumption of food cold stores. *Appl Therm Eng* 62 (2014) pp. 697-705.

Fluch J, Brunner C, Grubbauer A. Potential for energy efficiency measures and integration of renewable energy in the European food and beverage industry based on the results of implemented projects. *Energy Procedia* 123 (2017) pp. 148-155.

Glaser L, Morrison RM. Ag and Food Sectors and the Economy. U.S. Department of Agriculture, Economic Research Service. May 5, 2016.

Govindan K. Sustainable consumption and production in the food supply chain: A conceptual framework. *Int J Prod Econ* 195 (2018) pp. 419-431.

International Energy Agency (IEA). World Energy Statistics 2017.

Isleroglu H, Kaymak-Ertekin F. Modelling of heat and mass transfer during cooking in steam-assisted hybrid oven. *J Food Eng* 181 (2016) pp. 50-58.

Lee CL, Jou CJ. G. Saving fuel consumption and reducing pollution emissions for industrial furnace. *Fuel Process Technol* 92 (2011) pp. 2335-340.

Kabeel AE, El-Samadony YAF, Khiera MH. Performance evaluation of energy efficient evaporatively air-cooled chiller. *Appl Therm Eng* 122 (2017) pp. 204-213.

Lee CW, Zhong J. Top down strategy for renewable energy investment: Conceptual framework and implementation. *Renew Energ* 68 (2014) pp. 761-773.

Lee AP, Barbano DM, Drake MA. The influence of ultra-pasteurization by indirect heating versus direct steam injection on skim and 2% fat milks. *J Dairy Sci* 100 (2017) pp. 1688-1701.

Lim SAH, Antony J. Statistical process control readiness in the food industry: Development of a self-assessment tool. *Trends Food Sci Tech* 58 (2016) pp. 133-139.

Lin B, Xie X. Factor substitution and rebound effect in China's food industry. *Energy Convers Manag* 105 (2015) pp. 20-29.

Lin B, Xie X. CO_2 emissions of China's food industry: an input - output approach. *J Clean Prod* 112 (2016) pp. 1410-1421.

Lokers R, Knapen R, Janssen S, van Randen Y, Jansen J. Analysis of Big Data technologies for use in agro-environmental science. *Environ Modell* Softw 84 (2016) pp. 494-504.

Muller DCA, Marechal FMA, Wolewinski T, Roux PJ. An energy management method for the food industry. *Energ Effic* 7 (2014) pp. 2677-2686.

Nunes J, Neves D, Gaspar PD, Silva PD, Andrade LP. Predictive tool of energy performance of cold storage in agrifood industries: the Portuguese case study. *Energy Convers Manag* 88 (2014) pp. 758-767.

Nunes J, Silva PD, Andrade LP, Gaspar PD. Key points on the energy sustainable development of the food industry – Case study of the Portuguese sausages industry. *Renew Sustain Energy Rev* 57 (2016) pp. 393-411.

Odyssee-Mure. Decomposition of the final energy consumption in the European Union. October 2016.

Paudel E, Van der Sman RGM, Westerik N, Ashutosh A, Dewi BPC, Boom RM. More efficient mushroom canning through pinch and exergy analysis. *J Food Eng* 195 (2017) pp. 105-113.

Pereira RN, Vicente AA. Environmental impact of novel thermal and non-thermal technologies in food processing. *Food Res Int* 43 (2010) pp. 1936-1943.

Ramírez CA, Patel M, Blok K. From fluid milk to milk powder: energy use and energy efficiency in the European dairy industry. *Energy* 31 (2006a) pp. 1984-2004.

Ramírez CA, Patel M, Blok K. How much energy to process one pound of meat? A comparison of energy use and specific energy consumption in the meat industry of four European countries. *Energy* 31 (2006b) pp. 2047-2063.

Seck GS, Guerassimoff G, Maïzi N. Heat recovery with heat pumps in non-energy intensive industry: a detailed bottom-up model analysis in the French food & drink industry. *Appl Energy* 111 (2013) pp. 489-504.

Seck GS, Guerassimoff G, Maïzi N. Heat recovery using heat pumps in non-energy intensive industry: are energy saving certificates a solution for the food and drink industry in France? *Appl Energy* 156 (2015) pp. 374-389.

Shindo J, Yanagawa A. Top-down approach to estimating the nitrogen footprint of food in Japan. *Ecol Indic* 78 (2017) pp. 502-511.

Silva FLC, Souza RC, Cyrino Oliveira FL, Lourenco PM, Calili RF. A bottom-up methodology for long term electricity consumption forecasting of an industrial sector - Application to pulp and paper sector in Brazil. *Energy* 144 (2018) pp. 1107-1118.

Suntivarakorn R, Treedet W. Improvement of Boiler's Efficiency Using Heat Recovery and Automatic Combustion Control System. *Energy Procedia* 100 (2016) pp. 193-197.

Swain MJ, Evans JA, James SJ. Energy consumption in the UK food chill chain - primary chilling. *Food Manufacturing Efficiency* 2 (2008) pp. 1-9.

United Nations, Department of Economic and Social affairs population division. The 2017 revision of world population prospects. June 2017.

van Holsteijn F, Kemna R. Minimizing food waste by improving storage conditions in household refrigeration. *Resour Conserv Recy* 128 (2018) pp. 25-31.

Walmsley TG, Atkins MJ, Walmsley MRW, Neale JR. Appropriate placement of vapour recompression in ultra-low energy industrial milk evaporation systems using Pinch Analysis. *Energy* 116 (2016) pp. 1269-1281.

Wang L. Energy efficiency technologies for sustainable food processing. *Energy Effic* 7 (2014) pp. 791-810.

Wei X, Xu G, Kusiak A. Modeling and optimization of a chiller plant. *Energy* 73 (2014) pp. 898-907.

Wolfert S, Ge L, Verdouw C, Bogaardt MJ. Big Data in Smart Farming – A review. Energy efficiency technologies for sustainable food processing. *Agr Syst* 153 (2017) pp. 69-80.

Wojdalski J, Dróżdż B, Grochowicz J, Magryś A, Ekielski A. Assessment of Energy Consumption in a Meat-Processing Plant: a Case Study. *Food Bioprocess Tech* 6 (2013) pp. 2621-2629.

Xu T, Flapper J, Kramer KJ. Characterization of energy use and performance of global cheese processing. *Energy* 34 (2009) pp. 1993-2000.

Xu Y, Chen Y, Cao Y, Xia W, Jiang Q. Application of simultaneous combination of microwave and steam cooking to improve nutritional quality of cooked purple sweet potatoes and saving time. *Innov Food Sci Emerg* 36 (2016) pp. 303-310.

Xu Y, Szmerekovsky J. System dynamic modeling of energy savings in the US food industry. *J Clean Prod* 165 (2017) pp. 13-26.

Zuberi MJS, Patel MK. Bottom-up analysis of energy efficiency improvement and CO_2 emission reduction potentials in the Swiss cement industry. *J Clean Prod* 142 (2017) pp. 4294-4309.

3. Presentation of the research work

3.1. Thermal design of complex systems for food processing

The design of a food processing system involves the application of basic principles to address the following critical issues: (1) minimisation of capital and operating costs, while satisfying food processing steps, food safety regulations and required quality of final food product and (2) minimisation of energy consumption, of water use and of food waste. The principles involved include: careful choosing of the site and of the technologies, adoption of numerical tools and careful measures for safety of people.

This thesis provides an original both theoretical and applied design method for steam batch thermal processes in unsteady state conditions.

3.2. Innovative food processing plant

Successful food and beverage innovation is essential in helping industries achieve sustainability and profitability. To be acceptable to the consumer, the new process must deliver a product that shows significant advantage relative to a conventionally processed product.

This thesis presents an innovative food freezing plants at very low temperature. In particular, the new plant was designed to be operated by a reversed Brayton cycle.

3.3. Energy monitoring and systems simulation

Thoughts about energy saving measures often goes to more efficient technologies, such as: condensing boilers, high efficiency electric motors, variable speed drives, LED lighting, new refrigerators and/or freezers, etc. However, in order to achieve sustainable energy reduction results, energy monitoring is of the foremost importance to understand how energy systems are used and regulated. Only through consistent energy monitoring can energy costs and use be efficiently reduced. The continuous measurement and evaluation of all energy flows is the basis for successful energy management. Indeed, the adoption of an energy monitoring system gives energy managers of companies and domestic households information in the analysis of energy data.

This thesis reports examples of two monitoring campaigns where electricity consumption and temperatures were monitored in domestic cold appliances and in a multi-energy system for a chocolate industry. In the last case, the monitored data were also used to set out a simulation model of the system.

4. Thermal design of a complex system for food processing

4.1. First paper

Applied Thermal Engineering 118 (2017) pp. 638-651

DOI: 10.1016/j.applthermaleng.2017.03.004

Steam batch thermal processes in unsteady state conditions: Modelling and application to a case study in the food industry

Alessandro Biglia [a], Lorenzo Comba [b], Enrico Fabrizio [b,*], Paolo Gay [a], Davide Ricauda Aimonino [a]

[a] DiSAFA – Universitá degli Studi di Torino, 2 Largo Paolo Braccini, Grugliasco (TO) 10095, Italy

[b] DENERG – Politecnico di Torino, 24 Corso Duca degli Abruzzi, Torino 10129, Italy

* Corresponding author: Tel. +39 011 090 4465
e-mail address: enrico.fabrizio@polito.it

Abstract

Many industrial processes require high amounts of steam. Design and operation of steam plants are particularly complex when the steam supply is required for short periods and with a varying time schedules. To fulfil the discontinuous needs of steam users, avoiding the steam boiler oversizing to the peak value of the steam request, a thermal energy storage (TES) system can be adopted. The proper sizing of TES systems, which, in this application, is constituted by a steam accumulator vessel installed between the steam generator and the consumer, cannot be based on the sole initial and final state conditions of the steam storage, since a performance prediction of the process time-evolution is also required.

In this paper, a model of steam batch processes for industrial thermal treatments, able to describe unsteady operative conditions, is presented. More in detail, a three-stage steam plant, with a sequentially interconnected steam boiler, steam accumulator and processing tank, was considered. The dynamic model of the charging and discharging processes

of the steam accumulator was applied to a real case study in the food industry: the batch debacterisation process of cocoa beans. Nevertheless, the obtained results can be profitably employed in the design and the performance assessments of a wide set of applications involving the steam processing fluid, such as desalination plants, solar thermal power plants, retorts, steam ovens and others.

Keywords: Steam batch process, Steam accumulator, Tank steam filling, Unsteady process, Food industry.

Nomenclature

a	constant of Redlich-Kwong EoS	-
a_{cb}	length of the cocoa beans	m
b	constant of Redlich-Kwong EoS	-
b_{cb}	width of the cocoa beans	m
$c_{p,\mathrm{f}}$	specific heat of the food product at constant pressure	J kg^{-1} K^{-1}
$c_{p,\mathrm{shs}}$	specific heat of the superheated vapour at constant pressure	J kg^{-1} K^{-1}
$c_{p,\mathrm{w}}$	specific heat of the water film at constant pressure	J kg^{-1} K^{-1}
c_v	vapour specific heat at constant volume	J kg^{-1} K^{-1}
d_{p}	thickness of the cocoa beans	m
f	friction coefficient in the pipe connection	-
g	gravitational acceleration	m s^{-2}
$h_{1,\mathrm{v}}$	steam boiler enthalpy	J kg^{-1}
$h_{2,\mathrm{l}}$	liquid water enthalpy in the steam accumulator	J kg^{-1}
$h_{2,\mathrm{v}}$	vapour enthalpy in the steam accumulator	J kg^{-1}
$h_{3,\mathrm{w}}$	heat transfer coefficient between vapour and food product	W m^{-2} K^{-1}
$\bar{h}_{3,\mathrm{w}}$	corrected heat transfer coefficient between vapour and food product	W m^{-2} K^{-1}
$h_{\mathrm{p,v}}$	vapour specific enthalpy in the connection pipe	J kg^{-1}
$k_{3,\mathrm{w}}$	water film thermal conductivity	W m^{-1} K^{-1}
l_{m}	mechanical work per unit of mass	J kg^{-1}
l_{v}	total work per unit of mass of the vapour	J kg^{-1}
m_2	mass in the steam accumulator	kg

$m_{2,\mathrm{l}}$	liquid water mass in the steam accumulator	kg
$m_{2,\mathrm{v}}$	vapour mass in the steam accumulator	kg
$m_{3,\mathrm{f}}$	food product mass in the processing tank	kg
$m_{3,\mathrm{l}}$	liquid water mass in the processing tank	kg
$m_{3,\mathrm{v}}$	vapour mass in the processing tank	kg
$\dot{m}_{12,\mathrm{v}}$	steam flow rate from steam boiler to steam accumulator	kg s^{-1}
$\dot{m}_{23,\mathrm{v}}$	steam flow rate from steam accumulator to processing tank	kg s^{-1}
$\dot{m}_{3,\mathrm{c}}$	vapour condensation rate on the external surface of the food product	kg s^{-1}
p_1	steam boiler pressure	Pa, bar
p_2	steam accumulator pressure	Pa, bar
$\hat{p}_2$	steam accumulator pressure from references	Pa, bar
p_3	processing tank pressure	Pa, bar
p_{p}	vapour pressure in the initial section of the connection pipe	Pa, bar
Δp_{p}	pressure losses in the pipe connection	Pa, bar
$p_{\mathrm{v}} v_{\mathrm{v}}$	vapour pressure work	J kg^{-1}
q_{v}	vapour heat per unit of mass	J kg^{-1}
$u_{2,\mathrm{l}}$	liquid water specific internal energy in the steam accumulator	J kg^{-1}
$u_{2,\mathrm{v}}$	vapour specific internal energy in the steam accumulator	J kg^{-1}
$u_{3,\mathrm{v}}$	vapour specific internal energy in the processing tank	J kg^{-1}
$v_{2,\mathrm{l}}$	liquid water specific volume in the steam accumulator	m^3 kg^{-1}
$v_{2,\mathrm{v}}$	vapour specific volume in the steam accumulator	m^3 kg^{-1}
$v_{3,\mathrm{v}}$	vapour specific volume in the steam accumulator	m^3 kg^{-1}
$v_{\mathrm{p,v}}$	vapour specific volume in the connection pipe	m^3 kg^{-1}
w_{v}	vapour velocity	m s^{-1}
$w_{\mathrm{p,v}}$	vapour velocity in the connection pipe	m s^{-1}
x_2	vapour quality in the steam accumulator	-
y_{a}	air mass fraction	-
A_2	steam accumulator external area	m^2
$A_{3,\mathrm{f}}$	food product heat exchange surface	m^2

D_{p}	diameter of the connection pipe	m
K_2	steam accumulator thermal transmittance	W m^{-2} K^{-1}
$L_{3,\mathrm{f}}$	characteristic length of the food product	m
L_{p}	length of the connection pipe	m
$\dot{Q}_{2,\mathrm{e}}$	thermal losses between steam accumulator and ambient	W
$\dot{Q}_{3,\mathrm{e}}$	thermal losses between processing tank and ambient	W
$\dot{Q}_{3,\mathrm{w}}$	heat flow from vapour to food product	W
$\dot{W}_{2,\mathrm{e}}$	mechanical work between steam accumulator and ambient	W
$\dot{W}_{3,\mathrm{e}}$	mechanical work between processing tank and ambient	W
R	universal gas constant divided by molar mass of the fluid	J kg^{-1} K^{-1}
S_{p}	connection pipe section	m^2
t_0	simulation initial time	s
t_f	simulation final time	s
T_1	steam boiler temperature	K, °C
T_2	steam accumulator temperature	K, °C
T_{e}	environment temperature	K, °C
$T_{3,\mathrm{f}}$	food product temperature in the processing tank	K, °C
$T_{3,\mathrm{v}}$	vapour temperature in the processing tank	K, °C
$T_{3,\mathrm{sat}}$	vapour temperature in saturation condition in the processing tank	K, °C
$T_{3,\mathrm{shs}}$	superheated vapour temperature in the processing tank	K, °C
$T_{3,\mathrm{w}}$	water film temperature	K, °C
U_2	internal energy in the steam accumulator	J
$U_{3,\mathrm{v}}$	vapour internal energy in the processing tank	J
V_2	steam accumulator volume	m^3
$V_{3,\mathrm{v}}$	vapour volume in the processing tank	m^3
Z	compressibility factor	-
β_{cr}	critical pressure ratio	-
γ	adiabatic coefficient of expansion	-
$\bar{\gamma}$	corrected adiabatic coefficient of expansion	-
ε_∞	ℓ_∞ norm-based measure of the relative distance between $p_2(t)$ and $\hat{p}_2(t)$	-

ε_2	ℓ_2 norm-based measure of the relative distance between $p_2(t)$ and $\hat{p}_2(t)$	-
$\mu_{3,\mathrm{w}}$	water film viscosity	kg m^{-1} s^{-1}
$\xi_{2,\mathrm{l}}$	liquid water filling ratio in the steam accumulator	-
$\rho_{2,\mathrm{l}}$	liquid water density in the steam accumulator	kg m^{-3}
$\rho_{2,\mathrm{v}}$	vapour density in the steam accumulator	kg m^{-3}
$\rho_{3,\mathrm{sat}}$	vapour density in saturation condition in the processing tank	kg m^{-3}
$\rho_{3,\mathrm{w}}$	water film density in the processing tank	kg m^{-3}
$\Lambda_{3,\mathrm{w}}$	latent heat during condensation in the processing tank	J kg^{-1}
$\bar{\Lambda}_{3,\mathrm{w}}$	corrected latent heat during condensation in the processing tank	J kg^{-1}
ψ_1	valve 1 installed between steam boiler and steam accumulator	-
ψ_2	valve 2 installed between steam accumulator and processing tank	-

1. Introduction

The adoption of steam as a heat carrier is affirmed in many industrial thermal processes (Tam et al., 1989; Industrial Steam systems optimization experts training, 2012; Walker et al., 2013), thanks to the high value of latent energy per unit of mass (James et al., 2000) which, during the condensation, is available to be transferred at a constant temperature and with a very high heat transfer coefficient. When the thermal energy required by the consumers is low compared with production, the produced steam can be accumulated in insulated tanks, implementing a thermal energy storage (TES) system (Pirasaci and Yogi Goswami, 2016). Therefore, steam is a convenient energy carrier, even if its production is rather expensive. To ensure the steam boiler optimal working condition is thus essential in order to increase the system efficiency, which results in a consequent less expensive steam production (Sun et al., 2016). This can be achieved by coupling the steam boiler with a TES system, which increases the energy efficiency by managing the demand-side. Several profitable applications of TES systems can be found in literature (Comodi et al., 2016; Grange et al., 2016; Kishor Johar et al., 2016; Schreiber et al., 2015; Palacio et al., 2014; Cao and Cao, 2006), where TES system are

adopted to lower, smooth or shift the thermal, electrical or cooling load time profile.

In industrial applications, steam can be saturated or superheated. Usually, superheated steam is adopted to prevent condensation during its distribution, due to a decrease in temperature under the saturation value, at the particular processing pressure (Karimi, 2010; Cenkowski et al., 2007). Thanks to its capability to quickly heat up the food product surface, due to the high quantity of thermal energy transmitted per unit of time, steam is widely employed in thermal food industrial processes. Indeed, with the involved high temperatures, undesired pre-cooking process may occur in the presence of a too slow heat exchange between food products and the carrier fluid.

Moreover, with respect to hot air systems, the adoption of steam can reduce oxidation phenomena (Zzaman, 2014), even if the possible condensation phenomena on the product surfaces, when undesired, is a not negligible disadvantage.

In many cases, the amount of steam required at the use-side, in terms of instantaneous flow rate, is not constant. Batch processes, as e.g. retort sterilisation or debacterisation, require a huge amount of steam for short periods of time. Since steam boilers cannot react instantaneously to demand variations, usually they are sized on the base of the peak demand value, resulting in an oversized design. A TES system, based on the flash steam accumulator technology, could be adopted in order to: (1) fulfil the peak demands that occur for short time periods; (2) protect the steam boiler from operating under capacity (Steambook, Fischer).

An application where the coupling between a steam boiler and a steam accumulator represents an effective solution is the one of solar thermal power plants (Xu et al., 2012; Bai and Xu, 2011; Baldini et al., 2009; Steinmann and Eck, 2006). During periods of low solar radiation, the heat stored in the steam accumulator is discharged, while, during periods of high solar radiation, the excess part of the produced steam is used to recharge the steam accumulator.

For these reasons, the adoption of steam accumulators results to be essential in those processes where the supply of huge amount of steam is

required for limited periods of time, with respect to an average working cycle values, and/or where the energy source is intermittent.

In the food industry, many effective applications of the coupling between a steam boiler and a steam accumulator can be found. Several industrial food processes require the supplying of large quantities of saturated or superheated steam during short periods of time, maybe with a particular time schedule. This is the case, for example, of batch pasteurisation and sterilisation processes for retort, debacterisation, blanching, etc. With different temperatures and time durations, all these examples are representative of thermal processes applied to food products with the goal of reducing microbial charge and enzymatic activity to stabilize the product and reducing quality deterioration.

In this paper, a model of steam batch processes for industrial thermal treatments, able to describe unsteady operative conditions, is presented. More in detail, a three-stage steam plant, with a sequentially interconnected steam boiler, steam accumulator and processing tank, has been considered. The objective of the model is to predict the working condition of the various components of the systems (steam accumulator, connection pipe and processing tank) with different sizing and initial conditions, the pressurisation of the processing tank and the heat exchange between the vapour and the product to be processed. The time evolution of the steam temperature and pressure in the accumulator, the steam accumulator volume, the steam boiler capacity, the volume and the time evolution of temperature and pressure of the processing tank are some of the features provided by the application of the proposed model.

The proposed model demonstrates its effectiveness as a design tool, employable during plant sizing or to verify the operating conditions and the energy requirements of a given plant. Indeed, the model allows to study the proper trade-off between the steam boiler capacity, the steam accumulator volume and the processing tank volume and others design parameter, predicting the performance on the entire process.

The assumptions and simplifications adopted in the modelling framework, discussed in Section 3, are related to the required level of detail. Regarding the steam accumulator, for instance, different modelling approaches exist. A simple one, based to the sole initial and final conditions of the

accumulator, in terms of pressure or temperature (Steinmann and Eck, 2006), provides result only suitable for a preliminary rough sizing of the component. In order to evaluate the dynamic evolution of the temperature and pressure in the steam accumulator, models based on the equilibrium and non-equilibrium conditions between the vapour and liquid phases were developed. In the equilibrium model (Bai and Xu, 2011), the vapour and liquid phases are considered at the same saturation temperature and pressure, allowing to determine the complete thermodynamic state of the steam accumulator as a function of the sole pressure or temperature. Moreover, during thermodynamic change the evaporation and condensation rates are considered instantaneous. Lately, studies aiming at defining the dynamic behaviour of the steam accumulator, considering the nonlinear non-monotonic changing phenomenon that modifies the equilibrium solution, have been conducted (Stevanovic et al., 2015; Sun et al., 2015; Stevanovic et al., 2012). This latter approach requires to consider separately pressure and temperature evolutions of the two water phases (liquid and vapour) in the accumulator and to compute the evaporation and condensation finite rates defining two parameters, the evaporation and condensation relaxation times, obtained through empirical procedures. Indeed, as described in (Sun et al., 2015), different initial conditions of the steam accumulator (e.g. in terms of water filling ratio, of pressure, of temperature etc.) leads to a not predictable variation in the value of these two parameters. Considering that the scope of this article is to predict the behaviour – for design purposes – of a complex system where the steam accumulator is one component, and since the two evaporation and condensation relaxation times are experimental parameters which are unknown and cannot be precisely estimated before implementing a steam accumulator, in our work a dynamic model based on equilibrium conditions between the two phases was adopted for the steam accumulator. The developed modelling framework has been applied to a real case study of the food industry: a cocoa beans debacterisation plant. The considered steam plant is composed by a steam boiler, a steam accumulator and a debacterisation tank.

The paper is organised as follows: the technological features and the operating principles of the steam loop system are presented in Section 2;

Section 3 introduces the balance equations integrated in the model while, in Section 4, the model is applied to a case study. Finally, the conclusions are reported in the last section.

2. Description of the technology

In order to describe the developed model, an illustrative three-stage steam plant is introduced, which is constituted by a sequentially interconnected steam boiler, steam accumulator and processing tank (Fig. 1). The steam flow rates $\dot{m}_{12,v}$, from the steam boiler to the steam accumulator, and $\dot{m}_{23,v}$, from this last to the processing tank, are regulated by valves ψ_1 and ψ_2 respectively.

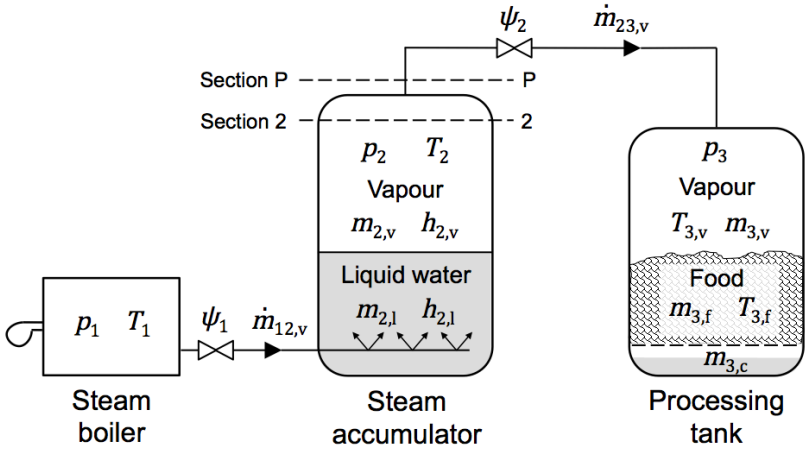

Fig. 1. Scheme of a three-stage steam plant for batch thermal process of food products constituted by a steam boiler, a steam accumulator and a processing tank.

The steam produced by the boiler is injected through a set of nozzle into the lower edge of the steam accumulator. During the charging phase of the accumulator, the incoming steam, injected under the surface level of the water already presents in the accumulator, rapidly condensates leading to an increment of the pressure p_2 and temperature T_2 of the accumulator. The charging process occurs at the initial start-up, when the water contained in the accumulator is in equilibrium with the environment temperature, or when the temperature and/or the pressure values in the accumulator decrease below certain thresholds.

Once the steam accumulator is pressurised, the downstream valve ψ_2 is opened when a supply of steam is required. The steam flow rate from the accumulator to the processing tank, which is affected by the pressure difference between the two interconnected tanks, p_2 and p_3 respectively, can be intercepted by closing the valve ψ_2 when the thermal process does not require additional heat. The processing tank contains the food product, properly arranged to be treated by the steam.

2.1. Steam accumulator

A steam accumulator is made by a pressurised vessel and it is generally used as buffer storage when the load demand of steam is discontinuous, e.g. with temporary high flow rate for short periods of time, also with fast dynamics. In this way, the sizing of the steam boiler can be limited to the average steam load value, with respect to a standard working cycle, avoiding an oversizing to cover the peak value. With this solution, the steam boiler will charge the accumulator with continuity, ever working at its optimal efficiency.

However, since the density $\rho_{2,\mathrm{v}}$ of saturated steam is significantly lower than saturated liquid one $\rho_{2,\mathrm{l}}$, directly storing saturated or superheated steam (*dry accumulator*) requires higher storing volumes with respect to vessel containing saturated liquid water (*wet accumulator*). In the case of wet accumulator, the steam is produced by a pressure reduction in a pressurised storage of saturated liquid and vapour water, resulting in a not constant pressure steam production (*sliding pressure steam accumulators*). The process of fast evaporation caused by lowering the pressure is called *flashing*, which produces *flash steam*. In steam plants, flash tanks are also adopted for heat recovery of the steam condensate drainage; in this case vertical flash tanks are preferred since the enhanced separation provided between steam and water [24–25]. It should be noted that the flash steam production rate is limited by an upper boundary limit depending on the surface area of the liquid-vapour interface. Reference curves that express the maximum flash steam generation velocity per square meter of interface surface as a function of the pressure can be found in technical literature. For this reason, in order to increase the flash steam production rate for a given water mass, horizontal vessels are usually

preferred to vertical ones, because of the more favourable liquid-vapour interface surface.

The sliding pressure steam accumulator (Fig. 1) contains steam and liquid water which are heated by the steam boiler during the charging process. When the discharging process starts, the out coming steam flow rate $\dot{m}_{23,\mathrm{v}}$ leads to a pressure reduction in the accumulator and, consequently, to the evaporation of a portion of liquid in order to re-equilibrate the system. The high specific heat capacity and the low specific volume of liquid water allow great quantities of heat to be stored in the vessel and, therefore, a large quantity of steam to be produced.

The amount of produced steam depends on the initial and final pressure values of the discharge process. Usually, the lower $p_{2,\min}$ and maximum $p_{2,\max}$ pressure values of steam accumulator should not decrease or exceed the values specified by the required thermal process. The values of the two pressure limits $p_{2,\min}$ and $p_{2,\max}$ can give a first attempt to design a steam accumulator by defining the producible amount of flash steam $m_{2,\mathrm{v}}$ as

$$m_{2,\mathrm{v}} = \frac{m_{2,\mathrm{l}}\left(h_{2,\max} - h_{2,\min}\right)}{\Lambda} \tag{1}$$

where $m_{2,\mathrm{l}}$ represents the liquid water mass in the steam accumulator before the steam production, $h_{2,\min}$ and $h_{2,\max}$ the enthalpy of $m_{2,\mathrm{l}}$ at pressure $p_{2,\min}$ and $p_{2,\max}$ respectively, and Λ the latent heat of water. Eq. (1), however, does not take into account the evolution of the accumulator pressure and temperature over time, during both charging and discharging processes.

2.2. Processing tank

Several non-stationary food processes can be schematized by the considered illustrative plant (Fig. 1): in the final steam user, the processing tank downstream the steam accumulator, a microbial decontamination, a bleaching or a cooking process, such as a steam oven cooking, can take place.

Nowadays, the steam oven cooking is one of the widely adopted cooking process in food industry, particularly widespread in commercial processing and food service operation, thanks to the provided good quality

of the cooked products by the steam contact (Sakin-Yilmazer et al., 2013). The effectiveness of steam ovens has been proved by numerous studies: Bowers et al. (2012) investigated the positive effects of moist-heat with respect to the dry-heat cookery while Mora et al. (2011) compared the cooking results in the case of ovens with forced convection, with low steam or with high steam, at a temperature of 100 °C, noting good effects in terms of reduction of cooking time and reduction of dehydration phenomena, which usually occur with traditional oven cooking. The considered processing tank can also represent another food industry batch process: the steaming (Huang et al., 2013). This type of cooking, affirmed as one of the healthiest cooking techniques, is widely used e.g. in the preparation of Asian cuisines.

In the food industry, steam is also used to pressurise retorts in order to perform steam sterilisation cycles (Berteli et al., 2013; Lau et al., 2015; Singh et al., 2015). Lau et al. (2015) have developed and validated a numerical model of a retort, which allows to predict the transient vessel temperature and pressure profiles of an entire steam sterilisation cycle. Singh et al. (2015) conducted a set of experiments for evaluating the heat transfer phenomena inside a conventional static steam retort. An evaluation of the energy consumption in a steam retort has been performed by Berteli et al. (2013), comparing the conventional and alternative venting processes.

3. Modelling framework

3.1. Steam boiler model

In this study, the steam boiler has been considered as an ideal steam generator, producing a stationary steam flow rate $\dot{m}_{12,\mathrm{v}}$, at constant pressure p_1 and temperature T_1, when it is active. The produced steam flow, characterized by a certain enthalpy $h_{1,\mathrm{v}}$, reaches the downstream steam accumulator through the valve ψ_1, which is kept open until the pressure p_2 of the steam accumulator does not exceed the maximum allowed value $p_{2,\max}$.

3.2. Steam accumulator model

A steam wet accumulator can be modelled as a pressurised vessel containing liquid and vapour water. Considering the dynamic of the water evaporation and of the steam condensation much faster than the charging and discharging processes, the water-vapour accumulator system is considered in thermodynamic equilibrium and, thus, the accumulator thermodynamic state can be completely defined by its temperature or pressure. The mass of liquid water $m_{2,\mathrm{l}}$ in the accumulator is function of the volumetric filling fraction of water $\xi_{2,\mathrm{l}}$, of the steam accumulator volume V_2 and of the water density $\rho_{2,\mathrm{l}}$.

The state of the steam accumulator has been described by the following two state variables: the mass m_2, which is the sum of the water mass and vapour mass content, and the overall internal energy U_2, in accordance with literature works (Moran and Shapiro, 2006).

Considering that charging and discharging processes of the steam accumulator may simultaneously occur, the accumulator mass balance is

$$\frac{dm_2}{dt} = \dot{m}_{12,\mathrm{v}} - \dot{m}_{23,\mathrm{v}} \tag{2}$$

where $\dot{m}_{12,\mathrm{v}}$ is the accumulator inlet steam flow rate and $\dot{m}_{23,\mathrm{v}}$ the steam flow rate provided to the consumer, described in Section 3.4.

The energy balance in the steam accumulator control volume, neglecting the kinetic and potential energy effects, is

$$\frac{dU_2}{dt} = \dot{Q}_{2,\mathrm{e}} + \dot{m}_{12,\mathrm{v}} h_{1,\mathrm{v}} - \dot{m}_{23,\mathrm{v}} h_{2,\mathrm{v}} \tag{3}$$

where $\dot{m}_{12,\mathrm{v}} h_{1,\mathrm{v}}$ and $\dot{m}_{23,\mathrm{v}} h_{2,\mathrm{v}}$ represent the energy flow rate entering and exiting the steam accumulator, respectively. The heat transfer rate $\dot{Q}_{2,\mathrm{e}}$, introduced to account for the vessel thermal losses, is a function of the external surface A_2 and the thermal transmittance K_2 of the accumulator, as

$$\dot{Q}_{2,\mathrm{e}} = A_2 K_2 (T_{\mathrm{e}} - T_2) \tag{4}$$

where T_{e} is the environment temperature, which has been considered constant.

The dynamic of the accumulator is therefore described by the two differential equations Eqs. (2) and (3).

Considering the internal dynamics of the steam accumulator as a succession of equilibrium conditions between the vapour and the liquid phases, the pressure p_2 and vapour quality x_2 can be determined by assuring the saturation condition, solving the system of non-linear equations

$$\begin{cases} V_2 = m_2 \left(x_2 v_{2,\mathrm{v}}(p_2) + (1 - x_2) v_{2,\mathrm{l}}(p_2) \right) \\ U_2 = m_2 \left(x_2 u_{2,\mathrm{v}}(p_2) + (1 - x_2) u_{2,\mathrm{l}}(p_2) \right) \end{cases} \quad (5)$$

The specific volume v and specific internal energy u, of both liquid and vapour phases were computed by a set of splines interpolating functions, using the Wagner and Kretzschmar (2008) steam data table as nodes. Finally, the others thermodynamic properties of the steam accumulator can be easily evaluated as a function of the sole pressure.

3.3. Processing tank model

During the filling phase of the processing tank by means of the steam flow rate $\dot{m}_{23,\mathrm{v}}$, the steam pressure p_3 and temperature $T_{3,\mathrm{v}}$ evolutions are linked. Indeed, the incoming high pressure steam flow performs a compression work to the low pressure air/steam mixture, leading to an increase of the internal energy $U_{3,\mathrm{v}}$, and consequently of $T_{3,\mathrm{v}}$ (Fundamentals of Thermodynmics, 2009). Moreover, during the food processing, a portion of the steam internal energy is being transferred to the food product, through a thin film of water, resulting from a condensation phenomenon on the food surfaces.

The developed thermodynamic model of the processing tank, during the filling process, takes into account two concurrent aspects: (1) the steam temperature and pressure evolution inside the tank during the pressurisation process and (2) the heat exchange from the vapour to the food product.

3.3.1. Steam state evolution

The dynamic of the steam into the processing tank is described by the variables $T_{3,\mathrm{v}}$ and p_3.

Several thermodynamic analyses of the filling phase of tanks can be found in literature, in particular for the cases of hydrogen and natural gas. In the work of Ruffio et al. (2014), temperature and pressure evolutions during tank filling have been derived from thermodynamic database (NIST) and by three different equations of state (EoS). Results obtained with Redlich-Kwong EoS and with NIST database were in good agreement. The refilling process of a gaseous hydrogen tank was modelled in (Li et al., 2014; Striednig et al., 2014), where a compressibility factor has been defined to take into account the real behaviour of the gas. Moreover, regarding the fast filling process of hydrogen storage cylinders, in (Li et al., 2012; Liu et al., 2010), experimental trials have been carried out to investigate the concurrent increased of temperature and pressure as a function of different parameters.

In the present work, temperature and pressure dynamics are studied by combining the Redlich-Kwong EoS with the first law of thermodynamics. Using the first law of thermodynamics for an open system the derivative of the internal energy $U_{3,\mathrm{v}}$, expressed as the product of mass $m_{3,\mathrm{v}}$ and specific internal energy $u_{3,\mathrm{v}}$, is

$$\frac{dU_{3,\mathrm{v}}}{dt} = m_{3,\mathrm{v}}\frac{du_{3,\mathrm{v}}}{dt} + \dot{m}_{23,\mathrm{v}}u_{3,\mathrm{v}} = \dot{Q}_{3,\mathrm{e}} + \dot{m}_{23,\mathrm{v}}h_{2,\mathrm{v}} - \dot{Q}_{3,\mathrm{w}} \tag{6}$$

where $\dot{Q}_{3,\mathrm{e}}$ represents the heat flow per unit of time towards the outdoor environment, $\dot{m}_{23,\mathrm{v}}h_{2,\mathrm{v}}$ represents the heat flow supplied by the steam accumulator during the tank filling and $\dot{Q}_{3,\mathrm{w}}$ is the heat flow from the steam to the food product. The derivative of $u_{3,\mathrm{v}}$ can be expressed as

$$\frac{du_{3,\mathrm{v}}}{dt} = c_{\mathrm{v}}dT_{3,\mathrm{v}} + \left[T_{3,\mathrm{v}}\left(\frac{\partial p_{3,\mathrm{v}}}{\partial T_{3,\mathrm{v}}}\right)_{\mathrm{v}} - p_3\right]dv_{3,\mathrm{v}} \tag{7}$$

Using the Redlich-Kwong EoS to define the pressure p_3 (Redlich and Kwong, 1949), and computing the partial derivative of the pressure with respect to the temperature at constant volume, Eq. (7) can be integrated between a generic time instant t and the initial reference one t_0, obtaining

$$u_{3,\mathrm{v}}(t) = u_{3,\mathrm{v}}(t_0) + c_{\mathrm{v}}\left(T_{3,\mathrm{v}}(t) - T_{3,\mathrm{v}}(t_0)\right) + \\ + \frac{3a}{2b\sqrt{T_{3,\mathrm{v}}(t)}}\left[\log\left(\frac{V_{3,\mathrm{v}} + bm(t_0)_{3,\mathrm{v}}}{V_{3,\mathrm{v}} + bm(t)_{3,\mathrm{v}}}\right)\right] \tag{8}$$

where a and b represent two parameters of the Redlich-Kwong Eos depending on the type of fluid.

Substituting Eqs. (7) and (8) into Eq. (6), the state equation of the steam temperature $T_{3,\mathrm{v}}$ can be expressed

$$\frac{dT_{3,\mathrm{v}}}{dt} = \frac{\dot{m}_{23,\mathrm{v}}}{C_{\mathrm{I}}}\left(h_{2,\mathrm{v}} - C_{\mathrm{II}} + \frac{3am_{3,\mathrm{v}}}{2\left(V_{3,\mathrm{v}} - bm_{3,\mathrm{v}}\right)\sqrt{T_{3,\mathrm{v}}}}\right) + \\ - \frac{\left(\dot{Q}_{3,\mathrm{w}} - \dot{Q}_{3,\mathrm{e}}\right)}{C_{\mathrm{I}}} \tag{9}$$

with

$$C_{\mathrm{I}} = m_{3,\mathrm{v}}c_{\mathrm{v}} - \frac{3am_{3,\mathrm{v}}}{4bT_{3,\mathrm{v}}^{1.5}}\left[\log\left(\frac{V_{3,\mathrm{v}} + bm(t_0)_{3,\mathrm{v}}}{V_{3,\mathrm{v}} + bm_{3,\mathrm{v}}}\right)\right]$$

and

$$C_{\mathrm{II}} = u(t_0)_{3,\mathrm{v}} + c_{\mathrm{v}}\left(T_{3,\mathrm{v}} - T(t_0)_{3,\mathrm{v}}\right) + \\ + \frac{3a}{2b\sqrt{T_{3,\mathrm{v}}}}\left[\log\left(\frac{V_{3,\mathrm{v}} + bm(t_0)_{3,\mathrm{v}}}{V_{3,\mathrm{v}} + bm_{3,\mathrm{v}}}\right)\right]$$

The state equation of the steam pressure p_3 can be obtained by deriving the Redlich-Kwong EoS as

$$\frac{dp_3}{dt} = C_{\mathrm{III}}\frac{dT_{3,\mathrm{v}}}{dt} + C_{\mathrm{IV}}\frac{V_{3,\mathrm{v}}}{m_{3,\mathrm{v}}^2}\dot{m}_{23,\mathrm{v}} \tag{10}$$

with

$$C_{\mathrm{III}} = \frac{R}{v_{3,\mathrm{v}} - b} + \frac{a}{2\left(v_{3,\mathrm{v}}^2 + bv_{3,\mathrm{v}}\right)T_{3,\mathrm{v}}^{1.5}}$$

and

$$C_{\mathrm{IV}} = \frac{RT_{3,\mathrm{v}}}{\left(v_{3,\mathrm{v}} - b\right)^2} - \frac{a\left(2v_{3,\mathrm{v}} + b\right)}{\left(v_{3,\mathrm{v}}^2 + bv_{3,\mathrm{v}}\right)^2\sqrt{T_{3,\mathrm{v}}}}$$

The set of Eqs. (9) and (10) describes, thus, the steam temperature $T_{3,\mathrm{v}}$ and pressure p_3 evolution in the processing tank during the filling phase.

3.3.2. Steam-food heat exchange model

Part of the steam flow rate injected in the processing tank condenses on the external surface of the food product. With the condensation process, a high quantity of energy is released by the steam with the formation of a thin film of water on the food surface, allowing a fast increment of the external temperature of the food product. The heat transfer coefficient $h_{3,\mathrm{w}}$ between steam and food product was estimated by using the Nusselt correlation (Holman, 2010) and, in particular, the heat flow $\dot{Q}_{3,\mathrm{w}}$ can be written as

$$\dot{Q}_{3,\mathrm{w}} = \bar{h}_{3,\mathrm{w}} A_{3,\mathrm{f}} \left(T_{3,\mathrm{sat}} - T_{3,\mathrm{f}}\right) = \dot{m}_{3,\mathrm{c}} \overline{\Lambda}_{3,\mathrm{w}} \tag{11}$$

where $\bar{h}_{3,\mathrm{w}}$ is the corrected form of the heat transfer coefficient $h_{3,\mathrm{w}}$ during condensation (Soponronnarit et al., 2006; Kittiworrawatt and Devahastin, 2009; Sa-adchom et al., 2011), $A_{3,\mathrm{f}}$ is the heat exchange surface between steam and food product, $T_{3,\mathrm{sat}}$ and $T_{3,\mathrm{f}}$ are the steam saturation temperature at pressure p_3 and the food product temperature respectively, $\dot{m}_{3,\mathrm{c}}$ the mass rate of steam condensation on the product and $\overline{\Lambda}_{3,\mathrm{w}}$ the corrected latent heat during condensation. The condensed water, once collected in the lower part of the processing tank and separated by a grid from the food to be processed, is discharged at the batch cycle completion.

The corrected heat transfer coefficient $\bar{h}_{3,\mathrm{w}}$ takes into account three aspects: (a) the presence of superheated steam and subcooled condensate, (b) the presence of air and (c) the arrangement layout of the food product inside the processing tank. More in detail:

(a) The presence of superheated steam during the pressurisation and subcooled condensate, due to the food product temperature lower than the condensation temperature of the steam at pressure p_3, leads to an increment of the heat transfer coefficient (Marto, 1998). To consider the sensible amount of energy transmitted between the steam and the food product, the corrected latent heat $\overline{\Lambda}_{3,\mathrm{w}}$ is

$$\overline{\Lambda}_{3,\mathrm{w}} = c_{\mathrm{p,shs}} \left(T_{3,\mathrm{shs}} - T_{3,\mathrm{sat}}\right) + \Lambda_{3,\mathrm{w}} + \frac{3}{8} c_{\mathrm{p,w}} \left(T_{3,\mathrm{sat}} - T_{3,\mathrm{f}}\right) \tag{12}$$

where $c_{\mathrm{p,shs}}$ is the specific heat of the superheated steam at constant pressure, $T_{3,\mathrm{shs}}$ is the superheated temperature of the steam equal to $T_{3,\mathrm{v}}$ when $T_{3,\mathrm{v}} > T_{3,\mathrm{sat}}$, $c_{\mathrm{p,w}}$ is the water film specific heat.

(b) The reduction of the heat transfer coefficient $h_{3,\mathrm{w}}$ due to the presence of air, which does not condensate, can be taken into account accordingly to (Lau et al., 2015; Rocca-Poliméni et al., 2011) by introducing the F_{a} coefficient

$$F_{\mathrm{a}} = -0.5\left[e^{\left(-47.7294 y_{\mathrm{a}}^{0.6246}\right)} + e^{\left(-2.8235 y_{\mathrm{a}}^{0.3533}\right)}\right] \tag{13}$$

where y_{a} is the ratio between the air mass and the total mass (air and steam).

(c) The food product arrangement into the processing tank, reducing the overall food surface involved in the heat exchange due to overlapping layers, can be taken into account with the corrective coefficient $n^{-0.25}$ (Rose et al., 1999; Boiling, Condensation, and Gas-Liquid Flow, 1987).

Based on the proposed considerations, the corrected heat transfer coefficient results

$$\bar{h}_{3,\mathrm{w}} = F_{\mathrm{a}} \frac{\alpha}{n^{-0.25}} \left[\frac{\rho_{3,\mathrm{w}}\left(\rho_{3,\mathrm{w}} - \rho_{3,\mathrm{sat}}\right) g \bar{\Lambda}_{3,\mathrm{w}} k_{3,\mathrm{w}}}{\mu_{3,\mathrm{w}}\left(T_{3,\mathrm{w}} - T_{3,\mathrm{f}}\right) L_{3,\mathrm{f}}}\right]^{0.25} \tag{14}$$

where $\rho_{3,\mathrm{w}}$ and $\rho_{3,\mathrm{sat}}$ are the densities of the water film and of the steam at saturation pressure p_3 respectively, $k_{3,\mathrm{w}}$ and $\mu_{3,\mathrm{w}}$ are the thermal conductivity and viscosity of the water film, g is the gravitational acceleration, $L_{3,\mathrm{f}}$ is the characteristic length of the food product defined as the ratio between the volume and the external surface, and α is a coefficient that depends on the geometry of the food product. The thermal properties $\rho_{3,\mathrm{w}}$, $k_{3,\mathrm{w}}$ and $\mu_{3,\mathrm{w}}$ have to be calculated taking into account the water film temperature $T_{3,\mathrm{w}}$, expressed as the mean temperature between the steam saturation temperature and the temperature of the food product.

3.3.3. Processing tank complete system of differential equations

By using $\bar{h}_{3,\mathrm{w}}$, $A_{3,\mathrm{f}}$, $T_{3,\mathrm{sat}}$, $T_{3,\mathrm{f}}$ and $\bar{\Lambda}_{3,\mathrm{w}}$, it is possible to calculate the heat transfer rate $\dot{Q}_{3,\mathrm{w}}$ in Eq. (11) and the steam condensation rate $\dot{m}_{3,\mathrm{c}}$. Besides the state variables $T_{3,\mathrm{v}}$ and p_3 (Eqs. (9) and (10)), vapour mass $m_{3,\mathrm{v}}$,

condensed liquid mass $m_{3,\mathrm{l}}$ and mean temperature of the food product $T_{3,\mathrm{f}}$ have to be studied.

The vapour mass $m_{3,\mathrm{v}}$ and condensed liquid mass $m_{3,\mathrm{l}}$ can be obtained by integrating over the time the steam flow rate $\dot{m}_{23,\mathrm{v}}$ and steam condensation rate $\dot{m}_{3,\mathrm{c}}$.

Hence, the dynamics of the processing tank state is described by the system of differential equations (SoDE)

$$\begin{cases} \dfrac{dT_{3,\mathrm{v}}}{dt} = \dfrac{\dot{m}_{23,\mathrm{v}}}{C_{\mathrm{I}}}\left(h_{2,\mathrm{v}} - C_{\mathrm{II}} + \dfrac{3am_{3,\mathrm{v}}}{2\left(V_{3,\mathrm{v}} - bm_{3,\mathrm{v}}\right)\sqrt{T_{3,\mathrm{v}}}}\right) - \dfrac{\left(\dot{Q}_{3,\mathrm{w}} - \dot{Q}_{3,\mathrm{e}}\right)}{C_{\mathrm{I}}} \\ \dfrac{dp_3}{dt} = C_{\mathrm{III}}\dfrac{dT_{3,\mathrm{v}}}{dt} + C_{\mathrm{IV}}\dfrac{V_{3,\mathrm{v}}}{m_{3,\mathrm{v}}^2}\dot{m}_{23,\mathrm{v}} \\ \dfrac{dm_{3,\mathrm{v}}}{dt} = \dot{m}_{23,\mathrm{v}} - \dot{m}_{3,\mathrm{c}} \\ \dfrac{dm_{3,\mathrm{l}}}{dt} = \dot{m}_{3,\mathrm{c}} \\ \dfrac{dT_{3,\mathrm{f}}}{dt} = \dfrac{\dot{m}_{23,\mathrm{v}}}{m_{3,\mathrm{f}}c_{\mathrm{p,f}}} \end{cases} \tag{15}$$

where the temperature of the food product $T_{3,\mathrm{f}}$ is obtained by using a lumped parameter model with the food product mass $m_{3,\mathrm{f}}$ and specific heat $c_{\mathrm{p,f}}$.

3.4. Accumulator-to-processing tank steam flow rate model

The processing tank is connected to the steam accumulator by a pipe of constant section S_{p} with an on-off valve ψ_2 that can intercept the steam flow rate $\dot{m}_{23,\mathrm{v}}$ (Fig. 1). When the valve ψ_2 is open, $\dot{m}_{23,\mathrm{v}}$ is not constant, since the pressure of the upstream and downstream interconnected tanks varies over time. A similar problem can be found in the case of gas vehicle reservoirs fuelling (Farzaneh-Gord and Deymi-Dashtebayaz et al., 2013; Winters et al., 2012; Farzaneh-Gord et al., 2008; Kountz).

In order to evaluate the evolution of $\dot{m}_{23,\mathrm{v}}$, the steam velocity w_{v} can be derived applying the energy conservation of steam between the steam accumulator (Section 2 in Fig. 1) and the pipe connection (section P in Fig. 1), by using the differential form of the first principle of thermodynamics

$$dq_{\mathrm{v}} = dl_{\mathrm{m}} + d(p_{\mathrm{v}}v_{\mathrm{v}}) + d\left(p_{\mathrm{v}}v_{\mathrm{v}} + \frac{w_{\mathrm{v}}^2}{2} + gz\right) \tag{16}$$

Neglecting the terms dq_{v}, dl_{m} and dgz (no significant potential energy variation), and by using the definition of enthalpy, the steam velocity value $w_{\mathrm{p,v}}$ in the connection pipe can be computed as

$$w_{\mathrm{p,v}} = \sqrt{2\left(h_{2,\mathrm{v}} + h_{\mathrm{p,v}}\right)} \tag{17}$$

where $h_{2,\mathrm{v}}$ and $h_{\mathrm{p,v}}$ are the steam enthalpy inside the steam accumulator and in the connection pipe. Considering Section 2 not close to the inlet of the connection pipe, as reported in Fig. 1, steam velocity in the steam accumulator can be neglected.
Using the corrected ideal gas EoS (Çengel and Boles)

$$pv = ZRT \tag{18}$$

the enthalpy can be written as

$$h_{\mathrm{v}} = c_{\mathrm{v}}T_{\mathrm{v}} + ZRT_{\mathrm{v}} = \frac{1}{(\gamma - 1)}\left(\gamma + \frac{1 - Z}{Z}\right)p_{\mathrm{v}}v_{\mathrm{v}} \tag{19}$$

where γ is the adiabatic coefficient of expansion. The value of the compressibility factor Z, equal to 0.93, was settled considering saturated steam at 8 bar pressure (Çengel and Boles). Substituting Eq. (19) in Eq. (17), the steam velocity can now be written as a function of the pressure and of the specific volume of steam in the accumulator and in the connection pipe as

$$w_{\mathrm{p,v}} = \sqrt{\frac{1}{(\gamma - 1)}\left(\gamma + \frac{1 - Z}{Z}\right)\left(p_{\mathrm{v}}v_{2,\mathrm{v}} - p_{\mathrm{p}}v_{\mathrm{p,v}}\right)} \tag{20}$$

where the specific volume and the pressure can be related considering the expansion of the steam from the accumulator to pipe being adiabatic.
By using Eq. (20) and considering an uniform flow in the connection pipe of constant section S_{p}, the steam flow rate $\dot{m}_{23,\mathrm{v}}$ can be written as

$$\dot{m}_{23,\mathrm{v}} = S_{\mathrm{p}}\sqrt{C_{\mathrm{V}}p_{\mathrm{p}}\rho_{2,\mathrm{v}}\left[\left(\frac{p_{\mathrm{p}}}{p_2}\right)^{2/\bar{\gamma}} - \left(\frac{p_{\mathrm{p}}}{p_2}\right)^{\bar{\gamma}+1/\bar{\gamma}}\right]} \tag{21}$$

where $\bar{\gamma}$ is the corrected adiabatic coefficient ($\bar{\gamma} = (\gamma - 1)Z + 1$) and the term C_{V} is equal to

$$C_{\mathrm{V}} = \frac{2}{(\gamma - 1)}\left(\gamma + \frac{1 - Z}{Z}\right)$$

When the ratio between p_{p} and p_2 is lower than the critical pressure ratio β_{cr}, expressed as

$$\beta_{\mathrm{cr}} = \frac{p_{\mathrm{p}}}{p_2} = \left(\frac{2}{\bar{\gamma} - 1}\right)^{\frac{\bar{\gamma}}{\bar{\gamma}-1}} \tag{22}$$

the steam flow rate $\dot{m}_{23,\mathrm{v}}$ is critical otherwise it is in subcritical condition. In the case of pressure ratio p_{p}/p_2 lower than β_{cr}, substituting Eq. (22) into Eq. (21), the critical steam flow rate $\dot{m}_{23,\mathrm{v}}$ can be written as function of the sole pressure p_2 as

$$\left(\frac{\dot{m}_{23,\mathrm{v}}}{S_{\mathrm{p}}}\right)_{\mathrm{cr}} = \sqrt{\frac{C_{\mathrm{V}} C_{\mathrm{VI}}}{2}(\bar{\gamma} - 1) p_2 \rho_{2,\mathrm{v}}} \tag{23}$$

where C_{VI} is equal to

$$C_{\mathrm{VI}} = \left(\frac{2}{\bar{\gamma} + 1}\right)^{\frac{\bar{\gamma}+1}{\bar{\gamma}-1}}$$

Thus, the steam flow rate $\dot{m}_{23,\mathrm{v}}$ can be defined as

$$\dot{m}_{23,\mathrm{v}} = \begin{cases} S_{\mathrm{p}} \sqrt{C_{\mathrm{V}} p_{\mathrm{p}} \rho_{2,\mathrm{v}} \left[\left(\frac{p_{\mathrm{p}}}{p_2}\right)^{2/\bar{\gamma}} - \left(\frac{p_{\mathrm{p}}}{p_2}\right)^{\bar{\gamma}+1/\bar{\gamma}}\right]} & \text{if } \frac{p_{\mathrm{p}}}{p_2} \geq \beta_{\mathrm{cr}} \\ S_{\mathrm{p}} \sqrt{\frac{C_{\mathrm{V}} C_{\mathrm{VI}}}{2}(\bar{\gamma} - 1) p_2 \rho_{2,\mathrm{v}}} & \text{if } \frac{p_{\mathrm{p}}}{p_2} < \beta_{\mathrm{cr}} \end{cases} \tag{24}$$

Computing the pressure losses in the pipe Δp_{p}, the pressure p_{p} at the pipe inlet can be derived by the pressure in the processing tank p_3, as

$$p_{\mathrm{p}} = p_3 + \Delta p_{\mathrm{p}}(t) = p_3 + \frac{1}{2} f \frac{L_{\mathrm{p}}}{D_{\mathrm{p}}} \frac{\dot{m}_{23,\mathrm{v}}^2}{\rho_{2,\mathrm{v}} S_{\mathrm{p}}^2} \tag{25}$$

where L_{p} and D_{p} are the pipe length and diameter of the pipe, f is the friction coefficient, calculated by using the Petukhov relation (Çengel and Boles).

3.5. Model implementation

The presented model has been implemented in Matlab® environment (2015b version). The final number of differential equations (DE), fully describing the dynamics of the considered plant system, results to be seven, organized as follow: 2 DE for the steam accumulator state variables (Eqs. (2) and (3)), 5 DE for the processing tank (Eq. (15)). A scheme of the relationship between the model variables is represented in Fig. 2. The developed modelling framework allows to obtain the temporal variation of the thermodynamic state of the steam accumulator and of the processing tank, to evaluate the steam flow rate between the steam accumulator and the processing tank as a function of pressure difference of the tanks and also to calculate the food mean temperature during the thermal process. The initial conditions of the modelled system at time t_0 are reported on top of the scheme, while the set of plant parameters, such as the volume of the steam accumulator, the connection pipe section, the food product heat exchange surface etc. have been omitted in the scheme.

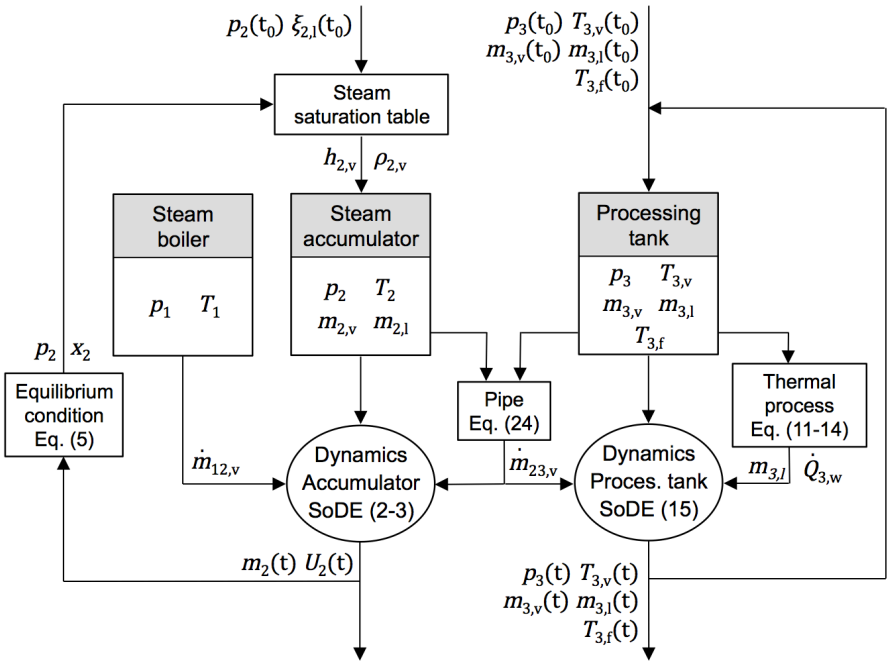

Fig. 2. Illustrative scheme of the developed model.

The developed modelling framework can be profitably used during the designing phase of steam accumulators. Indeed, the parameterised model

and initial plant conditions take into account all the typical sizing parameters and operative condition of these type of plants, allowing to find the proper configuration of boiler/steam accumulator/processing tank system.

3.5.1. Validation of the steam accumulator model

The results obtained by the proposed model were compared to data provided by (Stevanovic et al., 2015; Sun et al., 2015; Stevanovic et al., 2012), adopting the same parameters and initial conditions. Three validation tests were performed, where the accumulator charging and discharging processes have been simulated considering the three different steam flow rates reported in Fig. 3, from time instant $t_0 = 0$ and $t_f = 700$ s. The complete set of parameters and initial conditions, such as steam accumulator volume and pressure, inlet steam flow rate, etc., is collected in Table 1. More in detail, tests A and C were conducted considering the constant steam flow rate $\dot{m}_{12,v}$ and $\dot{m}_{23,v}$ respectively (Stevanovic et al., 2012), while the test B has been performed with a time-varying steam flow rate $\dot{m}_{12,v}$ (Stevanovic et al., 2015). Mass flow rate, pressure and temperature as a function of time have been shown in Fig. 3 for three different conditions.

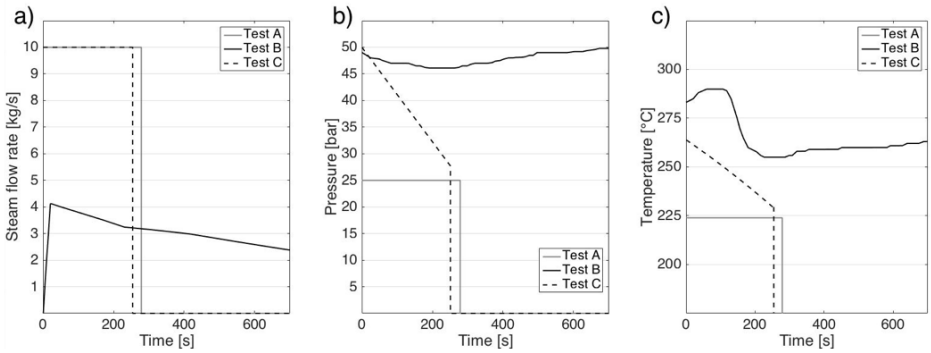

Fig. 3. Validation inputs: time evolution of mass flow rate (a), pressure (b) and temperature (c) of the steam flows.

Table 1. Accumulator parameters and initial conditions of validation tests.

	Test A	Test B	Test C
steam accumulator volume [m^3]	64	64	64
steam accumulator water filling ratio	0.5	0.5	0.5
steam accumulator initial pressure [bar]	25	-	50
initial state of valve ψ_1	open	closed	open
initial state of valve ψ_2	closed	open	closed

The simulation results, reported in Fig. 4, have been compared with the ones presented in (Stevanovic et al., 2012) and (Stevanovic et al., 2015), which have been reported in the same plot. The final steady state conditions and the times required to reach them are comparable. In addition, the accordance between the charging and discharging dynamics provided by the model and by the references has been quantified calculating ℓ_∞ and ℓ_2 norms based relative distances ε_∞ and ε_2 (Table 2) between the two functions $p_2(t)$ and $\hat{p}_2(t)$, the simulated time evolution of accumulator pressure and the reference one respectively. On the base of the obtained values for ε_∞ and ε_2, the developed steam accumulator model, based on the equilibrium conditions between vapour and liquid phases, can be considered adequately accurate to simulate different operating conditions.

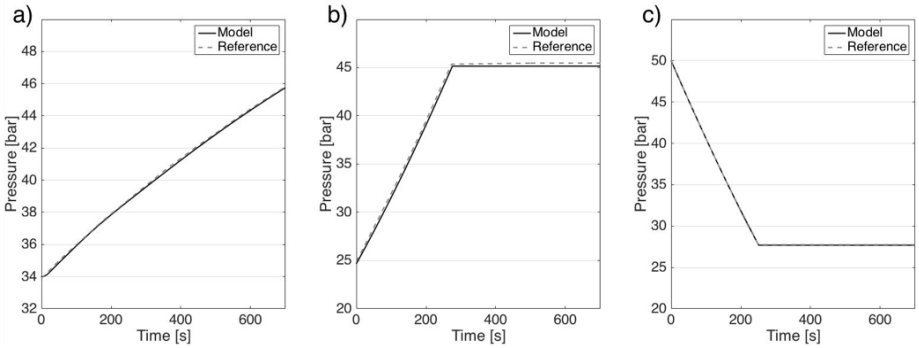

Fig. 4. Validation results: time evolution of the pressure p_2 in the steam accumulator, resulting from the validation test A (a), test B (b) and test C (c).

Table 2. ℓ_∞ and ℓ_2 norms based relative distances between model and reference dynamics.

	Test A	Test B	Test C
$\varepsilon_\infty = \frac{\lvert p_2(t^*) - \hat{p}_2(t^*)\rvert}{\lvert p_2(t^*)\rvert}$ with $t^* = arg \max_{t\in[t_0,t_f]} \lvert p_2(t) - \hat{p}_2(t)\rvert$	0.0035	0.0114	0.0038
$\varepsilon_2 = \frac{\int_{t_0}^{t_f}\left(p_2(t) - \hat{p}_2(t)\right)^2 dt}{\int_{t_0}^{t_f}\left(p_2(t)\right)^2 dt}$	$4.8013\cdot10^{-6}$	$7.7657\cdot10^{-5}$	$2.0237\cdot10^{-6}$

In (Stevanovic et al., 2012) and (Stevanovic et al., 2015), authors demonstrate how the approximations introduced by considering an equilibrium model translates in an estimation error in the prediction of the real maximum and minimum pressure values, with respect to the non-equilibrium model. However, the maximum detected differences between the non-equilibrium and the equilibrium model, for some operating conditions, result to be around 6%, and occur at valves opening/closure (Stevanovic et al., 2015). Moreover, the non-equilibrium model requires the measurement of a set of parameters on a physical existing plant, preventing its adoption in the sizing stage.

4. A case study: debacterisation of cocoa beans

The developed modelling framework was applied to the debacterisation process of cocoa beans, a typical batch thermal process in the food industry. The debacterisation process is preceded by a cleaning phase to remove waste materials and a roasting phase to intensify the aroma of the cocoa beans. In order to satisfy the quality and safety regulatory standards in food production, once the roasting process is completed, the bacterial charge of the cocoa beans has to be further reduced by a steam treatment. Therefore, the roasted cocoa beans, still at a temperature of about 90-100°C, are collected into a debacterisation tank. Once filled with the product and sealed, the processing tank is heated by steam insufflation, adopted to provide the heat for the debacterisation process.

Since a portion of the steam into the vessel, when it comes into contact with the cocoa beans surface, condenses forming a thin film of hot water,

particular technical solutions must be introduced in order to limit the condensed water to the quantity that does not compromise the food product. This can be achieved reducing as much as possible the time interval between the roasting and the debacterisation phases, in order to maintain a high beans surface temperature.
To further reduce condensation phenomena in the processing tank, it can be encased and pre-heated, so that the processing tank surface in contact with the food product is maintained at high temperature. In this case study, the considered processing tank layout allowed to assume thermal losses to the environment to be negligible.
After a fast pressurisation of the tank, which has a duration of 3-5 s, cocoa beans are mechanically mixed in order to assure the required uniformity to the debacterisation process. Usually, the mixing of cocoa beans is maintained throughout the entire duration of the process, which lasts about 5-10 min and finishes with the cocoa beans unloading procedure. Since the objective of this study is to model the pressurisation of the processing tank by the concurrent depressurisation of the steam accumulator, the mixing process of cocoa beans has not been considered in this model.

4.1. Simulation setup

At initial time t_0, the steam accumulator has been considered at a pressure $p_2(t_0)$ slightly lower than the maximum settled value $p_{2,\max}$, while the debacterisation tank is, initially, in equilibrium with the environment pressure. The temperature of the cocoa beans to be processed, when placed in the debacterisation tank, has been considered equal to 95 °C when the thermal treatment starts, after the valve ψ_2 opening. All the geometrical and physical properties of the plant components, together with their standard initial working conditions, are summarised in Table 3 organized by four groups: (1) the steam boiler; (2) the steam accumulator; (3) the debacterisation tank and (4) the connection pipe between the tanks (Biglia et al., 2015).

Table 3. Plant parameters and initial conditions of the case study simulation.

Steam boiler	
nominal steam flow rate $\dot{m}_{12,v}$ [kg s^{-1}]	0.097
nominal pressure $p_{1,v}$ [bar]	8
Steam accumulator	
volume V_2 [m^3]	4
external surface A_2 [m^2]	14.5
thermal losses coefficient K_2 [W m^{-2} K^{-1}]	0.7
water filling ratio $\xi_{2,l}$	0.5
initial pressure p_2 [bar]	7.98
maximum pressure $p_{2,max}$ [bar]	8
Debacterisation tank	
volume V_3 [m^3]	1
initial pressure p_3 [bar]	1
initial temperature $T_{3,v}$ [°C]	100
initial temperature of cocoa beans $T_{3,f}$ [°C]	95
mass of cocoa beans $m_{3,f}$ [kg]	50
number of cocoa beans N	26,000
Connection pipe	
length of the pipe L_p [m]	5
diameter of the pipe D_p [m]	0.05

In order to evaluate the heat exchange area $A_{3,f}$ between the water film and the food product, the shape of the cocoa beans was approximated to a geometrical shape made by a parallelepiped, the base of which has dimensions, a_{cb} and b_{cb} and a lateral area is considered rounded with a radius of $d_{cb}/2$, half of the parallelepiped height (Fig. 5). The dimensions a_{cb}, b_{cb} and d_{cb} have been considered equal to 2 cm, 1 cm and 0.4 cm respectively. Since in the debacterisation tank the cocoa beans are arranged in multiple layer, resulting in a vertical sequence of overlapping items, only the curved surface has been taken into account as heat exchange area between the water film and the cocoa beans. The resulting value of $A_{3,f}$ is used in Eq. (11) to evaluate $\dot{Q}_f$, while the coefficient α of Eq. (14), in the case of the cocoa beans geometry, is equal to 0.815. Moreover, the influence on the pressurisation process of the set of plant initial and working conditions, constituted by the accumulator maximum pressure

$p_{2,\max}$ and the filling ratio $\xi_{2,l}$, has been investigated. The effect of the plant components size (accumulator volume V_2 and connection pipe diameter D_p) in the process has been also analysed by simulations conducted with the developed modelling framework. All the simulations have been performed varying one parameter at time, while maintaining all the others settled to the values adopted during the initialization of the first case study (Table 3).

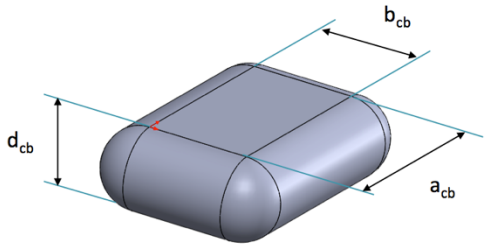

Fig. 5. Modelling representation of cocoa bean.

4.2. Simulation results

The model provides the time evolution of the thermodynamic state of the steam accumulator and of the debacterisation tank, the time evolution of the steam flow rate between the two tanks and the temperature evolution of the cocoa beans. Since the simulations confirmed the rapidity of the pressurisation process of the debacterisation tank, which mainly occurs in the first two seconds after the valve ψ_2 opening, the graphical output focuses on a short period of time, ten seconds long. During the first part of the simulation, the accumulator is charged by the steam flow $\dot{m}_{12,v}$, since $t_0 = 0$ s until $t_1 = 4.3$ s. At t_1, time instant when the accumulator pressure reaches the maximum settled value $p_{2,\max}$, the valve ψ_1 is closed (Fig. 6). During this phase, valve ψ_2 is still closed.

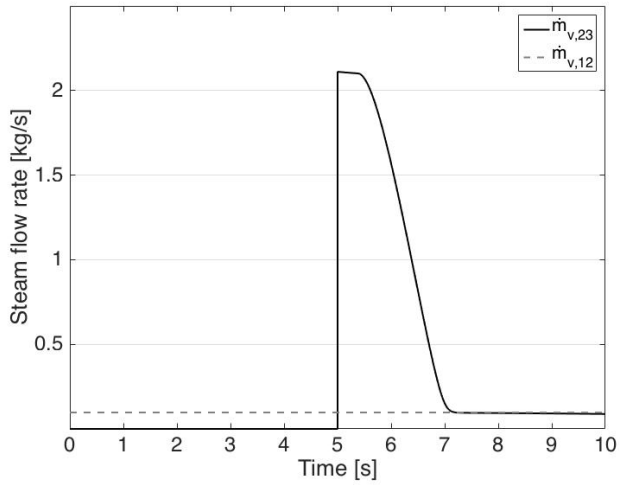

Fig. 6. Time evolution of the steam flow rate $\dot{m}_{12,\mathrm{v}}$, from the steam boiler to the accumulator, and of the steam flow rate $\dot{m}_{12,\mathrm{v}}$, from the accumulator to the debacterisation tank.

The pressurisation of the debacterisation tank starts at time instant $t_2 = 5$ s, when valve ψ_2 is opened and the steam flow rate $\dot{m}_{23,\mathrm{v}}$ is established. During the pressurisation, a rapid increment of the pressure p_3 in the debacterisation tank and a concurrent decrease of the pressure p_2 occur (Fig. 7), until an equilibrium between the pressure in the steam accumulator and the pressure in the processing tank is reached. It can be noted that, the equilibrium condition is reached in about two seconds, approximately at time instant $t_3 = 7$ s, when the pressure p_3 in the debacterisation tank reaches the maximum value, of about 7.75 bar. The steam flow rate $\dot{m}_{23,\mathrm{v}}$ between the two tanks is critical, reaching its maximum value of 2.11 kg s^{-1}, in the initial part of the pressurisation (time interval $t \in [5; 5.5]$ s), becoming sub-critical in the remaining part of the pressurisation (Fig. 6). It can be noted that, at the end of this process, the pressure $p_2(t_2)$ of the accumulator is slightly lower than the initial value $p_2(t_1)$, which was about 8 bar (Fig. 7). This behaviour can be caused by two main conditions: (1) the debacterisation tank volume V_3 is 4 times smaller than the steam accumulator one, V_2; (2) the pressurisation of the debacterisation tank is fast, therefore the steam mass exiting the steam accumulator, required to pressurise the processing tank, is small compared to the overall steam mass available in the accumulator. Even if the

maintenance of a high pressure value p_2 during the accumulator discharge is a valuable property, the simulation shows an oversizing of the installed accumulator, considering the sole debacterisation user process.

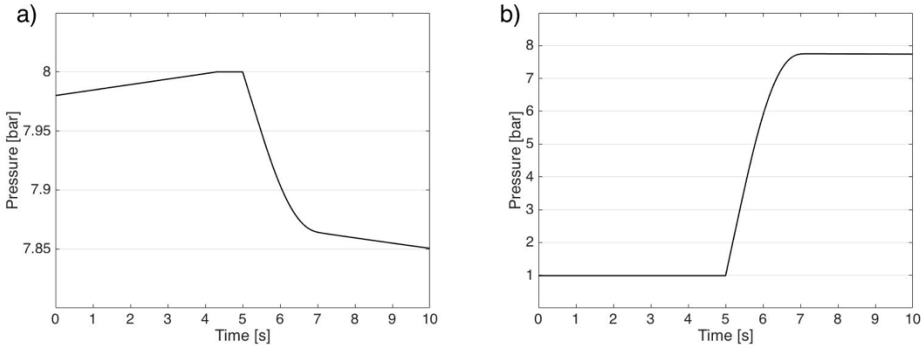

Fig. 7. Time evolution of the pressures p_2 in the accumulator (a) and p_3 in the debacterisation tank (b).

After the time instant t_3, when the pressurisation process of the debacterisation tank can be considered completed (the pressure p_3 becomes stationary, settled at the maximum value), a secondary phenomenon can be noticed. The accumulator discharge does not end after the pressurisation of the debacterisation tank: the steam flow rate $\dot{m}_{23,\mathrm{v}}(t)$, with $t \in [7;10]$ s, is settled to a low value, about 0.08 kg s^{-1}, without becoming completely null, and a remarkable change of the curve slope of the pressure p_2 denotes a slower dynamic in the system. This can be addressed to the slow condensing process of part of the steam $m_{3,\mathrm{v}}$ in the debacterisation tank, which leads to a gradual decrement of the pressure p_3 and, thus, to the consequent re-balancing steam flow $\dot{m}_{23,\mathrm{v}}$.

A contribution to the fast dynamic of the steam temperature $T_{3,\mathrm{v}}$ in the debacterisation tank (Fig. 8) is caused by the pressure work of the steam flow rate $\dot{m}_{23,\mathrm{v}}$, which contributes to the debacterisation tank internal energy increment. During the initial phase of the debacterisation process, the physical phenomenon of the pressurisation of the tank prevails over the heat exchange from the steam to the cocoa beans. After t_2, the steam flow rate $\dot{m}_{23,\mathrm{v}}$ decrement leads to a reduction of the heat provided to the processing tank from the accumulator, which becomes lesser than the one transferred to the cocoa beans: the steam temperature $T_{3,\mathrm{v}}$ in the debacterisation tank, thus, starts decreasing. At the end of the simulation,

the steam mass $m_{3,\mathrm{v}}$ in the debacterisation tank is about 3 kg while the final mass of condensed steam $m_{3,\mathrm{l}}$ on the cocoa beans surfaces results to be limited at about 0.2 kg, fulfilling the need of avoiding food product damages.

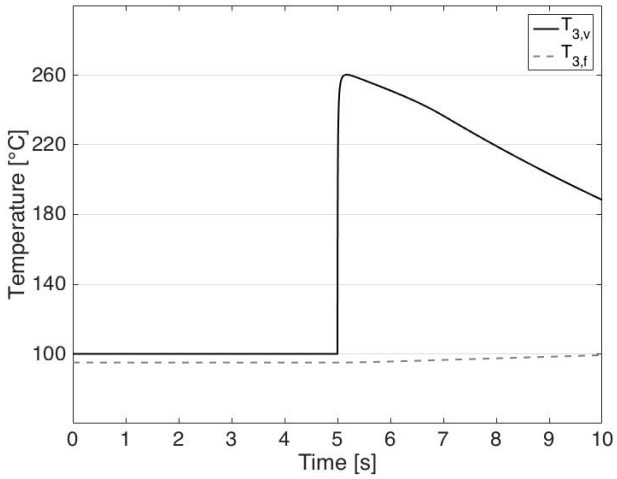

Fig. 8. Time evolution of the steam temperature $T_{3,\mathrm{v}}$ and of the cocoa beans temperature $T_{3,\mathrm{f}}$ in the debacterisation tank.

Further simulations have been carried out to investigate the effects of some operating conditions (e.g. maximum pressure of the steam accumulator) and of the sizing parameters (e.g. volume of the steam accumulator) on the dynamic evolution of the steam in the interconnected tanks. The most significant results of the simulations are reported in Figs. (9-14).

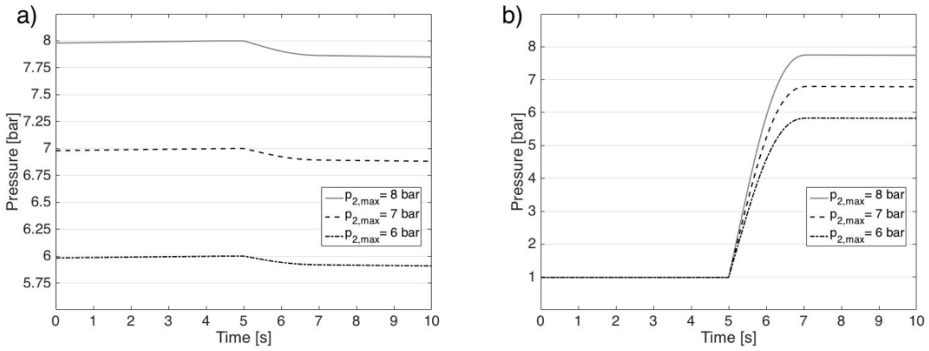

Fig. 9. Time evolution of pressures p_2 (a) and p_3 (b) during simulations with different values.

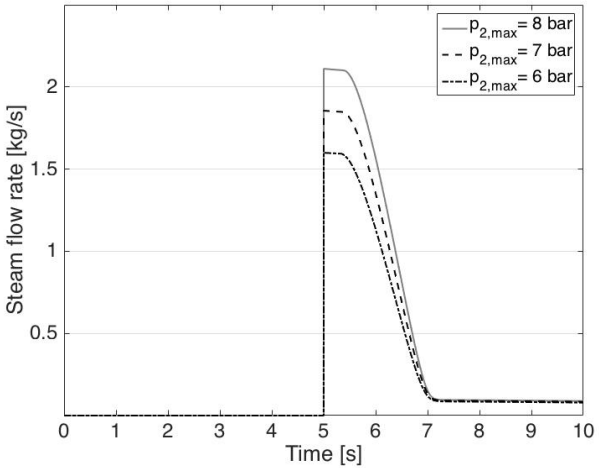

Fig. 10. Time evolution of steam flow rate $\dot{m}_{23,\mathrm{v}}$ during simulations with different $p_{2,\max}$ values.

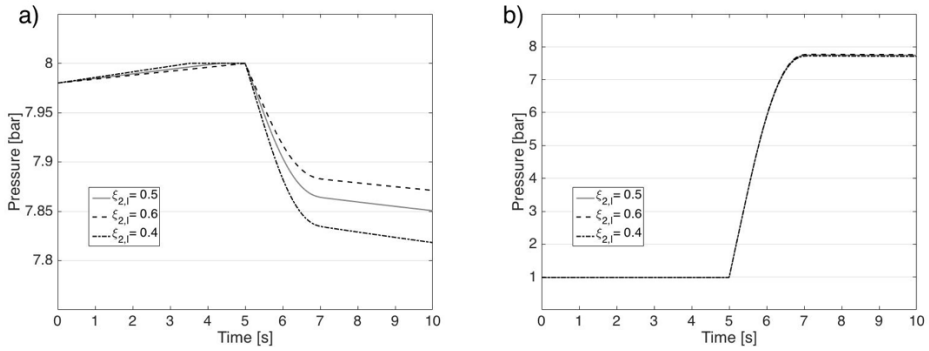

Fig. 11. Time evolution of steam pressures p_2 (a) and p_3 (b) during simulations with different $\xi_{2,\mathrm{l}}$ values.

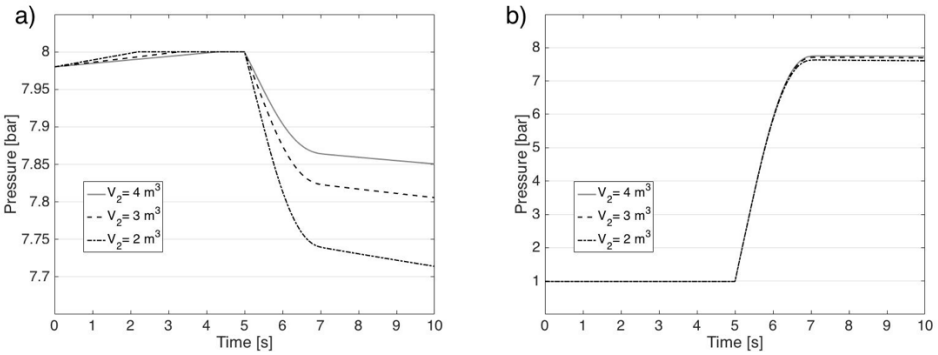

Fig. 12. Time evolution of steam pressures p_2 (a) and p_3 (b) during simulations with different V_2 values.

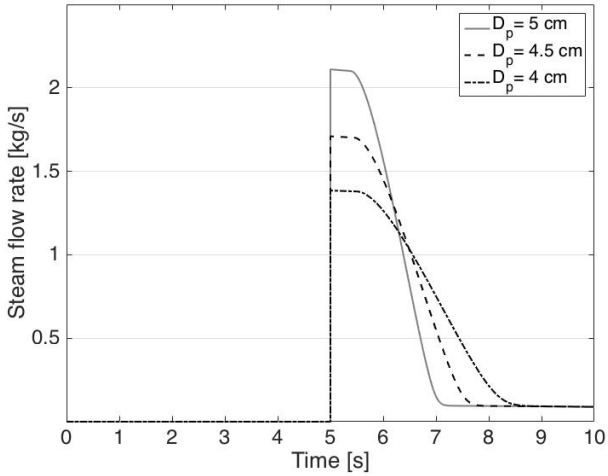

Fig. 13. Time evolution of steam flow rate $\dot{m}_{23,\mathrm{v}}$ during simulations with different D_{p} values.

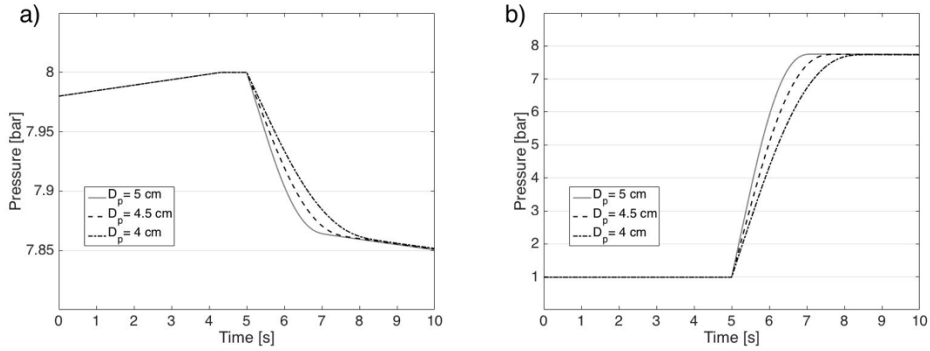

Fig. 14. Time evolution of steam pressures p_2 (a) and p_3 (b) during simulations with different D_{p} values.

Varying the maximum pressure of the accumulator, with values ranging from 8 to 6 bar, the evolution of the pressure in the steam accumulator and in the processing tank results to be modified as reported in Fig. 9. During the pressurisation of the processing tank, the pressure of the accumulator slightly decreases, reaching the steady state pressure values in around 2 s: 6.80 and 5.83 bar with $p_{2,\max}$ settled to 7 and 6 bar respectively. The effect on the steam flow rate $\dot{m}_{23,\mathrm{v}}$ of the pressure difference between the accumulator and the processing tank can be observed in Fig. 10 where, after the valve ψ_2 opening ($t_2 = 5$ s), the maximum value of the steam flow value decreases from 2.11 kg s^{-1} to 1.60 kg s^{-1} with the $p_{2,\max}$ decrement.

Acting on the filling ratio of the steam accumulator, a variation in the charging and discharging dynamic of the steam accumulator can be achieved. In particular, comparing the simulation results obtained with $\xi_{2,l}$ equal to 0.4 and 0.6 with those obtained with $\xi_{2,l} = 0.5$, a reduction of the charging process duration is observed in the case of filling ratio decrement (Fig. 11). Indeed, the mass of liquid to be heated up, in this case, is less and the energy required for the accumulator pressurisation is, thus, lower. Similarly, during the accumulator discharging process, a faster decrement of the pressure can be observed, because of the lower quantity of water (or energy) stored in the accumulator.

Steam plant sizing parameters have been also analysed. In particular, by considering steam accumulators with smaller volumes, during the charging process the maximum pressure $p_{2,\max}$ of 8 bar can be achieved in shorter times (Fig. 12). This behaviour is due to the small quantity of water to be heated up, which also affect the discharging phase. Indeed, after ψ_2 opening at time t_2, the user steam request lead to a faster depressurisation and to lower final pressure steady state in the accumulators with reduced volume (Fig. 12). It can be observed that, at the end of the simulation $t_4 = 10$ s, the final pressure in steam accumulator accounts for 7.81 and 7.71 bar with a steam accumulator volume of 3 and 2 m^3 respectively.

The effect to the steam flow rate of the pipe connection between the accumulator and the processing tank has been also investigated. In particular, by varying the section of the pipe, in the conducted simulations the maximum steam flow rate reduces from 2.11 kg s^{-1} to 1.38 kg s^{-1} (Fig. 13), considering pipe diameters values of 5, 4.5 and 4 cm. Even if the final steady state pressure in the two interconnected tanks results to be equal (Fig. 14), the pressure evolutions differ, being the time required to reach the equilibrium condition increased by the pipe diameter reduction.

5. Conclusions

In this paper, a model of a food processing plant, constituted by a boiler, a sliding pressure steam accumulator and a processing tank has been presented. The developed model, based on the mass and energy balances, also integrates the properties of the processed food in the last tank. The condensation and evaporation processes in the steam accumulator were

approximated with a succession of equilibrium state and the steam flow rate from this vessel to the processing pressurised tank was evaluated as a function of the pressure difference between the two tanks. The model has been also applied to a real system configuration for cocoa beans debacterisation; nevertheless, with limited appropriate changes, it can be profitably adapted to a wide set of different thermal processes of food industry employing sliding pressure steam accumulators to feed pressurised tanks.

Allowing to simulate the dynamics of a complete set of plant state variables, such as pressures, temperatures and flow rate/masses, during processes with different settings and initial conditions, the developed modelling framework has already proven its effectiveness in designing new processing plants. The sizing of the steam accumulator as well as the operative settings, such as the boiler steam supply pressure and flow rate, the initial water filling ratio of the accumulator etc., can be evaluated in advance for a wide range of plant configurations, allowing, for example, to properly size a system composed of steam boiler and steam accumulator when the steam demand profile of a user is known.

Acknowledgements

Authors would like to thank Prof. Bruno Panella, Prof. Mario Malandrone and Guido Gobino S.r.l. for their support.

References

Ahlgren RCE. Flash tanks for steam and boilers systems. *ASHRAE J* 33 (8) (1991) pp. 15-20.

ASHRAE. ASHRAE Systems and Equipment Handbook. ASHRAE, Atlanta, GA (2000).

Bai F, Xu C. Performance analysis of a two-stage thermal energy storage system using concrete and steam accumulator. *Appl Therm Eng* 31 (14–15) (2011) pp. 2764-2771.

Baldini A, Manfrida G, Tempesti D. Model of a solar collector/storage system for industrial thermal applications. *Int J Thermodyn* 12 (2009) pp. 83-88.

Berteli MN, Vitali AA, Berto Jr MI, Marsaioli A. Alternative venting in steam retorts – an approach to energy savings in thermal processing. *Chem Eng Process* 70 (2013) pp. 204-210.

Biglia A, Fabrizio E, Ferrara M, Gay P, Ricauda Aimonino D. Performance assessment of a multi-energy system for a food industry. *Energy Procedia* 82 (2015) pp. 540-545.

Bowers LJ, Dikeman ME, Murray L, Stroda SL. Cooked yields, color, tenderness, and sensory traits of beef roasts cooked in an oven with steam generation versus a commercial convection oven to different endpoint temperatures. *Meat Sci* 92 (2012) pp. 97-106.

Cao M, Cao J. Optimal design of thermal-energy stores for boiler plants. *Appl Energy* 83 (1) (2006) pp. 55-68.

Çengel YA, Boles MA, Thermodynamics: An Engineering Approach, fifth ed., McGraw-Hill.

Cenkowski S, Pronyk C, Zmidzinska D, Muir WE. Decontamination of food products with superheated steam. *J Food Eng* 83 (2007) pp. 68-75.

Comodi G, Carducci F, Nagarajan B, Romagnoli A. Application of cold thermal energy storage (CTES) for building demand management in hot climates. *Appl Therm Eng* 103 (2016) pp. 1186-1195.

Holman JP. Condensation and Boiling Heat Transfer. 10th ed., McGraw Hill, New York (2010) pp. 487–520.

Farzaneh-Gord M, Hashemi S, Farzaneh-Kord A. Thermodynamics analysis of cascade reservoirs filling process of natural gas vehicle cylinders. *World Appl Sci J* 5 (2008) pp. 143-149.

Farzaneh-Gord M, Deymi-Dashtebayaz M. Optimizing natural gas fueling station reservoirs pressure based on ideal gas model. *Pol J Chem Technol* 15 (1) (2013) pp. 88-96.

Grange B, Dalet C, Falcoz Q, Ferrière A, Flamant G. Impact of thermal energy storage integration on the performance of a hybrid solar gas-turbine power plant. *Appl Therm Eng* 105 (2016) pp. 266-275.

Huang S-R, Yang JI, Lee Y-C. Interactions of heat and mass transfer in steam reheating of starchy foods. *J Food Eng* 114 (2013) pp. 174-182.

Karimi F. Applications of superheated steam for drying of food products. *Int Agrophys* 24 (2010) pp. 195-204.

Kittiworrawatt S, Devahastin S. Improvement of a mathematical model for low-pressure superheated steam drying of a biomaterial. *Chem Eng Sci* 64 (2009) pp. 2644-2650.

Kountz KJ. Modelling the fast fill process in natural gas vehicle storage cylinders, Institute of Gas Technology Chicago, IL 60632.

Industrial Steam Systems Optimization (SSO) Experts Training. United Nations Industrial Development Organization (2012) October.

James C, Göksoy EO, Corry JEL, James SJ. Surface pasteurisation of poultry meat using steam at atmospheric pressure. *J Food Eng* 45 (2000) pp. 111-117.

Kishor Johar D, Sharma D, Lal Soni S, Gupta PK, Goyal R. Experimental investigation on latent heat thermal energy storage system for stationary C.I. engine exhaust. *Appl Therm Eng* 104 (2016) pp. 64-73.

Lau WL, Reizes J, Timchenko V, Kara S, Kornfeld B. Numerical modeling of an industrial steam-air sterilization process with experimental validation. *Appl Therm Eng* 75 (2015) pp. 122-134.

Li Q, Zhou J, Chang Q, Xing W. Effects of geometry and inconstant mass flow rate on temperatures within a pressurized hydrogen cylinder during refueling. *Int J Hydrogen Energy* 37 (2012) pp. 6043-6052.

Li C, Peng Y, Dong J. Prediction of compressibility factor for gas condensate under a wide range of pressure conditions based on a three-parameter cubic equation of state. *J Nat Gas Sci Eng* 20 (2014) pp. 380-395.

Liu YL, Zhao YZ, Zhao L, Li X, Chen HG, Zhang LF, et al. Experimental studies on temperature rise within a hydrogen cylinder during refueling. *Int J Hydrogen Energy* 35 (2010) pp. 2627-2632.

Marto PJ, Condensation, in: W.M. Rohsenow, Harnett JP, Cho YI (Eds.), Handbook of Heat Transfer, third ed., McGrawhill (1998), Chapter 14.

Mora B, Curti E, Vittadini E, Barbati D. Effect of different air/steam convection cooking methods on turkey breast meat: physical characterization, water status and sensory properties. *Meat Sci* 88 (2011) pp. 489-497.

Moran MJ, Shapiro HN. Fundamentals of Engineering Thermodynamics. John Wiley & Sons (fifth ed.), Chichester (2006).

Palacio SN, Valentine KF, Wong M, Zhang KM. Reducing power system costs with thermal energy storage. *Appl Energy* 129 (2014) pp. 228-237.

Pirasaci T, Yogi Goswami D. Influence of design on performance of latent heat storage system for a direct steam generation power plant. *Appl Energy* 162 (2016) pp. 644-652.

Redlich O, Kwong JNS. On the thermodynamics of solutions. *Chem Rev* 44 (1949) pp. 233-244.

Rocca-Poliméni R, Flick D, Vasseur J. A model of heat and mass transfer inside a pressure cooker. *J Food Eng* 107 (2011) pp. 393-404.

Rose J, Uehara H, Koyama S, Fujii T, Film condensation, in: Kandlikar SG, Shoji M, Dhir VK (Eds.), Handbook of Phase Change: Boiling and Condensation, Taylor & Francis (1999) pp. 523–80.

Ruffio E, Saury D, Petit D. Thermodynamic analysis of hydrogen tank filling. Effects of heat losses and filling rate optimization. *Int J Hydrogen Energy* 39 (2014) pp. 12701-12714.

Sa-adchom P, Swasdisevi T, Nathakaranakule A, Soponronnarit S. Mathematical model of pork slice drying using superheated steam. *J Food Eng* 104 (2011) pp. 499-507.

Sakin-Yilmazer M, Kemerli T, Isleroglu H, Ozdestan O, Guven G, Uren A, et al. Baking kinetics of muffins in convection and steam assisted hybrid ovens. *J Food Eng* 119 (2013) pp. 483-489.

Schreiber H, Graf S, Lanzerath F, Bardow A. Adsorption thermal energy storage for cogeneration in industrial batch processes: experiment, dynamic modelling and system analysis. *Appl Therm Eng* 89 (2015) pp. 485-493.

Singh AP, Singh A, Ramaswamy HS. Modification of a static steam retort for evaluating heat transfer under reciprocation agitation thermal processing. *J Food Eng* 153 (2015) pp. 63-72.

Soponronnarit S, Prachayawarakorn S, Rordprapat W, Nathakaranakule A, Tia W. A superheated-steam fluidized-bed dryer for parboiled rice: testing of a pilot-scale and mathematical model development. *Dry Technol* 24 (2006) pp. 1457-1467.

Steambook, Steam Applications, Fischer.

Steinmann WD, Eck M. Buffer storage for direct steam generation. *Sol Energy* 80 (10) (2006) pp. 1277-1282.

Stevanovic VD, Maslovaric B, Prica S. Dynamics of steam accumulation. *Appl Therm Eng* 37 (2012) pp. 73-79.

Stevanovic VD, Petrovic MM, Milivojevic S, Maslovaric B. Prediction and control of steam accumulation. *Heat Transfer Eng* 36 (5) (2015) pp. 498-510.

Striednig M, Brandstätter S, Sartory M, Klell M. Thermodynamic real gas analysis of a tank filling process. *Int J Hydrogen Energy* 39 (2014) pp. 8495-8509.

Sun B, Guo J, Lei Y, Yang L, Li Y, Zhang G. Simulation and verification of a non-equilibrium thermodynamic model for a steam catapults steam accumulator. *Int J Heat Mass Trans* 85 (2015) pp. 88-97.

Sun L, Doyle S, Smith R. Understanding steam costs for energy conversation projects. *Appl Energy* 161 (2016) pp. 647-655.

Tam KW, Leung CW, Probert SD. Energy management in a dairy-products plant. *Appl Energy* 32 (2) (1989) pp. 83-100.

The First Law of Thermodynamics, in: Borgnakke C, Sonntag RE (Eds.), Fundamentals of Thermodynamics. seventh ed., John Wiley & Sons (2009) pp. 180–237.

Wagner W, Kretzschmar HJ. International steam tables Properties of Water and Steam Based on the Industrial Formulation IAPWS-IF97 (second ed.), Springer, Berlin (2008).

Walker ME, Zhen Lv, Masanet E. Industrial steam systems and the energy-water nexus. *Environ Sci Technol* 47 (2013) pp. 13060-13067.

Winters WS, Evans GH, Rice SF, Greif R. An experimental and theoretical study of heat and mass transfer during the venting of gas from pressure vessels. *Int J Heat Mass Trans* 55 (2012) pp. 8-18.

Xu ES, Wang ZF, Wei G. Dynamic simulation of thermal energy storage system of Badaling 1 MW solar power tower plant. *Renew Energy* 39 (2012), pp. 455-462.

Zzaman W, Bhat R, Yang TA. Application of response surface methodology to optimize roasting conditions in Cocoa Beans subjected to superheated steam treatments in relevance to antioxidant compounds and activities. *Dry Technol* 32 (2014) pp. 1104-1111.

5. Innovative food processing plant

5.1. Second paper

International Journal of Refrigeration 81 (2017) pp. 82-95

DOI: 10.1016/j.ijrefrig.2017.05.022

Reversed Brayton cycle for food freezing at very low temperatures: Energy performance and optimisation

Alessandro Biglia [a], Lorenzo Comba [b,*], Enrico Fabrizio [b], Paolo Gay [a], Achille Mannini [c], Adriano Mussinatto [d], Davide Ricauda Aimonino [a]

[a] DiSAFA – Universitá degli Studi di Torino, 2 Largo Paolo Braccini, Grugliasco (TO) 10095, Italy

[b] DENERG – Politecnico di Torino, 24 Corso Duca degli Abruzzi, Torino 10129, Italy

[c] Dyria Sistemi Srl – 57 Via Veglia, Torino 10136, Italy

[d] Criotec Impianti Srl – 32/A Via Francesco Parigi, Chivasso (TO) 10034, Italy

* Corresponding author: Tel. +39 011 090 4519
e-mail address: lorenzo.comba@polito.it

Abstract

Freezing is a valuable method to increase food shelf life and to ensure high quality standards during long-term storage. Additional benefits to frozen food quality can be achieved by freezing at very low temperatures (« -50 °C): small ice crystals formation during fast freezing reduces food cell wall rupture, preventing water and texture loss during thawing.

This paper presents the design of an innovative food freezing system operating at very low temperatures, based on a modified reversed Brayton cycle (rB cycle). The plant is composed of two interconnected sub-systems: a primary thermodynamic closed loop, operated by an rB cycle, and a secondary airflow loop which is devoted to food freezing by batch process. Relevant features of the designed rB cycle rely on the adopted environmentally safe working fluid, the optimised thermodynamics working conditions and the innovative cycle layout.

A modelling framework for the system was developed to identify and design efficient operative settings for the plant components (turbo-machineries, heat exchangers, etc.) and to assess, via sensitivity analysis, the influence of the main design parameters on the global energy performance. The proposed system configuration, designed to maximise the Coefficient of Performance (CoP) value of the plant, was determined by means of nonlinear multivariable optimisation. In addition, the energy performance of the system can be increased by recovering waste heat available from the rB cycle.

Keywords: Food industry, Food freezing, Reversed Brayton cycle, Low temperatures, Energy performance, Optimisation.

Nomenclature

Plant component	
BC	bootstrap compressor
BU	bootstrap unit
CHX	cold heat exchanger
HX1	first heat exchanger
HX2	second heat exchanger
M	electric motor
PC	primary compressor
RHX	regenerative heat exchanger
TB	turbine
Component 'x' parameters	
l_x	work per mass unit [J kg^{-1}]
q_x	heat per mass unit [J kg^{-1}]
$\dot{Q}_x$	thermal capacity [W]
$\dot{W}_x$	mechanical power [W]
β_x	pressure ratio
Δp_x	pressure drop [Pa]
ε_x	heat exchanger effectiveness
ζ_x	electric efficiency
η_x	isentropic efficiency
Other symbols	
f_{BU}	bootstrap unit mechanical losses
$\dot{m}_N$	nitrogen mass flow rate [kg s^{-1}]

p_i	pressure at i-th thermodynamic state [Pa]
T_i	temperature at i-th thermodynamic state [°C]
CoP	coefficient of performance

1. Introduction

Freezing is a valuable method to increase food shelf life, to preserve organoleptic and nutritional food properties, and to ensure high quality standards during long-term storage (Soyer et al., 2010). Contrary to other methods of food storage, such as drying (Tian et al., 2016), vacuum packaging (Li et al., 2014), salting (Lerfall et al., 2016), and smoking (Ledesma et al., 2016), freezing technology can be applied to almost any kind of food category.

In the freezing process, a cooling fluid (medium) removes sensible and latent heat from the food by convection through its surface while thermal conduction occurs at its interior (Castro-Giráldez et al., 2014). Usually, cold air is used as the medium in food industry freezing systems since it is not expensive and corrosive to plant components, it is environmentally friendly and does not contaminate foods (James and James, 2002): these systems are known as air blast freezers (Dempsey and Bansal, 2012). There are two categories of air blast freezers: batch freezers and continuous freezers. In batch freezing, the food is loaded into an insulated closed room and the process runs until the product is completely frozen. After that, the freezing room compartment is unloaded and the process can be run for other unfrozen food lots (batch process). Inside the room, cold air circulation is forced by fans during the freezing process. This kind of system is usually adopted to freeze medium to large sized products, such as meat, fish, bread, and even packaged foods. In continuous freezing, food products, usually arranged in a single layer, are moved through a freezing tunnel by a conveyor belt. This is a suitable process for freezing small foods such as legumes, prawns, slices of vegetables, etc. Since the food flow is continuous, air deflectors and/or movable shutters, properly placed at the inlet and outlet of the tunnel, have to be adopted in order to limit warm air infiltrations. Conveyor speed and tunnel length depend on the freezing time required by the kind of food to be processed.

Freezing time is a relevant parameter as it deeply affects the quality of the final product (Kim et al., 2015). Quick-freezing is preferred because water contained in the food is turned into minute ice crystals (Kaale et al., 2011). If the freezing process is too slow, the ice crystals tend to agglomerate and to grow in size, causing mechanical damage to food cell membranes. This unfavourable phenomenon results in texture and food nutrients being lost after thawing. Freezing time mainly depends on the following factors (ASHRAE, 2010; Huan et al., 2003; Perussello et al., 2011): (1) the chemical composition and shape of the food; (2) the initial and final temperatures of the food and (3) the temperature and velocity of the medium.

A food core temperature of about -18 °C, which is recommended for frozen products, has to be reached in the shortest possible time. A reduction of the freezing time can be achieved by modifying medium temperature and/or velocity (Biglia et al., 2016), properties that deeply influence heat transfer between the product and the medium itself.

In the food industry, air blast systems typically adopt cold air, with temperatures ranging between -20 and -40 °C and velocities from 1 to 6 $m \cdot s^{-1}$. Vapour compression chillers are normally used to reduce air temperature until the desired design value. The Coefficient of Performance (CoP) of these systems depends on the temperature lift between the evaporator and the condenser of the chiller. Considering that the standard working temperature of a chiller for food freezing is usually within the range [-50, -30] °C in the evaporator and [20, 40] °C in the condenser, the resulting temperature lift leads to a high-pressure ratio in the compressor, which can barely be obtained with a single compression stage. A valuable solution consists in performing the compression in two different stages (Llopis et al., 2015). Even if this technical feature allows the system's efficiency to be increased, it is very difficult to obtain high CoP values. Alternatively, cascade refrigeration systems (Dopazo and Fernández-Seara, 2012), which use two different refrigeration circuits interconnected with a heat exchanger, can be adopted to reach low evaporator temperatures. Their installation and maintenance are, thus, more complex (Foster et al., 2011) than the one required for a single stage chiller. For

these reasons, producing air significantly colder than -30 °C by using vapour compression chillers is complex and expensive.

Another possibility to enhance heat transfer, in order to bypass the difficulty of lowering the medium temperature, is to increase air velocity. Two different air blast freezer technologies, with the air at velocities higher than 20 $m \cdot s^{-1}$ (Dempsey and Bansal, 2012), were developed: the fluidised bed (Di Matteo et al., 2003; Reynoso and Calvelo, 1985) and the impingement (Salvadori and Mascheroni, 2002; Kaale et al., 2011). In these systems, the adopted air temperature is usually about -20 °C, since a sufficient heat transfer coefficient between food and air is guaranteed by the high medium velocity. In the fluidised bed, the product is moved through a freezing tunnel on a conveyor grid by an upward and sideways injection of cold air, making the product float and tumble. This technology is used to freeze small-sized food items, such as peas, blueberries, etc. In the impingement technology, cold air is injected with nozzles directly in proximity of the product surface, ensuring a very high heat exchange between the air and the product itself. Although a quick-freezing time is obtained, this technology can only be adopted to process a limited set of foods characterized by small thickness, such as peas, French fries, fruit slices etc. Indeed, large products, characterized by a thickness greater than 25 mm (Dempsey and Bansal, 2012), could be damaged by the freezer-burn phenomena on the external surface.

Alternatively, a liquid medium (e.g. $CaCl_2$ or $C_2H_6O_2$ solutions, CO_2, etc.) may be used in food freezing. An advantage of this solution is the enhanced heat transfer, which in the case of liquids is 10 to 20 times higher than the one obtained with air (Galetto et al., 2010; Islam et al., 2014; Xu et al., 2016).

Another solution is based on liquid nitrogen evaporation systems, in which the food is frozen by a mixture of air and nitrogen. The compressed liquid nitrogen is injected through nozzles in batch or tunnel freezers (Awonorin, 1997; Shaikh and Prabhu, 2007; Gazda, 2013) where it rapidly evaporates at ambient pressure, absorbing a large amount of heat from the food. These systems are operated with an open cycle as the refrigerant cannot be recovered at the end of the freezing process (Foster et al., 2011). Therefore,

liquid nitrogen systems are characterised by high running costs due to the onerous supplying chain of the refrigerant.

Low temperatures for freezing purposes can also be achieved by means of a reversed Brayton cycle (rB cycle) (Chang et al., 2009; Streit and Razani, 2013; Giannetti and Milazzo, 2014). The rB cycle's main components are the compressor, the turbine, and the heat exchanger. A relevant characteristic of the rB cycle, compared to the direct one, is the different set of working fluid temperatures in the turbo-machineries: e.g. in the rB cycle, the turbine is designed to operate at very low temperatures, even below -100 °C, while in the direct one, the turbine is designed to receive very hot gases at the inlet (about 1200 °C in power plant stations and 2000 °C in air craft engines).

Nowadays, the application of the rB cycle is still limited to a few specific sectors, mainly in the temperature range [0, 10] °C. This is the case, for example, of air conditioning and cabin pressurisation of airplanes and high-speed trains, and of air cycle heat pumps. In these applications, the advantages of a cooling system based on the rB cycle are reliability, the reduced dimensions and weight of plant components, and the safety level given by the adoption of air as the working fluid (Rogers, 1994) since it is non toxic, non flammable and with null ozone depletion and global warming potential. The design and performance analysis of aircycle refrigeration systems conducted by Spence et al. (2004, 2005) confirmed the profitable application of this system to road transport air conditioning. Other applications of rB cycles, over 0 °C, concerned air conditioning on ships and for supermarket facilities (Elsayed et al., 2006; Hou et al., 2008). The optimal conditions and different layouts of regenerated air cycle heat pumps were analysed by several authors (see e.g. Bi et al., 2008, 2009, 2012; Ahmadi et al., 2016; Li et al., 2017).

For freezing applications, an open rB cycle was studied by Hou and Zhang (2009), but cold air temperature was limited to -55 °C. Foster et al. (2011) developed a first closed air cycle cooling and heating prototype able to reach working fluid temperature (air) even lower than -100 °C at the outlet of the turbine and at the same time recovering large quantities of heat at a temperature higher than 150 °C at the compression stage outlet. A

compressor-turbine unit, also named bootstrap unit, developed for aircraft air conditioning was used.

The objective of this work is to design a new system based on an innovative modified rB cycle configuration, able to produce cooling energy at a very low temperature (below -110 °C) with an improved efficiency level. Indeed, facing the limitations of previous published plant concepts, the proposed system is characterised by an enhanced efficiency of the thermodynamic cycle. Together with the description of the design features, a performance evaluation of the proposed freezing plant is hereby presented. With this aim, a numerical model of the system was developed (1) to investigate the performance of the plant at steady-state conditions; (2) to identify which components affect the performance of the plant the most and (3) to optimise the overall thermodynamic cycle (Ahmadi et al., 2014; Ahmadi and Ahmadi, 2016). The proposed plant scheme turns out to be an effective technological alternative to liquid nitrogen freezing plants in very-low temperature freezing processes.

The paper is structured as follows. Section 2 describes the structure of the reversed Brayton cycle, which is the basis of the new thermodynamic cycle proposed in Section 3. Section 4 describes the modelling framework of the designed modified rB cycle, which was adopted to perform the sensitive analysis presented in Section 5. The energy performance optimisation and the results are discussed in Section 6, while the conclusions are reported in Section 7.

2. Introduction to the reversed Brayton cycle

In a closed reversed Brayton cycle (Fig. 1a), the gaseous working fluid, from the initial condition of pressure p_{1a} and temperature T_{1a}, is compressed to pressure p_{2a} by a compressor (PC), which increases its temperature to T_{2a}. Then, it is involved in a cooling process through a heat exchanger (HX1) where it releases heat q_{HX1} to a warm region. Once cooled at temperature T_{3a}, the working fluid is expanded through a turbine (TB) until it reaches pressure p_{1a} and minimum cycle temperature $T_{min,a}$, low enough to remove heat from the cold region. Indeed, downstream from the turbine and before re-entering the compressor, the working fluid passes through a cold heat exchanger (CHX) where it is heated up by absorbing

heat from the region that has to be cooled. The heat q_{CL} received by the working fluid in the CHX represents the *cooling load* of the thermodynamic cycle. Moreover, the working fluid does not change phase during the thermodynamic transformations. By installing the compressor and the turbine on the same shaft, the mechanical work l_{CP} required by the compressor can be partially supplied by the mechanical work of turbine l_{TB}. The resulting mechanical unbalance between driving and resistance forces has to be compensated by an external mechanical power source, such as an electric motor (M). The Gibbs diagram of the cycle is presented in Fig. 1b.

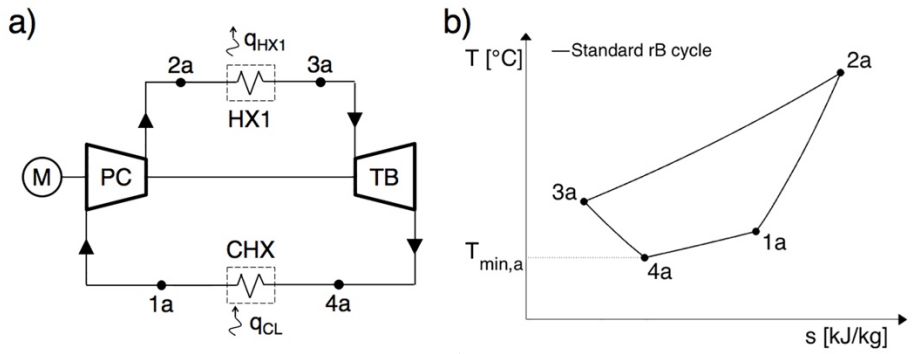

Fig. 1. Standard rB cycle scheme (a) and Gibbs diagram (b). The working fluid, sequentially, undergoes a compression (1a-2a), a cooling phase (2a-3a), an expansion process (3a-4a) and, finally, once the lowest temperature of the cycle $T_{\mathrm{min,a}}$ is reached, the fluid is heated removing heat q_{CL} from the cooled volume (4a-1a).

Applicative examples of the rB cycle are mainly referred to as open cycle, where the working fluid is not recovered after the CHX, having been expelled out of the cycle. In aircraft cabin refrigeration and pressurisation, the compressed air can be directly bled from the aircraft engine compressor, avoiding the installation of a dedicated compressor. The bled pressurised air is cooled in a heat exchanger and then, after being expanded by a turbine, is injected in the cabin.

The rB cycle's Coefficient of Performance, assessed by comparing the heat removed from the cold heat exchanger and the work supplied by the electric motor, can be defined as

$$CoP = \frac{h_{1a} - h_{4a}}{\left((h_{2a} - h_{1a}) - (h_{3a} - h_{4a})\right)\zeta_M^{-1}} \quad (1)$$

where h is the specific enthalpy of the working fluid and ζ_M the efficiency of the electric motor.

Temperature value $T_{min,a}$, much lower than 0 °C, cannot be easily obtained in the plant scheme of Fig. 1, making that configuration unsuitable for freezing processes. A reduction of the temperature at the turbine outlet can be obtained, for example, by reducing the inlet turbine temperature. This task can be performed by adopting a regenerative heat exchanger (RHX) installed to intercept the working fluid exiting the HX1 at one side of the heat exchanger and exiting the CHX at the other side of the heat exchanger (Fig. 2). This configuration allows lower temperature values $T_{min,b}$ to be achieved after the expansion, making the cooling load q_{CL} effective at lower temperatures.

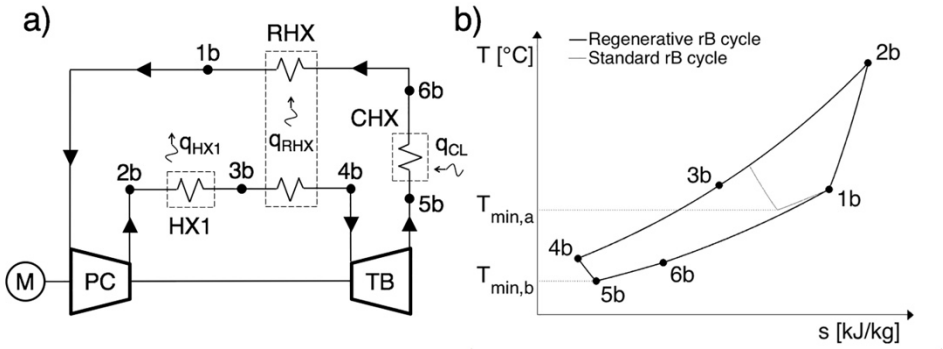

Fig. 2. Regenerative rB cycle scheme (a) and Gibbs diagram (b).

Compared to the cycle represented in Fig. 1, this configuration has a lower CoP, considering all the unchanged cycle parameters (e.g. the same compressor ratio, the same isentropic efficiency of the turbo machineries, the same inlet compressors pressure and temperature and the same q_{CL}). Even if the efficiency of the thermodynamic cycle of Fig. 2 is reduced, it should be noted that the introduction of an RHX is essential to achieve the required low temperature at the turbine outlet. Working at lower temperatures, the mechanical unbalance between turbine and compressor increases, leading to an unfavourable increment of the required external mechanical power.

3. Modified reversed Brayton cycle

To comply with the discussed technical features of standard rB cycles and to overcome the limitations of plant configurations presented in literature (see Section 1.), an innovative modified rB cycle has been designed. The proposed cycle involves new features regarding the scheme configuration (Fig. 3), the temperature and pressure levels of the primary circuit, the adopted working fluid and, finally, the food freezing process technique.

The proposed freezing plant can be outlined into two sub-systems: (1) a primary closed system, operated by an rB cycle, which cools a gaseous working fluid at very low temperatures and (2) a secondary system, where food is processed by batch in a freezer room by controlled recirculation of cold air. A cold heat exchanger (CHX), where the medium fluid (air) of the secondary loop is cooled by the working fluid of the primary closed loop, connects the two systems. The modified rB cycle has been designed to ensure a mean operative air temperature of the batch freezer of about -80 °C.

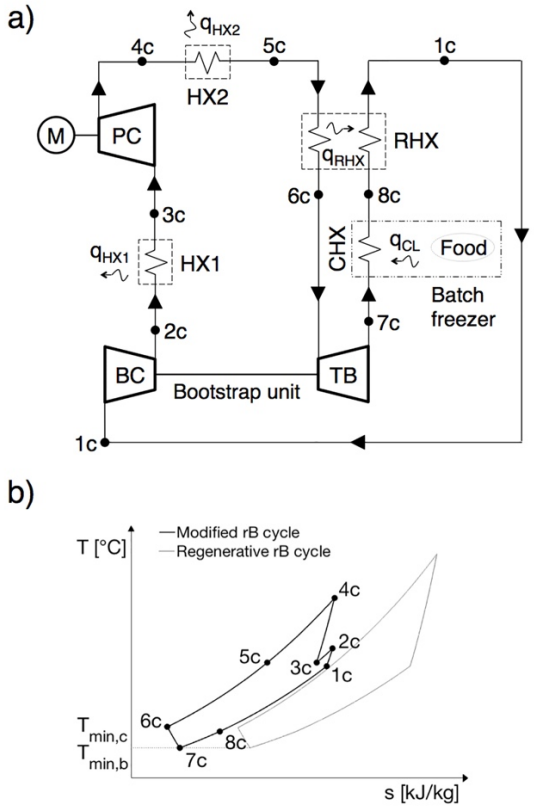

Fig. 3. Innovative modified rB cycle scheme (a) and Gibbs diagram (b). The working fluid compression phase occurs in BC (1c-2c) and PC (3c-4c), with the introduction of an intercooling (2c-3c). Once compressed, the working fluid is sequentially cooled in HX2 (4c-5c) and in RHX (5c-6c), and then expanded in TB (6c-7c). The resulting cold working fluid is reheated in CHX, by absorbing heat from the batch freezer (7c-8c), and in RHX (8c-1c).

In the loop, the presence of chemical compounds with freezing point above the lowest temperature of the system is a critical problem due to the possibility of solids formation (e.g. ice, in case of moisture) that may lead to serious damage and/or malfunctions of the mechanical components (first of all, the turbine). As a trace of moisture is usually released by the food during the freezing process, the modified rB cycle working fluid cannot be directly used inside the freezing room. This leads to the adoption of two separate systems. To further reduce the occurrence of icing in the primary loop, the adoption of an anhydrous working fluid (e.g. nitrogen) has been conceived. The design of two distinct systems also allows the operation of the modified rB cycle at loop pressure, which is always greater than 101 kPa, which allows (1) to improve cycle efficiency; (2) to reduce pipe and heat exchangers sizes and (3) to prevent external (moist) air infiltration in the loop. The problem of ice formation cannot be completely avoided in the batch freezer: in addition to the moisture released by the food and absorbed by the medium fluid, moist air from the environment enters the freezer during door opening and food loading and unloading. A defrosting procedure of the CHX is thus required to remove ice formation on the cold surfaces and to prevent heat exchange rate degradation.

More in detail, the compression of the working fluid has been divided into two separate stages. The first compression is performed by a bootstrap unit, which is constituted by the compressor (BC) and the turbine (TB), installed on the same shaft. In this configuration, the mechanical work required by the bootstrap compressor is completely supplied by the turbine. The second compression stage is then performed by the primary compressor (PC), which is driven by an electric motor (M). In order to reduce the required electric power, the working fluid is cooled, from T_{2c} to T_{3c}, by the heat exchanger HX1 placed between the two compressors.

Once compressed at pressure p_{4c}, and before entering the turbine, the working fluid is cooled down in the second heat exchanger (HX2) and in the regenerative heat exchanger RHX, reaching temperature T_{6c}. Water cools the HX1 and HX2. Downstream from the turbine and before re-entering the compressor BC, the working fluid passes through the cold heat exchanger (CHX) installed in the batch freezer and, finally, through the second duct of the RHX. In the CHX, the working fluid cools the air in the batch freezer by absorbing q_{CL}.

Differently from Foster et al.'s (2011) system, where the compression of the working fluid is sequentially performed by the primary compressor followed by the bootstrap unit, in the proposed plant layout the primary compressor is installed after the bootstrap unit to obtain a reduction of the working temperature gap among the components. The gaseous working fluid was selected to avoid solids formation in the colder components of the plant and, in addition, the minimum pressure value of the rB cycle (BC inlet) should be higher than the atmospheric one, allowing an increase in cycle performance.

The CoP of the proposed plant configuration is defined as

$$CoP = \frac{h_{8c} - h_{7c}}{(h_{4c} - h_{3c})\zeta_M^{-1}} \quad (2)$$

which is the ratio of the working fluid enthalpy differences in the CHX and in the PC, taking into account the electric motor efficiency ζ_M.

Since in the food industry hot water and/or steam are typically required for several thermal processes – e.g. blanching (Xin et al., 2015), cooking, washing, heating (Comba et al., 2010; Comba et al., 2011; Biglia et al., 2015), pasteurisation, debacterisation (Biglia et al., 2017), etc. – the heat released by the working fluid in the HX1 and HX2 may be favourably recovered, as demonstrated and tested in the air cycle prototype developed by Foster el at. (2011). In particular, the heat supplied by the HX1 may be used to warm a fluid, generally water, up to [40, 60] °C while the thermal level of the heat available in the HX2 might even allow production of low-pressure steam. In addition, the rejected heat from the HX1 and HX2 may also be used for space heating or to pre-heat water entering a boiler. Considering the concurrent cooling and heating effect production, heat

recovery (Ashrafi et al., 2015) represents a relevant advantage of rB cycles with respect to other freezing technologies, such as liquid nitrogen evaporation.

4. Plant modelling framework

A numerical model of the proposed modified rB cycle plant (Fig. 3) has been developed in order to evaluate the energy performance of the freezing plant. Each component was modelled by using the conservation of energy for one-inlet one-outlet control volume with one-dimensional flow (Moran and Shapiro, 2006). In particular, steady-state conditions were considered and heat losses across the components as well as potential and kinetic energy terms were neglected. Moreover, given the required level of detail, pressure drops were considered constant in the heat exchangers and null in the connection pipes. The thermodynamic state of the working fluid, in terms of temperature and/or pressure values, in a set of loop nodes was defined by physical and plant constructive constraints.

The model was implemented by using the Matlab® environment (version R2015b). Since the system of non-linear equations describing the thermodynamic and mechanic equilibrium among the loop components cannot be solved analytically, the Levenberg-Marquardt numerical solving method was adopted.

The thermodynamic properties of gaseous nitrogen, adopted as the working fluid in the loop, were evaluated by integrating the Reference Fluid Thermodynamic and Transport Properties (REFPROP) database, developed by the National Institute of Standards and Technology (NIST, version 9.1), directly with the model framework of the plant.

It should be noted that all the results were normalised by the cooling load $\dot{Q}_{CL}$.

4.1. Thermodynamic model of the components

The steady state form of the energy rate balance has been used to develop the thermodynamic model of the plant's components. The energy rate balance of the compressors (and - analogously - of the turbine) can be expressed as

$$\dot{W} = \dot{m}_N(h_{in} - h_{out}) \quad (3)$$

where h_{in} and h_{in} account for the specific enthalpy of the nitrogen mass flow rate $\dot{m}_N$ at the component inlet and outlet, respectively, and $\dot{W}$ is the net rate of energy transfer by work across the turbo machinery. The specific enthalpy difference $(h_{in} - h_{out})$ is related to the pressure ratio β and to the isentropic efficiency η of the turbo machinery, in addition to the thermodynamic properties of the fluid.

With the same approach, the net heat rate across the heat exchangers can be expressed as

$$\dot{Q} = \dot{m}_N(h_{in} - h_{out}) \quad (2)$$

In this case, the specific enthalpy difference $(h_{in} - h_{out})$ depends on the pressure drops Δp and on the effectiveness ε of the heat exchanger. The balance equations of each loop component (Fig. 3) are summarised in Table 1.

Parameters $\dot{W}$ and $\dot{Q}$ of each component were normalised per unit of cooling load $\dot{Q}_{CL}$.

Table 1. Balance equations of the modified rB cycle components.

Bootstrap compressor BC	$\dot{W}_{BC} = \dot{m}_N\,(h_{1c} - h_{2c})$
Heat exchanger HX1	$\dot{Q}_{HX1} = \dot{m}_N\,(h_{2c} - h_{3c})$
Primary compressor PC	$\dot{W}_{PC} = \dot{m}_N\,(h_{3c} - h_{4c})$
Heat exchanger HX2	$\dot{Q}_{HX2} = \dot{m}_N\,(h_{4c} - h_{5c})$
Regenerator RHX	$\dot{Q}_{RHX} = \dot{m}_N\,(h_{5c} - h_{6c}) = \dot{m}_N\,\lvert(h_{8c} - h_{1c})\rvert$
Turbine TB	$\dot{W}_{TB} = \dot{m}_N\,(h_{6c} - h_{7c})$
Heat exchanger CHX	$\dot{Q}_{CL} = \dot{m}_N\,(h_{7c} - h_{8c})$

4.2. Thermodynamic constraints and specifications

The set of feasible working parameters of the modified rB cycle is constrained by the technical specifications of the components and/or by the boundary conditions. The constraints considered in the model implementation concerned:

- nitrogen pressure at the compressor BC inlet p_{1c} and at the compressor PC outlet p_{4c}. The atmospheric pressure, to avoid external moist air infiltration, was considered to be the limit for the minimum pressure of the plant p_{1c}. The maximum value of pressure p_{4c} was limited to fulfil the mechanical constraints due to the resistance of the heat exchangers,

which is usually referred to about 3 MPa. Therefore, the pressure of the plant is subject to both upper and lower boundary conditions;

- nitrogen temperatures T_{3c} and T_{5c} at the outlet of heat exchangers HX1 and HX2 respectively. The values of T_{3c} and T_{5c} are related to the temperature of the cooling fluid and to the technology adopted in the HX1 and HX2. Assuming the HX1 and HX2 are cooled by using water at 30 °C (standard operating temperature of the cooling water tower) and considering a pinch point of 10 °C between the inlet cooling water and the outlet cooled nitrogen, temperatures T_{3c} and T_{5c} were considered fixed;
- the isentropic efficiency of turbo machineries η_{BC}, η_{PC}, η_{TB}. Even if the fine tuning of the machines efficiency values is affected by the power size of the components and the adopted technical solution, these values were considered constant and equal to standard design values for such types of components;
- the effectiveness of the regenerator RHX. The regenerator effectiveness ε_{RHX} was considered constant in the thermodynamic model of the plant;
- the operating parameters of the cold heat exchanger CHX. In particular, the outlet nitrogen temperature T_{8c}, the nitrogen temperature difference ΔT_{CHX} between the inlet and the outlet of the CHX and the cooling load $\dot{Q}_{CL}$ were considered constant.

4.3. Cycle equilibrium solution

The setting of the plant parameters must guarantee the mechanical and thermodynamic balance between plant components. Due to the relationships and the constraints linking the nitrogen thermodynamic states (Section 4.2.), the pressure ratios β_{BC} and β_{PC} of the bootstrap and the primary compressor have been assumed as design variables (independent variables). Indeed, the bootstrap and primary compressor working pressures affect the bootstrap unit mechanical balance according to

$$\dot{m}_N\left(h_{6c}(T_{6c}, p_{1c}\beta_{BC}\beta_{PC}) - h_{7c}(T_{7c}, p_{7c})\right) = \\ = \frac{\dot{m}_N\left(h_{2c}(T_{2c}, \beta_{BC}) - h_{1c}(T_{1c}, p_{1c})\right)}{f_{BU}} \quad (5)$$

and the turbine isentropic efficiency

$$\eta_{TB} = \frac{h_{6c} - h_{7c}}{(h_{6c} - h_{7c,is})} = \frac{\left(h_{6c}(T_{6c}, p_{1c}\beta_{BC}\beta_{PC}) - h_{7c}(T_{7c}, p_{7c})\right)}{\left(h_{6c}(T_{6c}, p_{1c}\beta_{BC}\beta_{PC}) - h_{7c}(T_{7c,is}, p_{7c})\right)} \quad (6)$$

where f_{BU} and h_{is} account for the mechanical losses in the bootstrap and the isentropic specific enthalpy respectively. The values of pressure ratios β_{BC} and β_{PC}, which guarantee the solution of non-linear equations (5) and (6), were numerically obtained by means of a Levenberg-Marquardt algorithm, implemented in Matlab®.

5. Energy performance analysis of the modified rB cycle

The effect of a set of thermodynamic parameters on the energy efficiency of the modified rB cycle, measured by the CoP index (Eq. 2), was investigated by means of a performance analysis. In order to quantify the individual effect of a parameter on the overall system performance, the behaviour of the plant was simulated for a set of configurations generated by varying only one parameter at a time, within a specified range, while keeping all the others constant. During new systems design, performance analysis is an effective tool to identify the plant components which affect system efficiency the most, with the aim of properly focusing improvement efforts, and of obtaining preliminary results by helping system optimisation. The performance analysis was carried out on the modified rB cycle operated with the thermodynamic parameters listed in Table 2.

Table 2. Reference parameters of the modified rB cycle performance analysis.

Variable	Value	
p_{1c}	100	[kPa]
Δp_{HX1}	8	[kPa]
Δp_{HX2}	11	[kPa]
Δp_{RHX}	14 (each side)	[kPa]
Δp_{CHX}	16	[kPa]
T_{3c}	40	[°C]
T_{5c}	40	[°C]
T_{8c}	-85	[°C]
ΔT_{CHX}	30	[°C]
ε_{RHX}	0.925	[-]
η_{BC}	0.725	[-]
η_{TB}	0.810	[-]
f_{BU}	0.920	[-]
η_{PC}	0.680	[-]
ζ_{M}	0.950	[-]

5.1. Effect of the system's pressurisation

In order to assess the effect of the working fluid pressure on system performance, the CoP was computed for a set of plant configurations with loop minimum pressure p_{1c} varying within the range [100, 1000] kPa. The resulting growing trend of the modified rB cycle efficiency, related to increments of the p_{1c} value (Fig. 4a), is due to the reduction of the required pressure ratio β_{PC} of the primary compressor (Fig. 4b) and to the increment in the working fluid density, which lead to a reduction in the required compression work (Fig. 4c). Since the incremental rate of the system's performance due to loop pressurisation significantly decreases for p_{1c} values above 500 kPa (Fig 4a), the pressurisation of the system may be settled to a value which benefits the CoP and to the required mechanical resistance of the plant components.

The heat exchangers' normalised capacity per unit of cooling load is reported in Fig. 4d. The pressurisation of the system mainly affects the capacity of the heat exchanger HX2, which decreases with an increment of p_{1c}, while the capacities of exchangers HX1 and RHX can be considered constant according to the adopted hypothesis. Since the temperatures T_{3c} and T_{5c} at the PC inlet and HX2 outlet respectively are

fixed and equal in value, the result is a comparable trend of the normalised power of the two consecutive loop components (Figs. 4c, 4d). For p_{1c} values above 500 kPa, the normalised power $\dot{W}_{PC}$ required by the PC is about 3 times larger than the one required by the BC, while the capacity of heat exchangers HX2 and RHX is about 4 times larger than the one of the HX1.

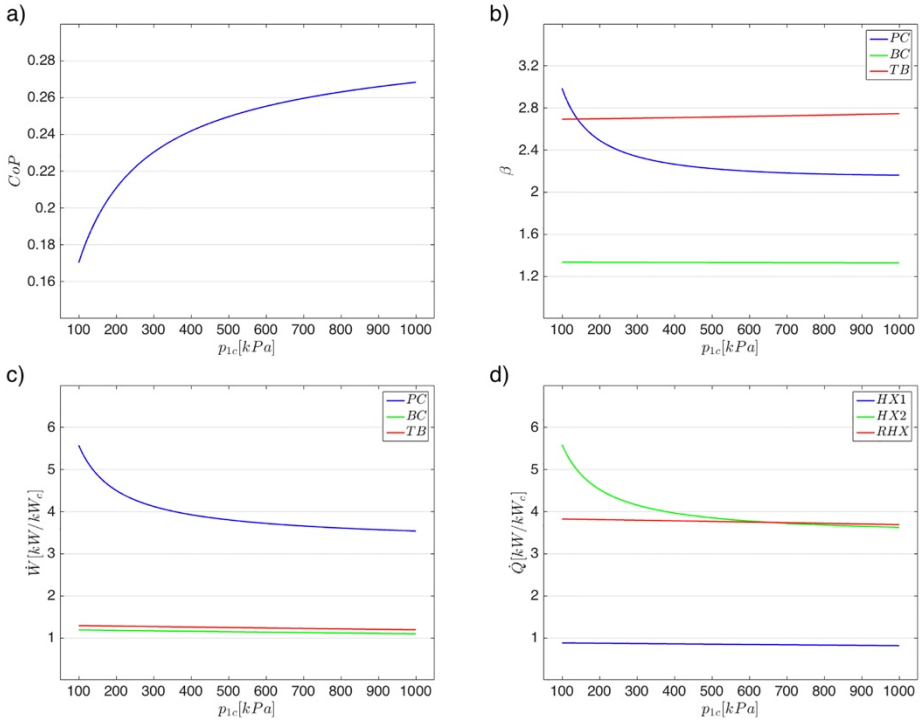

Fig. 4. Effect of the system's pressurisation on the modified rB cycle CoP (a), turbo-machineries pressure ratios β_{PC}, β_{BC} and β_{TB} (b), normalised power $\dot{W}_{PC}$, $\dot{W}_{BC}$ and $\dot{W}_{TB}$ (c) and, finally, on the heat exchangers normalised capacity $\dot{Q}_{HX1}$, $\dot{Q}_{HX2}$ and $\dot{Q}_{RHX}$ (d).

5.2. Effect of the working fluid's temperature at the HX1 and HX2 outlets

The effect of the nitrogen temperature at the outlets of heat exchangers HX1 and HX2 on the system's CoP was investigated by simulating the modified rB cycle behaviour by varying T_{3c} and T_{5c}, values within the range [30, 50] °C (Fig. 5a). A slight reduction of the plant's CoP can be noted with higher T_{3c} and T_{5c} temperature values. Indeed, an increment of T_{3c} corresponds to an intercooling reduction between the two nitrogen

compression stages, which leads the mechanical work of the compressor PC to increase. The effect of T_{5c} on the whole system's CoP is more complex and can be linked to the changes led to the thermodynamic state of the working fluid at the turbine TB inlet. Indeed, with constant regenerator effectiveness ε_{RHX}, an increment in the T_{5c} value determines a resulting turbine inlet temperature T_{6c} increment. In order to maintain the cooling load constant, which results in a fixed temperature T_{7c} and pressure p_{7c} at the turbine outlet, an increment of temperature T_{6c} requires a higher p_{6c} value before the nitrogen expansion. The resulting slight increments β_{TB} and β_{PC} (Fig. 5b) lead to a CoP reduction. Temperatures T_{3c} and T_{5c} may be set as low as possible, according to the adopted typology of heat exchangers HX1 and HX2 and to the cooling fluid mass flow rate and temperature. Within the considered temperature range of T_{3c} and T_{5c}, the mechanical power of turbo-machineries (Fig. 5c) does not change significantly with respect to the heat exchanger's capacity (Fig. 5d): an increment of the nitrogen temperature at the outlet of one heat exchanger (HX1 or HX2) leads to a reduction of its capacity, while a capacity increment of all the others is required to balance the loop equilibrium.

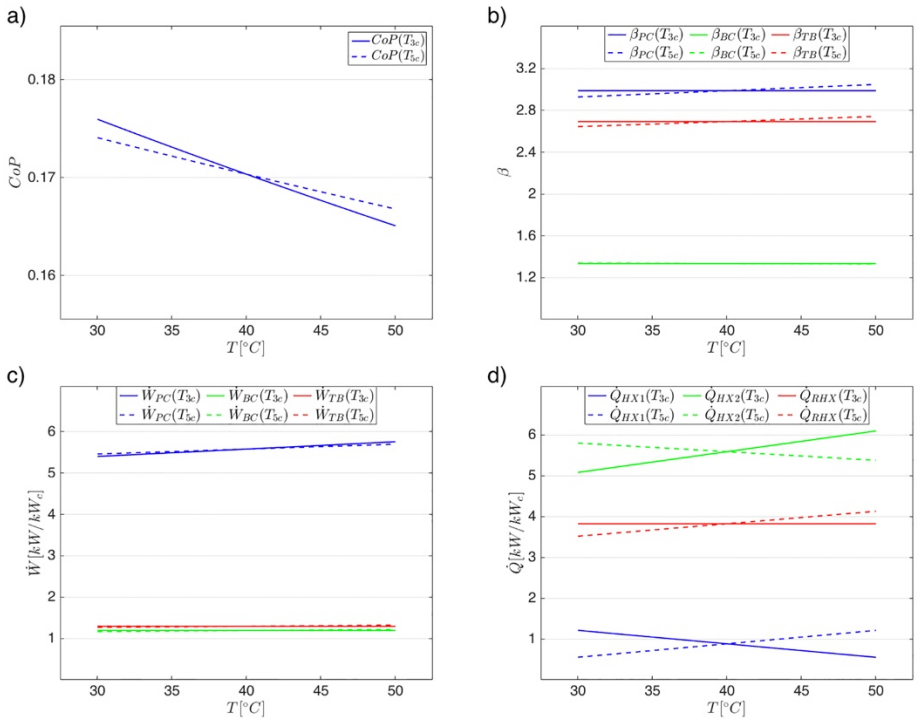

Fig. 5. Effect of the working fluid's temperature at HX1 and HX2 outlets on the modified rB cycle CoP (a), turbo-machineries pressure ratios β_{PC}, β_{BC} and β_{TB} (b), normalised power $\dot{W}_{PC}$, $\dot{W}_{BC}$ and $\dot{W}_{TB}$ (c) and, finally, on the heat exchangers normalised capacity $\dot{Q}_{HX1}$, $\dot{Q}_{HX2}$ and $\dot{Q}_{RHX}$ (d).

5.3. Effect of the working fluid's temperature gap in the CHX

The variation of the plant's CoP was analysed by considering a working fluid temperature difference ΔT_{CHX} between the heat exchanger CHX inlet and outlet varying within the range [20, 70] °C. The efficiency of the modified rB cycle is deeply sensitive to the ΔT_{CHX} parameter (Fig. 6a), showing a non-monotonous trend with a maximum value within the considered range of values. By affecting both the required nitrogen flow rate $\dot{m}_N$ and the outlet turbine temperature T_{7c}, the effect of ΔT_{CHX} on system performance is relevant. Indeed, given a certain cooling load $\dot{Q}_{CL}$, the product of the nitrogen mass flow rate $\dot{m}_N$ and $\Delta h(\Delta T, \Delta p)_{CHX}$ must be constant. Benefits to the overall CoP value can be achieved with low $\dot{m}_N$ values, which involve a low turbo machineries power $\dot{W}$ (Fig. 6c), and/or a low ΔT_{CHX} value, which corresponds to a higher T_{7c} temperature at the turbine outlet and, thus, a reduction of the turbine pressure ratio β_{TB} (Fig.

6b). The positive effect of this last phenomenon to the system's CoP can be easily attributed to the required lower pressure ratio β_{PC} of the primary compressor (Fig 6b). Therefore, the correct choice of ΔT_{CHX} allows the performance of the system to be maximised.

Fig. 6d shows the capacity of the heat exchangers per unit of cooling load as a function of the temperature difference in the CHX. It can be noticed that the capacity of the HX1 is constant compared to the increase of ΔT_{CHX}.

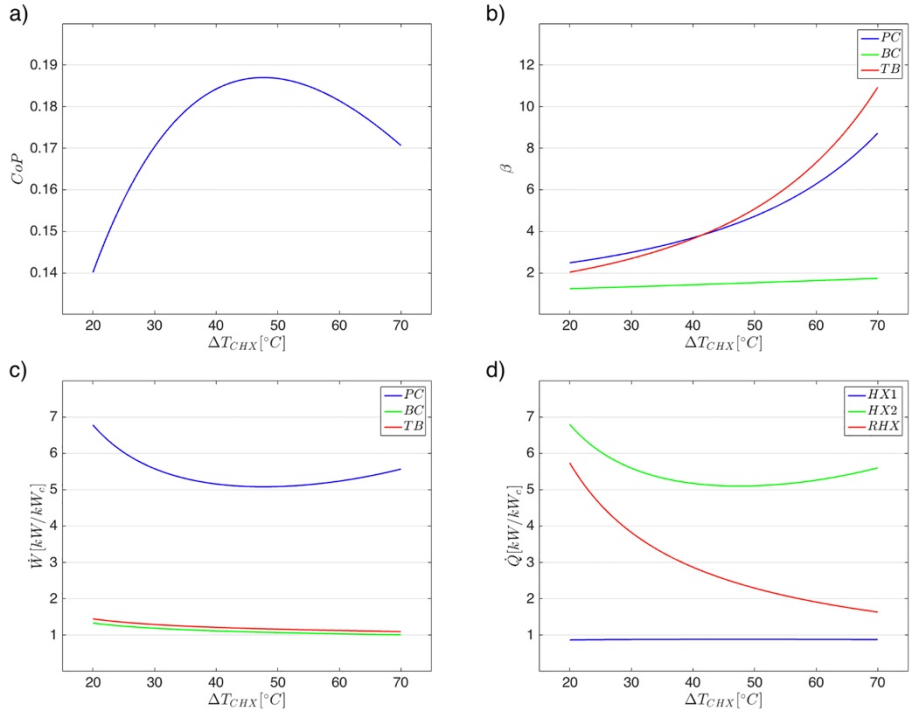

Fig. 6. Effect of the working fluid's temperature gap in CHX on the modified rB cycle CoP (a), turbo machines pressure ratios β_{PC}, β_{BC} and β_{TB} (b), normalised power $\dot{W}_{PC}$, $\dot{W}_{BC}$ and $\dot{W}_{TB}$ (c) and, finally, on the heat exchangers normalised capacity $\dot{Q}_{HX1}$, $\dot{Q}_{HX2}$ and $\dot{Q}_{RHX}$ (d).

5.4. Effect of the turbo-machineries' isentropic efficiency

The sensitivity of the system's CoP to the isentropic efficiency of the compressors and of the turbine was evaluated for a set of plant configurations with η_{PC} varying within the range [0.65, 0.71], η_{BC} within the range [0.70, 0.75] and, finally, η_{TB} within the range [0.78, 0.84]. Even if, of course, a positive effect on the CoP was found in connection to an increment of all the turbo machineries efficiencies (Fig. 7a), the CoP

turned out to be more affected by the isentropic efficiency of the primary compressor and of the turbine, compared to the bootstrap compressor.

More in detail, considering a constant cooling load $\dot{Q}_{CL}$, the adoption of bootstrap components - BC and TB - with higher isentropic efficiency values, allows a PC pressure ratio β_{PC} reduction (Fig. 7b). Indeed, given a fixed thermodynamic state at the turbine outlet and an invaried mechanical power balance at the bootstrap unit shaft (Fig. 7c), an increment in η_{BC} and η_{TB} lets the pressure ratio and the mechanical power of the primary compressor to decrease. Even if η_{BC} has a minor effect on the overall system's performance with respect to η_{TB}, an increment in its value would allow the mechanical power supplied by the turbine to be more effective, leading to favourable β_{BC} increments and β_{PC} reductions.

The isentropic efficiency η_{PC} of the primary compressor mainly affects the required electric power and, thus, the system's CoP (Fig. 7a and 7c).

Regarding the power and heat capacity of the cycle components, it should be noted that an increment in the turbo-machineries isentropic efficiency leads to a significant reduction in the sole primary compressor power (Fig. 7c) and in the capacity of heat exchanger HX2 (Fig. 7d). On the contrary, the normalised power per unit of cooling load of the bootstrap unit (Fig. 7c) and the capacity per cooling load of heat exchangers HX1 and RHX (Fig. 7d) are less affected since temperatures T_{3c}, T_{5c}, T_{8c} and the lower pressure p_{1c} are fixed parameters.

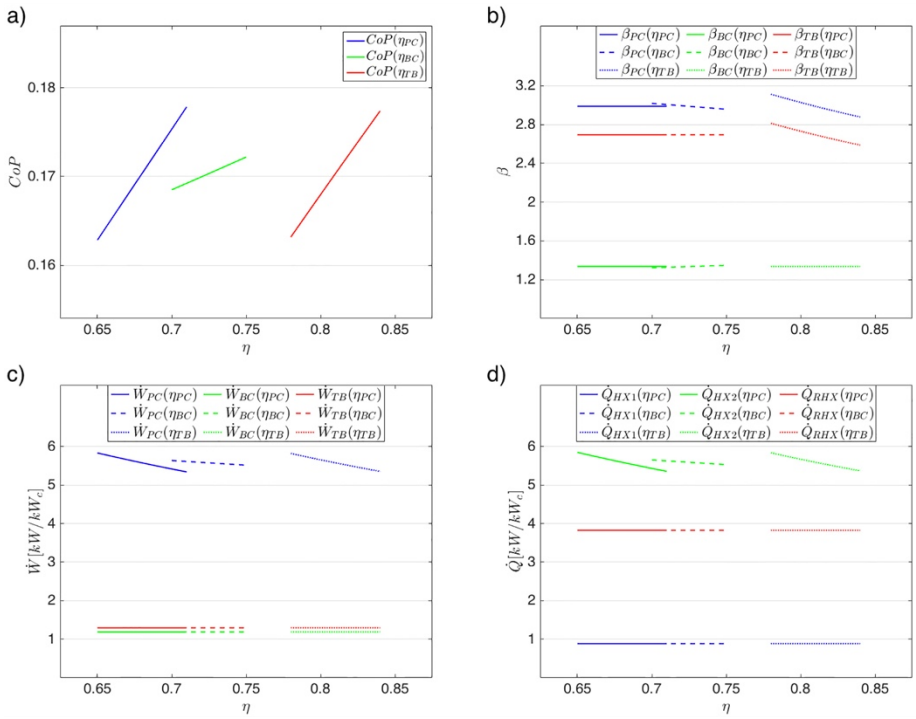

Fig. 7. Effect of the turbo-machineries' isentropic efficiency on the modified rB cycle CoP (a), turbo-machineries pressure ratios β_{PC}, β_{BC} and β_{TB} (b), normalised power $\dot{W}_{PC}$, $\dot{W}_{BC}$ and $\dot{W}_{TB}$ (c) and, finally, on the heat exchangers normalised capacity $\dot{Q}_{HX1}$, $\dot{Q}_{HX2}$ and $\dot{Q}_{RHX}$ (d).

5.5. Effect of the regenerator's effectiveness

The effect of regenerator effectiveness ε_{RHX} on the modified rB cycle performance was investigated by varying its value within the range [0.90, 0.95]. An increment of the system's CoP (Fig. 8a) can be obtained by increasing regenerator effectiveness. Indeed, given regenerator inlet temperatures T_{5c} and T_{8c} of the hot and cold sides respectively, higher ε_{RHX} values lead to a reduction of nitrogen temperatures T_{6c} and T_{1c} at the RHX outlets, allowing the turbine and bootstrap compressors to work with lower inlet temperatures and, consequently, with lower pressure ratios β_{TB} and β_{BC}, to fulfil the imposed constant cooling load $\dot{Q}_{CL}$. Thus, the turbo machineries' normalised power per cooling load decreases with higher ε_{RHX} values (Figs. 8b and 8c). The capacity $\dot{Q}_{HX1}$ per unit of cooling load of the HX1 is less affected by ε_{RHX} (Fig. 8d), while the capacity $\dot{Q}_{HX2}$ of

heat exchanger HX2 and $\dot{Q}_{\mathrm{RHX}}$ of the regenerator decrease and increase, respectively.

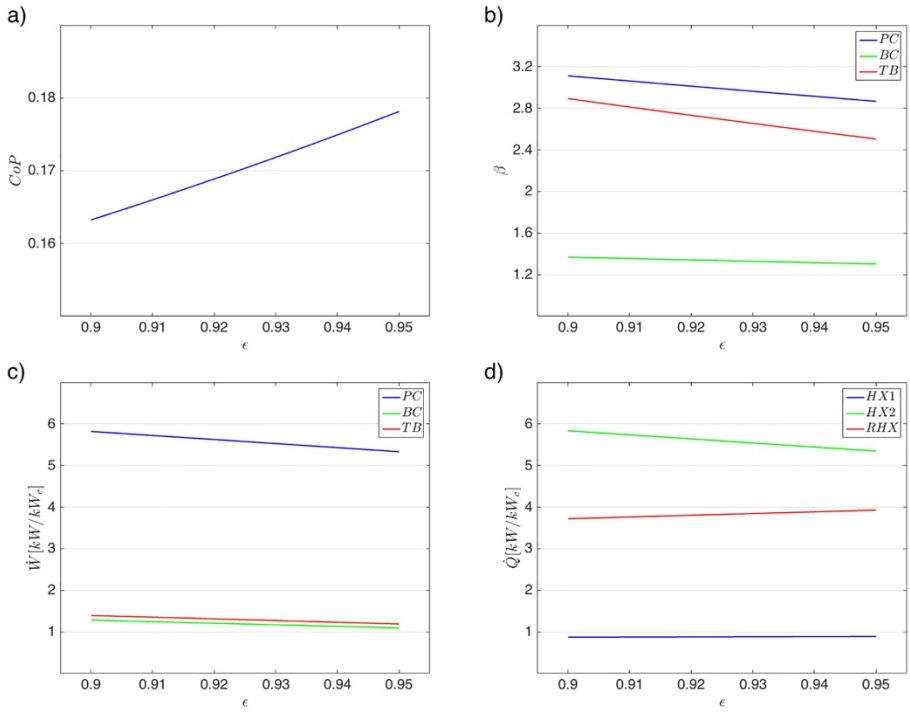

Fig. 8. Effect of the regenerator's effectiveness on the modified rB cycle CoP (a), turbo-machineries pressure ratios β_{PC}, β_{BC} and β_{TB} (b), normalised power $\dot{W}_{\mathrm{PC}}$, $\dot{W}_{\mathrm{BC}}$ and $\dot{W}_{\mathrm{TB}}$ (c) and, finally, on the heat exchangers normalised capacity $\dot{Q}_{\mathrm{HX1}}$, $\dot{Q}_{\mathrm{HX2}}$ and $\dot{Q}_{\mathrm{RHX}}$ (d).

6. Energy performance optimisation

An optimisation algorithm was coupled with the cycle equilibrium solver (Section 4.3.) to identify the best configuration of the modified rB cycle. In line with the results of the performance analysis (Section 5), the most effective variables on the system's CoP were considered for the optimisation model. These are:

- Temperature difference in the CHX: ΔT_{CHX}
- Minimum pressure of the loop: $p_{1\mathrm{c}}$
- Turbo machineries isentropic efficiency: η_{PC}, η_{BC}, η_{TB}
- Regenerator effectiveness: $\varepsilon_{\mathrm{RHX}}$

and can be arranged as $x = [\Delta T_{\mathrm{CHX}}, p_{1\mathrm{c}}, \eta_{\mathrm{PC}}, \eta_{\mathrm{BC}}, \eta_{\mathrm{TB}}, \varepsilon_{\mathrm{RHX}}]^{\mathrm{T}}$. The lower and upper bounds for each variable, summarised in Table 3, were set according to the performance analysis and component specifications. Constant parameters used in the optimisation problem were also reported in Table 3.

The optimisation problem can be expressed as $\max_{x} f(x)$ where

$$f(x) = \frac{h_{8\mathrm{c}} - h_{7\mathrm{c}}}{(h_{4\mathrm{c}} - h_{3\mathrm{c}})\zeta_{\mathrm{M}}^{-1}} \tag{7}$$

which represents the plant's CoP of Fig. 3.

The optimisation solver was implemented in the Matlab® by adopting an interior-point method developed to solve nonlinear optimisation problems.

6.1. Optimisation results

The highest value of the system's CoP, obtained by the optimisation process, is equal to 0.322, which involves an electric engine power of 3.11 kW per unit of cooling load in the CHX. This plant configuration is characterised by the minimum pressure value of the system, turbo machineries isentropic efficiency and regenerator effectiveness equal to the prescribed upper bound of Table 3, while the final ΔT_{CHX} value is 28.9°C. The set of optimal parameters can be summarised as $x_{\mathrm{opt}} = [28.9, 1000, 0.71, 0.75, 0.84, 0.95]^{\mathrm{T}}$.

The thermodynamic state of each loop node, in terms of nitrogen temperature and pressure values, of the obtained operating conditions of the modified rB cycle is reported in Table 4, together with the normalised net rate of energy transfer by work and heat across the loop components. The resulting value of the nitrogen mass flow rate is also provided in Table 4. The maximum and minimum temperatures of the cycle account for 131.2°C and -113.9°C, which are reached at the primary compressor ($T_{4\mathrm{c}}$) and turbine ($T_{7\mathrm{c}}$) outlets respectively. The maximum pressure of the cycle (primary compressor outlet, $p_{4\mathrm{c}}$) results in 2494 kPa, within the considered upper pressure limit prescribed for heat exchangers. The normalised mechanical power of the bootstrap compressor, of the primary compressor and of the turbine account for 1.03, 2.95 and 1.12 respectively. Please note that the normalised mechanical power of the primary compressor and the

electric engine power are connected to the efficiency of the electric engine. The required turbine power is larger than the power of the bootstrap compressor to balance the mechanical losses of the bootstrap unit.

In addition to the cooling load supply, which is effective at very low temperatures in the CHX, a normalised thermal power of 0.84 kW and 3.02 kW, per each kW of cooling load, may be profitably recovered from the HX1 and in the HX2 respectively. It should be noted that the thermal level is different in the two heat exchangers (about 65 °C in the HX1 and 130 °C in the HX2); therefore, depending on the end-user, different plant configurations may be adopted to profitably recover the available heat in the HX1 and HX2.

Considering an electricity price for industrial users of 0.16 €·kWh^{-1} (average commercial price in Italy, 2016), the running cost of the proposed plant can be estimated at 0.50 €·kWh^{-1}. This value is lower than a liquid-nitrogen plant running cost of 2.71 €·kWh^{-1}, obtained by calculating the required liquid nitrogen mass per unit of cooling load, considering a nitrogen latent heat (at saturation conditions at ambient pressure) of 199.44 kJ·kg^{-1} and a liquid nitrogen cost of 0.15 €·kg^{-1} (average commercial price in Italy, 2016).

7. Conclusions

The performance analysis of an innovative system, based on a modified reversed Brayton cycle, for food freezing at very low temperatures was investigated in this paper. The analysis showed the effect of the different design parameters on the thermodynamic cycle's CoP. The system can achieve very low temperatures (even lower than -100 °C) which are favourable for food fast freezing processes. Gaseous nitrogen was selected as the working fluid of the reversed Brayton cycle, to avoid solids formation in the coolest part the thermodynamic cycle. The food freezing process takes place in a batch freezer room, by means of recirculating air, cooled down by the primary working fluid.

A Coefficient of Performance of 0.322 was obtained by setting the cold heat exchanger (CHX) of the reversed Brayton cycle at an operating average temperature of –99.5 °C. In particular, the performance analysis showed that the performance of the thermodynamic cycle strictly depends

on the pressure level of the system, on the temperature difference through the cold heat exchanger and on the effectiveness of the regenerative heat exchanger. This latter component is essential to reach low temperatures at the turbine outlet of the thermodynamic cycle.

As a benefit, large quantities of waste heat, around 3.8 kW per unit of cooling load, may be recovered and used to produce heated water, which is widely adopted in the food industry (e.g. pre-cooking, blanching, heating, pasteurisation, etc.). In particular, 0.8 kW and 3 kW of waste heat per unit of cooling load may be available at temperatures of 65 °C and 130 °C respectively.

Considering an electricity cost of 0.16 €·kWh^{-1}, a running cost of 0.50 €·kWh^{-1} was estimated for the designed system. This value is lower than the estimated running cost of a liquid nitrogen plant, which is about 2.71 €·kWh^{-1}.

The proposed innovative food freezing system proves that it is possible to overcome the discussed limitations of the existing reversed Brayton cycle solutions assuring, in the meanwhile, favourable energy performance for food freezing purposes with respect to available technological solutions for food processing at low temperatures.

Acknowledgements

This research was partially funded by projects “SACS” (POR FESR 2007-2013, Polo Innovazione Agroalimentare, Grant No. ASF 285-226) and “CRYOFOOD” (POR FESR 2014-2020, Polo Innovazione AgriFood). The authors wish to thank Criotec Impianti S.r.l., Dyria Sistemi S.r.l. and ZOPPI S.r.l. project partners for their active collaboration.

References

Ahmadi MH, Ahmadi MA. Multi objective optimization of performance of three-heat-source irreversible refrigerators based algorithm NSGAII. *Renew Sustainable Energy Rev* 60 (2016) pp. 784-794.

Ahmadi MH, Ahmadi MA, Mohammadi AH, Feidt M, Pourkiaei SM. Multi-objective optimization of performance of an irreversible Stirling cryogenic refrigerator cycle. *Energ Convers Manage* 82 (2014) pp. 351-360.

Ahmadi MH, Ahmadi MA, Pourfayaz F, Bidi M. Thermodynamic analysis and optimization for an irreversible heat pump working on reversed Brayton cycle. *Energ Convers Manage* 110 (2016) pp. 260-267.

Ashrafi O, Bédard S, Bakhtiari B, Poulin B. Heat recovery and heat pumping opportunities in a slaughterhouse. *Energy* 89 (2015) pp. 1-13.

ASHRAE. Refrigeration ASHRAE Handbook. ISBN 978 1 933742 82 3 (2010).

Awonorin AO. An appraisal of the freezing capabilities of tunnel and spiral belt freezers using liquid nitrogen sprays. *J Food Eng* 34 (1997) pp. 179-192.

Bi Y, Chen L, Sun F. Heating load density and COP optimizations for an endoreversible air heat pump. *Appl Energy* 85 (2008) pp. 607-617.

Bi Y, Chen L, Sun F. Comparative performance analysis for endoreversible simple air heat pump cycles considering ecological, exergetic efficiency and heating load objectives. *Int J Exergy* 6 (2009) pp. 550-566.

Bi Y, Xie G, Chen L, Sun F. Heating load density optimization of an irreversible simple Brayton cycle heat pump coupled to counter-flow heat exchangers. *Appl Math Model* 36 (2012) pp. 1854-1863.

Biglia A, Comba L, Fabrizio E, Gay P, Ricauda Aimonino D. Case studies in food freezing at very low temperature. *Energy Procedia* 101 (2016) pp. 305-312.

Biglia A, Comba L, Fabrizio E, Gay P, Ricauda Aimonino D. Steam batch thermal processes in unsteady state conditions: modelling and application to a case study in the food industry. *Appl Therm Eng* 118 (2017) pp. 638-651.

Castro-Giráldez M, Balaguer B, Hinarejos E, Fito PJ. Thermodynamic approach of meat freezing process. *Innov Food Sci Emerg* 23 (2014) pp. 138-145.

Chang H-M, Chung MJ, Kim MJ, Park SB. Thermodynamic design of methane liquefaction system based on reversed-Brayton cycle. *Cryogenics* 49 (2009) pp. 226-234.

Comba L, Gay P, Piccarolo P, Ricauda Aimonino D. Thermal processes in the candy process of chestnut. *Acta Hortic* 866 (2010) pp. 587-594.

Comba L, Belforte G, Gay P. Modelling techniques for the control of thermal exchanges in mixed continuous-discontinuous flow food plants. *J Food Eng* 106 (2011) pp. 177-187.

Dempsey P, Bansal P. The art of air blast freezing: design and efficiency considerations. *Appl Therm Eng* 41 (2012) pp. 71-83.

Di Matteo P, Donsì G, Ferrari G. The role of heat and mass transfer phenomena in atmospheric freeze-drying of foods in a fluidised bed. *J Food Eng* 59 (2003) pp. 267-275.

Dopazo JA, Fernández-Seara J. Experimental evaluation of freezing processes in horizontal plate freezers using CO_2 as refrigerant. *Int J Refrig* 35 (2012) pp. 2093-2101.

Elsayed ES, Akisawa A, Kashiwagi T, Hamamoto Y. Using air cycle refrigerator integrated desiccant system for simultaneous usage in supermarket: refrigerating and ventilated air conditioning. Proc. of the 3rd Asian Conference on Refrigeration and Air-Conditioning (ACRA2006). May 21–23, vols. 1 and 2 (2006) Gyeongju, Korea.

Foster AM, Brown T, Gigiel AJ, Alford A, Evans JA. Air cycle combined heating and cooling for the food industry. *Int J Refrig* 34 (2011) pp. 1296-1304.

Galetto CD, Verdini RA, Zorrilla SE, Rubiolo AC. Freezing of strawberries by immersion in $CaCl_2$ solutions. *Food Chem* 123 (2010) pp. 243-248.

Gazda W. Application possibilities of the strategies of the air blast-cryogenic cooling process. *Energy* 62 (2013) pp. 113-119.

Giannetti M, Milazzo A. Thermodynamic analysis of regenerated air-cycle refrigeration in high and low pressure configuration. *Int J Refrig* 40 (2014) pp. 97-110.

Hou S, Zhang H. An open reversed Brayton cycle with regeneration using moist air for deep freeze cooled by circulating water. *Int J Therm Sci* 48 (2009) pp. 218-223.

Hou S, Li H, Zhang H. An open air-vapor compression refrigeration system for air-conditioning and desalination on ship. *Desalination* 222 (2008) pp. 646-655.

Huan Z, He S, Ma Y. Numerical simulation and analysis for quick-frozen food processing. *J Food Eng* 60 (2003) pp. 267-273.

Islam MN, Zhang M, Adhikari B, Xinfeng C, Xu B. The effect of ultrasound-assisted immersion freezing on selected physicochemical properties of mushrooms. *Int J Refrig* 42 (2014) pp. 121-133.

James SJ, James C. Meat Refrigeration. *Woodhead Publishing Series in Food and Science and Technology*, 1 85573 442 7 (2002).

Kaale LD, Eikevik TM, Rustad T, Kolsaker K. Superchilling of food: a review. *J Food Eng* 107 (2011) pp. 141-146.

Kim YHB, Liesse C, Kemp R, Balan P. Evaluation of combined effects of ageing period and freezing rate on quality attributes of beef loins *Meat Sci* 110 (2015) pp. 40-45.

Ledesma E, Laca A, Rendueles M, Díaz M. Texture, colour and optical characteristics of a meat product depending on smoking time and casing type. *LWT – Food Sci Technol* 65 (2016) pp. 164-172.

Lerfall J, Bendiksen EA, Olsen JV, Østerlie M. A comparative study of organic- versus conventional Atlantic salmon. II. Fillet color, carotenoid- and fatty acid

composition as affected by dry salting, cold smoking and storage. *Aquaculture* 451 (2016) pp. 369-376.

Li S, Wang S, Ma Z, Jiang S, Zhang T. Using an air cycle heat pump system with a turbocharger to supply heating for full electric vehicles. *Int J Refrig* 77 (2017) pp. 11-19.

Li X, Babol J, Bredie WLP, Nielsen B, Tománková J, Lundström K. A comparative study of beef quality after ageing longissimus muscle using a dry ageing bag, traditional dry ageing or vacuum package ageing. *Meat Sci* 97 (2014) pp. 433-442.

Llopis R, Sánchez D, Sanz-Kock C, Cabello R, Torrella E. Energy and environmental comparison of two-stage solutions for commercial refrigeration at low temperatures: fluids and systems. *Appl Energy* 138 (2015) pp. 133-142.

Moran MJ, Shapiro HN. Fundamentals of Engineering Thermodynamics (fifth ed.), John Wiley & Sons (2006).

National Institute of Standards and Technology (Standard Reference Data) NIST Reference Fluid Thermodynamic and Transport Properties Database: Version 9.1 United States Department of Commerce, Gaithersburg, MD (2013).

Perussello CA, Mariani VC, do Amarante ÁC. Combined modelling of thermal properties and freezing process by convection applied to green beans. *Appl Therm Eng* 31 (2011) pp. 2894-2901.

Reynoso RO, Calvelo A. Comparison between fixed and fluidized bed continuous pea freezers. *Int J Refrig* 8 (1985) pp. 109-115.

Rogers BH. Cooling in aircraft. *Proceedings of the Institute of Refrigeration* 91 (1994) pp. 4-11.

Salvadori VO, Mascheroni RH. Analysis of impingement freezers performance. *J Food Eng* 54 (2002) pp. 133-140.

Shaikh NI, Prabhu V. Mathematical modelling and simulation of cryogenic tunnel freezers. *J Food Eng* 80 (2007) pp. 701-710.

Soyer A, Özalp B, Dalmiş Ü, Bilgin V. Effects of freezing temperature and duration of frozen storage on lipid and protein oxidation in chicken meat. *Food Chem* 120 (2010) pp. 1025-1030.

Spence SWT, Doran WJ, Artt DW. Design, construction and testing of an air-cycle refrigeration system for road transport. *Int J Refrig* 27 (2004) pp. 503-510.

Spence SWT, Doran WJ, Artt DW, McCullough G. Performance analysis of a feasible air-cycle refrigeration system for road transport. *Int J Refrig* 28 (2005) pp. 381-388.

Streit J, Razani A. Thermodynamic optimization of reverse Brayton cycles of different configurations for cryogenic applications. *Int J Refrig* 36 (2013) pp. 1529-1544.

Tian Y, Zhao Y, Huang J, Zeng H, Zheng B. Effects of different drying methods on the product quality and volatile compounds of whole shiitake mushrooms. *Food Chem* 197 (2016) pp. 714-722.

Xin Y, Zhang M, Xu B, Adhikari B, Sun J. Research trends in selected blanching pretreatments and quick freezing technologies as applied in fruits and vegetables: a review. *Int J Refrig* 57 (2015) pp. 11-25.

Xu B, Zhang M, Bhandari B, Sun J, Gao Z. Infusion of CO_2 in a solid food: a novel method to enhance the low-frequency ultrasound effect on immersion freezing process. *Innov Food Sci Emerg* 35 (2016) pp. 194-203.

5.2. Third paper

Energy Procedia 101 (2016) pp. 305-312

DOI: 10.1016/j.egypro.2016.11.039

Case studies in food freezing at very low temperature

Alessandro Biglia [a], Lorenzo Comba [b], Enrico Fabrizio [b,*], Paolo Gay [a,c], Davide Ricauda Aimonino [a]

[a] DiSAFA – Universitá degli Studi di Torino, 2 Largo Paolo Braccini, Grugliasco (TO) 10095, Italy

[b] DENERG – Politecnico di Torino, 24 Corso Duca degli Abruzzi, Torino 10129, Italy

[c] CNR-IEIIT – 24 Corso Duca degli Abruzzi, Torino 10129, Italy

* Corresponding author: Tel. +39 011 090 4465
e-mail address: enrico.fabrizio@polito.it

Abstract

Freezing is one of the most widely used and effective processes to preserve foods shelf-life during long periods of time. This paper focuses on very low temperature freezing, and a thermal model, based on literature formulations, was developed to calculate the food freezing time considering several kinds of food, with different sizes, shapes and chemical composition. Moreover, once evaluated the food freezing time as a function of temperature and velocity of the cooling fluid, a chart reporting the food production rate, the freezing time and the cooling

capacity was developed to properly design the freezing equipment in terms of optimal choice of the process and type of freezer.

Keywords: Low temperature freezing, Food freezing time, Freezing process design.

1. Introduction

Every year, a huge amount of food is produced to satisfy the demand of consumers, which number is high and still rising. Nowadays, legislations concerning food storage methodology are becoming more restrictive in terms of final quality of food products and of transformation (Biglia et al., 2015) and storage processes efficiency. In this scenario, freezing assumes a relevant role, as it is a suitable method to retard food deterioration preserving, in the meanwhile, the food organoleptic properties (Castro-Giráldez et al., 2014).

Traditional industrial food freezers are based on air-blast system technology (Dempsey and Bansal, 2012), where cold air (the medium fluid) is adopted, due to its cheapness and the low risk of food contamination, to reduce the food temperature below the freezing point, until reaching a final temperature of about -18 °C in the inner part of the product. Typically, the medium fluid temperature varies from -40 °C to -20 °C, with a velocity that ranges between 1 and 6 m/s depending on the kind, size and shape of the food product to be processed. Food can be frozen through a batch process in a closed and insulated freezing room or an in-line process in a freezing tunnel.

A relevant factor affecting the final quality of frozen food products and, thus, the design of the food industry plant equipment, is the freezing time. This parameter is deeply conditioned by the food chemical composition, in terms of water content and percentage of soluble and insoluble solids (ASHRAE refrigeration, 2010), and by the properties of the medium fluid. During the freezing process, the phase change of the liquid content of food does not occur at constant temperature. Indeed, when the freezing process begins at the initial freezing temperature T_f, due to the crystallization of a portion of water, the concentration of solute in the remaining aqueous solution increases, thus reducing the freezing point of the unfrozen portion of the food. This phenomenon gradually leads to lower the temperature

required to maintain and continue the freezing process, until the complete freezing of the product is reached. In this process, the ice fraction x_{ice} of food is an important parameter describing the variable food thermal properties. Quick-freezing process, using a medium at very low temperature (even under -90/-80 °C), can assure the quickly turning of the water contained in the food into minute ice crystals, avoiding damaging the food cell membranes (Kim et al., 2015), as it may happen during freezing at standard temperature (-40/-20 °C).

Usually, very quick-freezing processes are obtained by the adoption of a cryogenic fluid or of the impingement technology, as discussed in literature. In the work of Agnelli and Mascheroni (2001), a cryogenic immersion freezer (using liquid nitrogen) coupled with an air-blast freezer (using air as medium fluid) was studied. The simulations and experimental results confirmed that reduced freezing time that can be obtained using medium fluids at a cryogenic temperature. The benefits of cryogenic freezing technique on the quality of frozen storage, in comparison with traditional air-blast systems, were also evaluated by Rodezno et al. (2013) and by Kim et al. (2015), where systems using a liquid carbon-dioxide and a liquid solution of calcium chloride were respectively studied. The cryogenic immersion technique allows to increase the heat transfer coefficient, thus reducing the freezing time, but its adoption is limited by the high cost of the liquid fluids and by the kind of food. Liquid nitrogen can also be adopted in tunnel freezers where, by means of particular nozzles, it is usually injected in proximity of the conveyor belt where food is placed to be processed. Here, absorbing a great quantity of heat by evaporation, the nitrogen cools down the tunnel at very low temperature. Alternatively, a favourable reduction of the freezing time can be achieved by impingement technology, which consists in using high velocity air jets (50÷100 m/s) directly to the food surface, with an air temperature usually equal to -20°C (Salvadori and Mascheroni, 2002). Even if this technique allows to reach freezing times comparable to those obtained by using cryogenic techniques, it can be applied only to limited kinds of foods, characterized by a high ratio surface/volume (such as peas, slices of vegetables or meat etc.).

A valuable alternative to cryogenic techniques and to the impingement is represented by air-blast freezing at very low temperatures, with values of around -90/-80 °C. Values of temperature in this range can be achieved, for example, coupling the freezer with a reversed Brayton cycle (Foster et al., 2011), where the fluid in this particular thermodynamic cycle can reach a temperature of about -140/-120 °C. In this paper, a thermal model, based on the Pham formula (Pham, 1984), of the freezing process with air-blast system at very low temperature is presented, which allows to evaluate the food freezing time and the proper design of the freezing equipment. This model can be applied to a wide set of food products: depending on the particular food size, shape, composition (USDA, 1996) and relative direction of the cooling air, the heat transfer coefficient between the medium and the food product has been evaluated by different formulation. A representative set of three food samples have been selected to describe the application of the proposed methodology. Indeed, the most suitable freezing process, in terms of type and mode (in-line process in tunnels, by batch in closed insulated rooms), can be determined depending on the peculiar food geometry and/or the available cooling capacity of the freezing plant and/or the medium fluid properties.

2. Thermal model

During freezing, foods are cooled by removing sensible and latent heat by means of a cooling medium. The process is a heat conduction problem, during which a phase change occurs inside the food product. The entire process can be divided into three steps: (1) food is pre-cooled from its starting temperature T_1 to the initial freezing temperature T_f (sensible heat); then (2) water contained in the food starts to solidify (latent heat) and finally (3) food is sub-cooled, until reaching the desired final temperature T_2 (sensible heat).

2.1. Food and medium fluid properties

Thermal properties of foods, essential for describing the dynamics of the freezing process, are strictly dependent on the composition and on the temperature of the product. The set of the main constituents of a food can be summarized as: water, proteins, fats, carbohydrates, fibre and vitamins. Foods composition, in terms of shares of each constituent, can deeply vary

among different kind of food, but also, at a minor scale, within the same class of products, depending on the current quality and/or on the adopted recipe. The properties of foods (such as density, specific heat, etc.) can be thus evaluated as a combination of the properties of each constituent, which are estimated by relations proposed by Choi and Okos (1986), as a function of the food temperature.

The freezing process is also influenced by the properties of the cooling medium. Indeed, the heat exchange is affected by the temperature and the velocity of the cooling medium. In the proposed thermal model, foods are cooled by air whose properties were evaluated by using the REFPROP database (NIST, version 9.1).

2.2. Determination of the heat transfer coefficient

The heat transfer coefficient h between the food and the cooling medium is a relevant parameter of the freezing process, since it describes the effectiveness of the heat exchange. It depends on the shape, size and kind of food and on the temperature and velocity (modulus and direction) of the medium fluid and can be calculated from the Nusselt number Nu. Modelling the food shape using elementary geometric forms (cylinder, sphere, flat plane, etc.) allows evaluating Nu by empirical formulations as a function of the Reynolds (Re) and Prandtl (Pr) numbers.

For example, in the case of food with a prevalent flat surface (e.g. slices of fruits or vegetables, hamburgers etc.) and a tangential direction of the medium fluid, Nu can be approximately calculated as (Holman, 2010):

$$\begin{cases} Nu = 0.037 Re^{0.8} Pr^{1/3} & \text{with } 5 \cdot 10^5 \le Re \le 10^7 \text{ and } 0.6 \le Pr \le 60 \\ Nu = 0.664 Re^{0.5} Pr^{1/3} & \text{with } Re < 5 \cdot 10^5 \end{cases} \quad (1)$$

For cylindrical shape volumes (e.g. carrots, sausages, cucumbers etc.) and medium fluid perpendicular to the lateral surface, Churchill and Bernstein equation (Holman, 2010) should be adopted

$$Nu = 0.3 + \frac{0.62 Re^{0.5} Pr^{1/3}}{(1 + (0.4/Pr)^{2/3})^{1/4}} \left(1 + (Re/282000)^{5/8}\right)^{4/5} \quad (2)$$

with $Re \cdot Pr > 0.2$

while for spherical items (e.g. peas, cherries, blueberries etc.), the Whitaker's formula (Holman, 2010)

$$Nu = 2 + \left(0.4Re^{0.5} + 0.06Re^{2/3}\right)Pr^{0.4}\left(\frac{\mu_{\text{medium}}}{\mu_{\text{food}}}\right)^{1/4} \quad (3)$$

with $3.5 \leq Re \leq 8 \cdot 10^4$ and $0.7 \leq Pr \leq 380$

should be used. Once Nu is defined, h can be easily obtained as

$$h = \frac{Nu \cdot k}{l} \quad (4)$$

where k and l are respectively the thermal conductivity and characteristic length of the food item.

2.3. Freezing time formulation

Freezing time τ, an important descriptive index of a freezing process of foods, is strictly related to the final quality of frozen food products, and its estimation is an aid to the plant designing phase in food industry. It can be calculated by the governing equation of a heat conduction problem, which can be written by using the Fourier's law, without internal heat generation,

$$\rho c_{\text{p}} \frac{\partial T}{\partial t} = \nabla(k \nabla T) \quad (5)$$

With the following assumptions: (1) in the case of a one-dimensional and steady-state problem; (2) considering only the latent heat that has to be removed from the food; (3) without taking into account the sensible heat needed to cool down the food from T_1 to T_{f} (pre-cooling stage) and from T_{f} to T_2 (sub-cooling stage); (4) assuming the temperature and the thermal properties of the product being constant during the phase change, the freezing time formula proposed by Plank is

$$\tau_{\text{plank}} = \frac{L}{T_{\text{f}} - T_{\text{m}}}\left(\frac{PD}{h} - \frac{RD^2}{k}\right) \quad (6)$$

where L is the latent heat, T_{f} the initial freezing temperature, T_{m} is the medium fluid temperature, h is the heat transfer coefficient, k is the thermal conductivity, P, R and D are shape food factors (for more detail see ASHRAE refrigeration, 2010).

To overcome Plank's formulation limits, Pham proposed a formulation (Pham, 1984) where the sensible heat released by the food during pre-cooling and sub-cooling stages is considered. In addition, a mean freezing temperature T_2, supposed to be 1.5 K below the initial freezing

temperature T_2, has to be adopted to consider the effect of the temperature variation during the food phase change. The here adopted Pham's formulation is

$$\tau_{\text{pham}} = f_{\text{pham}} \sum_{\text{i}=1}^{3} \tau_{\text{i}} \tag{7}$$

where τ_1 represents the time required to reduce the temperature from T_1 to T_{f} (pre-cooling), τ_2 the time required to freeze the food and τ_3 the time to reduce the temperature from T_{f} to T_2 (sub-cooling). The correction factor f_{pham}, proposed by Pham (2014), was introduced to take into account the effects of medium fluids at very low temperature ($\ll -40$°C) and it can be expressed as

$$f_{\text{pham}} = 1 + 0.41 R_{\text{T}}^{0.5} (1 - e^{-Bi}) \tag{8}$$

where R_{T} is the ratio between the food freezing temperature T_{f} and medium fluid temperature T_{m} while Bi represents the Biot number of the foods. More in detail, each time τ_{i} can be calculated as

$$f_{\text{pham}} = \frac{Q_{\text{i}}}{h A_{\text{s}} \Delta T_{\text{m,i}}} \left(1 + \frac{Bi_{\text{i}}}{k_{\text{i}}}\right) \tag{9}$$

where: Q_{i} represents the heat to be extracted during each stage; h the mean heat transfer coefficient between food product and the medium fluid; A_{s} the food heat exchange surface; $\Delta T_{\text{m,i}}$ the mean logarithmic temperature difference during the different freezing stages; Bi_{i} is the Biot number; k_{i} the Pham's formula coefficient. Parameters Q_{i}, $\Delta T_{\text{m,i}}$ and k_{i} can be evaluated according to ASHRAE refrigeration book (2010). Once defined the initial and the final food temperature T_1 and T_2 of the freezing process, the heat Q_{i} only depends on the properties of the food product, in particular specific heat and density, and on the volume of the food item. The effect of the food shape on the freezing process is integrated within the mean heat transfer coefficient h, the Biot number Bi and the heat exchange active surface A_{s}.

For a fixed couple of values of T_{m} and v_{m}, the freezing time is thus deeply affected by both the composition and the geometry/size of the food product: the first affects the properties of the food, while the second is involved in the heat exchange. For example, foods with a great content of

unbound water, which has specific heat higher than other constituents, a longer freezing time τ is required, with respect, for example, to fat-rich food. The geometry/size of foods, instead, affects the heat exchange in term of the ratio between external surface, brushed by the cooling medium, and volume: products with a higher ratio, such as small sized or thin sliced items, reach really shorter freezing times with respect to the others.
It should be noted that, for a given food product, considering a constant initial and a final temperature T_1 and T_2 and a fixed relative direction of the cooling medium respect to the product surfaces, the freezing time τ can be expressed as a function of the sole medium temperature T_{m} and velocity v_{m}.

3. Application to the design of the freeze process

The selection of the proper parameters for the freezing process design is not a trivial task since favourable conditions for a profitable food process has to be guaranteed while fulfilling possible technical specifications and requirements of the existing facilities of the factory. The final quality of frozen foods is related to the resulting freezing time τ that, in the case of adequate placement into the freezer (for example, number of products on a single tray, etc.) that limits the thermal interaction among single food items during the freezing process, is only affected by the characteristics of the cooling medium. In this situation, the most appropriate freezing time for a specific food can be obtained by finding the proper balance between medium temperature T_{m} and velocity v_{m}. Obviously, T_{m} and v_{m} must satisfy the technical features of the plant and the food characteristics, not exceeding, for example, a maximum medium velocity to avoid food freezing-burn: this constraint is particular limiting in the case of high volume items. Therefore, the freezing process at very low temperature -90/-80 °C plays an important role, allowing to obtain fast freezing processes for a wider set of food products.
Given the food production rate G of the plant, which is the mass of food that is processed per unit of time (kg h^{-1}), the overall cooling capacity Q_{c} of the freezing plant can be easily computed as

$$Q_{\mathrm{c}} = G \cdot \Delta H \tag{10}$$

where ΔH is the difference in food specific enthalpy (ASHRAE refrigeration, 2010) between the initial value at a temperature of the food T_1 and the final value at temperature T_2. It can be noted that the required cooling capacity Q_c is not affected by the medium properties, but it is only related to the type of food, in terms of composition of constituents, characterized by different properties and, thus, different enthalpy difference ΔH. With the objectives of assuring a certain productive capacity G, and at the same time guaranteeing a freezing process with the more appropriate conditions, the freezing plant has to be designed to provide the appropriate cooling capacity Q_c, which allows the medium temperature T_m to be maintained constant.

Once the most suitable freezing time τ has been evaluated on the base of the type of food, the selection of the more appropriate configuration of the freezing equipment, in terms of choice between a batch or an in-line process, can be performed evaluating the size of the batch lot M, defined as

$$M = G \cdot \tau \tag{11}$$

Indeed, in case of foods with particularly short freezing times, a batch process, where products are frozen by lots in a closed and insulated room, with loading and un-loading procedures, is not recommended. In this case, the batch freezing process results in a sequence of too short cycles, during which a small mass of product M is processed. Since the time required to the loading and unloading procedure of lots into and out of the freezing room will affect the overall cycle timing, it results in an inefficient management of the freezing plant. In this case, an in-line process, in which foods are processed in freezing tunnel on a conveyor belt, is more advantageous and recommended.

In case of in-line processes, the required food production rate G and freezing time τ of the product must be assured by the properly set-up of the width and the velocity of the conveyor belt and of the freezing tunnel length. The adoption of this configuration is limited, however, to values of freezing times that assure the constructive feasibility of the tunnels. Indeed, long freezing times can be obtained by both increasing the tunnel length or reducing the conveyor velocity, but, in order to guarantee the

required food production rate G, a too low velocity of the belt will lead to an excessive belt width. In the last case, a batch process should be preferred.

For a batch process, particularly relevance resides in the mass of the batch lot, which can be processed in the insulated room with a particular set of temperature T_{m} and velocity v_{m} of the cooling medium, and cooling capacity Q_{c} of the freezing plant. With this aim, a chart of the batch lot size has been defined (see Fig. 1b), in which iso-mass curves has been calculated as a function of the food production rate G, freezing time τ and of the cooling capacity Q_{c}. Therefore, given the production capacity G, the required cooling capacity Q_{c} can be easily obtained and, moreover, depending on the desired freezing time τ (or cooling medium temperature T_{m}), the proper size of the lot to be processed by batch can be obtained.

4. Case studies

The analysis of the trade-off between a batch process or an in-line process is here applied to three different case studies: (1) sausages, (2) peas and (3) slices of pineapple. The selected products represent different foods in terms of composition, size and shape. For each sample, standard values of composition (USDA, 1996) were adopted and the shapes were approximated by elementary geometric objects, depending on the heat exchange surface: a cylinder for the sausage, a sphere for the pea and a flat plate for the slice of pineapple. Air was selected as medium fluid since its cheapness, large availability and low risk of contaminating foods. Composition and shape data of the selected foods are reported in Table 1.

Table 1. Composition of food products and geometrical data.

	Sausage	**Pea**	**Pineapple**
Moisture fraction content: x_{wa} [%]	51.08	78.86	86.50
Protein fraction content: x_{pr} [%]	14.25	5.42	0.39
Fat fraction content: x_{ft} [%]	31.33	0.40	0.43
Carbohydrate fraction content: x_{ca} [%]	0.65	14.46	12.39
Fiber fraction of carbohydrate: x_{fb} [%]	0.00	5.10	1.20
Other fraction content: x_{ot} [%]	2.70	0.86	0.29
Bound water fraction: x_{bw} [%]	$0.4 \cdot x_{\mathrm{pr}}$	$0.4 \cdot x_{\mathrm{pr}}$	$0.4 \cdot x_{\mathrm{pr}}$
Initial temperature: T_1 [°C]	5	5	5

Initial freezing temperature: T_f [°C]	-1.7	-0.6	-1.0
Final temperature: T_2 [°C]	-18	-18	-18
Latent heat: L [kJ kg^{-1}]	171	263	289
Radius [cm]	1.25	0.3	5.5
Height [cm]	10	-	1.0

The results are reported into two types of charts that are related by reporting the same freezing time. The first one (Figs. 1a-3a) reports the freezing time as a function of the medium temperature and of the medium velocity. The second one (Figs. 1b-3b) reports the freezing time as a function of the food production rate and the cooling capacity. On this chart, iso-mass curves representing the batch size are also drawn. Once identified a suitable range of freezing time, as a function of the medium temperature and velocity on the first chart, it is possible to pass to the second chart where, the batch size lot can be found intersecting the same freezing time range with the desired food production rate. These charts were computed to determine the adequate lot size as a function of freezing time and of the desired food production rate G. For example, the vertical line indicated in Figs. 1b-3b is representative of all the different combination of design parameters (medium velocity and temperature) that assure a certain food production rate into a certain freezing time and that can be found on the first chart.

In particular, the time τ required to cool down and freeze the selected food products, from an initial temperature T_1 equal to 5°C until reaching a final temperature T_2 of -18°C, was evaluated with a medium temperature T_m and velocity v_m varying within the ranges (-110/-30 °C) and (0.4/20 m s^{-1}) respectively. In Figs. 1a-3a the resulting freezing time values τ for sausages, peas and slices of pineapple are reported as function of T_m and organized by curves for a set of discrete values of v_m. With the operative ranges, in terms of T_m and v_m, of an air-blast freezing system at very low temperature (Foster et al., 2011), highlighted by grey areas in Figs. 1a-3a, the freezing time of sausages, peas and slices of pineapple results to be within the ranges of (7/14), (0.7/1.5) and (14/28) minutes respectively.

It can be observed that, for low air velocity values, a reduction of the air temperature involves a remarkable decrease in the freezing time. Comparing the obtained freezing time of the selected food samples, the

effects of the food composition and of the geometry/size on the heat exchange (between food and cooling air) can be observed. In particular, the effect of the food composition can be easily identified comparing the behaviour of sausages (Fig. 1a) and slices of pineapple (Fig. 3a), which are food samples with a remarkable difference in the water content. In the case of the first sample, the same temperature difference $T_2 - T_1$ can be obtained in a significantly shorter time (about half time) with respect to the second one. Whereas, the effect of the geometry/size of different foods on the heat exchange is particularly evident in the freezing of peas (Fig. 2a), where shorter times, with also an order of magnitude of reduction, can be achieved comparing to product with a lower ratio surface/volume, such as slices of pineapple (Fig. 3a), a food product with different shape but a similar content of unbound water.

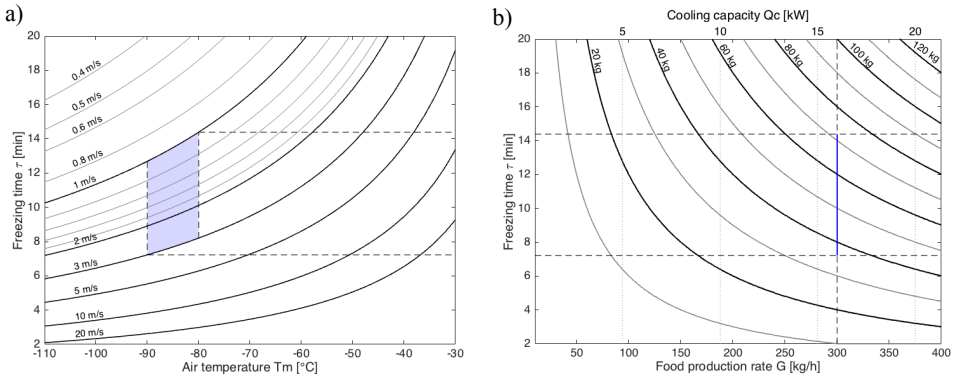

Fig. 1. Food sample: Sausage. (a) Freezing time as a function of air temperature and velocity. (b) Chart for freezing process design.

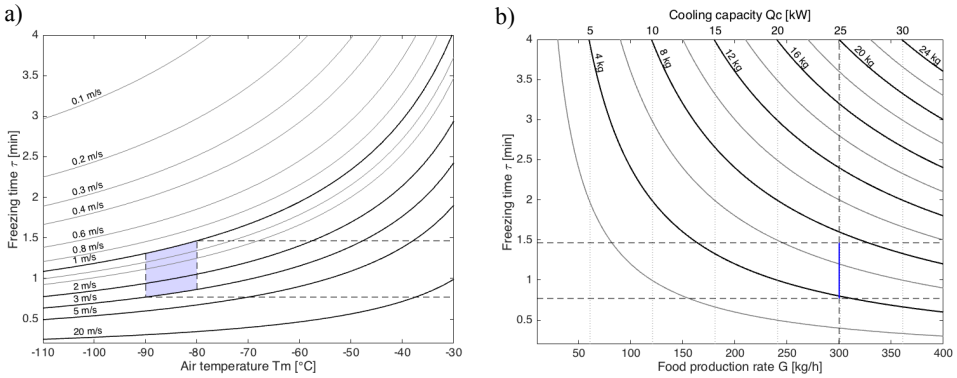

Fig. 2. Food sample: Pea. (a) Freezing time as a function of air temperature and velocity. (b) Chart for freezing process design.

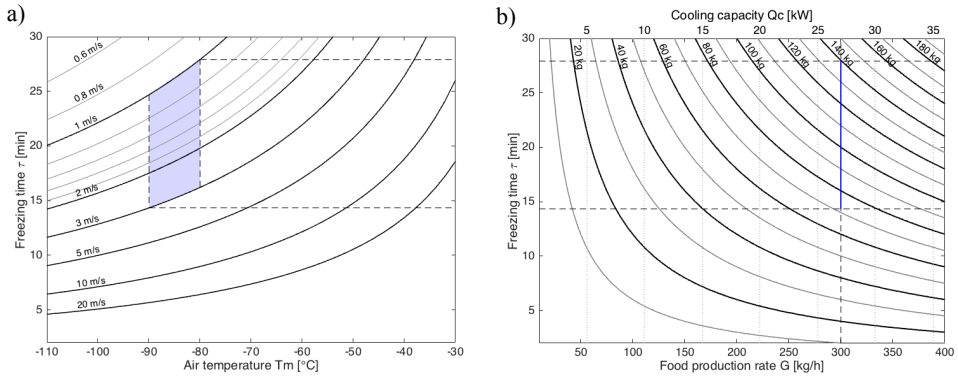

Fig. 3. Food sample: Pineapple. (a) Freezing time as a function of air temperature and velocity. (b) Chart for freezing process design.

The second chart can be used to size the freezing plant and to verify the options of using a batch or tunnel process. With the aim to freeze a certain quantity of food per unit of time G ensuring, at the same time, the maintenance of the more appropriate process environment (in terms of constant value of the medium temperature T_{m}), the designed freezing plant equipment must, of course, provide a suitable cooling capacity Q_{c}. Consider, for example, a plant with a desired food production rate G of 300 kg h^{-1}: the differences in contents composition of food samples deeply affect the required cooling capacity Q_{c}, which results in 16 kW for sausages (Fig. 1b), 25 kW for peas (Fig. 2b) and 27 kW for slices of pineapples (Fig. 3b). Once the ranges of freezing time τ for each food sample (highlighted by horizontal dashed lines in Figs. 1a-3a), obtained by the proper trade-off between values of T_{m} and v_{m}, has been determined, the most adequate lot size, in term of mass of food product, can be evaluated. At this point, the freezing time is uniquely determined and plays a key role in deciding whether a batch or in-line process should be used. Processing all the three food samples in the same environment (with medium temperature within the range (-90/-80 °C) and velocity of (1/3 m s^{-1}), the size of the required lot M, derived by Eq. (11), are determined to be in the range (35/70 kg) for sausages (Fig. 1b), (4/7 kg) for peas (Fig. 2b) and (70/140 kg) for slices of pineapple (Fig. 3b). In the case of peas, for example, a batch process is not reasonable.

5. Conclusions

In this work, useful charts for designing a low temperature freezing process and apprising the trade-off between the various design parameters (freezing time, cooling capacity, medium temperature, food production rate and type of food product) were determined. The developed methodology and the charts can be assists during the design of new industrial food freezers plants, being also a profitable aid in choosing between batch processes, where foods are frozen by lots in a closed and insulated room, or in-line ones, in which food is processed in freezing tunnel on a conveyor belt. Moreover, the thermal model adopted can be applied to all type of food products.

References

Agnelli ME, Mascheroni RH. Cryomechanical freezing. A model for the heat transfer process. *J Food Eng* 47 (2001) pp. 263-270.

ASHRAE. Refrigeration ASHRAE Handbook. (2010) ISBN 978 1 933742 82 3.

Biglia A, Fabrizio E, Ferrara M, Gay P, Ricauda Aimonino D. Performance assessment of a multi-energy system in a food industry. *Energy Procedia* 82 (2015) pp. 540-545.

Castro-Giráldez M, Balaguer N, Hinarejos E, Fito PJ. Thermodynamic approach of meat freezing process. *Innov Food Sci Emerg* 23 (2014) pp. 138-145.

Choi Y, Okos MR. 1986. Effects of temperature and composition on the thermal properties of foods. *Food Engineering and Process Applications* 1 (1986) pp. 93-101.

Dempsey P, Bansal P. The art of air blast freezing: Design and efficiency considerations. *Appl Therm Eng* 47 (2012) pp. 71-83.

Foster AM, Brown T, Gigiel AJ, Alford A, Evans JA. Air cycle combined heating and cooling for the food industry. *Int J Refrig* 34 (2011) pp. 1296-1304.

Holman JP. Heat Transfer. 10th ed. New York: McGraw-Hill Series in Mechanical Engineering (2010).

Kim BYH, Liesse C, Kemp R, Balan P. Evaluation of combined effects of ageing period and freezing rate on quality attributes of loins. *Meat Sci* 110 (2015) pp. 40-45.

NIST Reference Fluid Thermodynamic and Transport Properties Database: Version 9.1. National Institute of Standards and Technology (Standard Reference Data). United States Department of Commerce. Gaithersburg, Maryland.

Pham QT. An extension to Plank's equation for predicting freezing times for foodstuffs of simple shape. *Int J Refrig* 7 (1984) pp. 377-383.

Pham QT. Freezing time formulas for foods with low moisture content, low freezing point and for cryogenic freezing. *J Food Eng* 127 (2014) pp. 85-92.

Rodezno ELA, Sundararajan S, Mis Solvan K, Chotiko A, Li J, Zhang J, L. Alfaro, et al. Cryogenic and air blast freezing techniques and their effect on the quality of catfish fillets. *LWT- Food Sci Technol* 54 (2013) pp. 377-382.

Salvadori VO, Mascheroni RH. Analysis of impingement freezers performance. *J Food Eng* 54 (2002) pp. 133-140.

USDA. Nutrient database for standard reference. (1996) release 11. U.S. Department of Agriculture, Washington D.C.

6. Energy monitoring and systems simulation

6.1. Fourth paper

International Journal of Refrigeration (Article in press)

DOI: 10.1016/j.ijrefrig.2017.10.022

Temperature and energy performance of domestic cold appliances in households in England

Alessandro Biglia [a], Andrew J. Gemmell [b], Helen J. Foster [b], Judith A. Evans [c,*]

[a] DiSAFA – Universitá degli Studi di Torino, 2 Largo Paolo Braccini, Grugliasco (TO) 10095, Italy

[b] BRE – Bucknalls Lane, Garston, Watford, Hertfordshire WD25 9XX, United Kingdom

[c] School of the Built Environment and Architecture – London South Bank University, Churchill Building, Langford, Bristol BS40 5DU, United Kingdom

* Corresponding author: Tel. +44 (0)117 928 9300
e-mail address: j.a.evans@lsbu.ac.uk

Abstract

This paper reports the results of a large-scale survey in which 998 cold appliances were monitored in 766 properties in England. No surveys published to date analyse such a large dataset, which includes data on ambient temperature, cold appliance temperature (refrigerator and/or freezer) and electricity consumption of the cold appliance.

Simultaneous measurements of the temperature inside and outside of the cold appliances and the electricity consumption were taken over a period of seven days during a nine-month period in 2015. An interview was also conducted with the householders to collect further information about the cold appliances and their usage patterns.

The cold appliances monitored in the work included fridge-freezers (52%), refrigerators with ice-box (6%), larder fridges (14%), chest freezers (9%) and upright freezers (19%). It was found that for all monitored cold appliances with valid data that: the mean ambient temperature was 18.5°C;

the mean refrigerator temperature was 5.3°C; the mean freezer temperature was -20.3°C; and the mean electricity consumption was 354 kWh per year. Significant differences between the electricity consumption of different types of cold appliance were determined from statistical analysis.

Keywords: Survey, Domestic households, Refrigerator, Freezer, Temperature, Electricity consumption, England.

Nomenclature

n/a	not available
se	standard error
σ	standard deviation
ANOVA	analysis of variance
HRP	household reference person
N	number of samples
RSL	registered social landlord

1. Introduction

Domestic refrigerators and freezers are generally operated using a vapour compression thermodynamic cycle and many researchers have focused their work on increasing the energy efficiency of these appliances. The main parameters affecting the electricity consumption of cold appliances can be divided into two main groups: (1) technical features, for example air flow distribution, type of thermodynamic cycle, type of refrigerant, type of insulation used to reduce the heat gains, etc.; (2) cold appliance operation, for example number of door openings, ambient temperature, thermostat set point, and quantity/temperature of products placed in the appliance, etc.

1.1. Technical features

Concerning the first group, studies by researchers such as Avci et al. (2016), Belman-Flores et al. (2014), Kumlutaş et al. (2012), Laguerre et al. (2010), Amara et al. (2008), Gupta et al. (2007) and Laguerre et al. (2007) have used CFD (Computational Fluid Dynamics) models to identify and optimise the main design parameters, thermal stratification and air flow issues so as to improve the energy efficiency of domestic cold appliances. Other researchers such as Yang et al. (2015) have developed

new refrigeration cycles based on a 2-stage vapour compression cycle. Yoon et al. (2013) showed that the choice of insulation, in terms of type of material and thickness, enabled high energy savings to be achieved. For example, by using vacuum insulated panels instead of standard polyurethane foam insulation, 5-10% of the energy could be saved as reported by Hammond and Evans (2014).

Regarding different types of refrigerants, new European regulations of the European Parliament and Council (2014) restrict the use of high GWP (Global Warming Potential) refrigerants. Although the majority of refrigerated appliances in Europe operate using hydrocarbon refrigerants (e.g. R600a) there is still ongoing work to replace R134a as a refrigerant in locations where hydrocarbons are not generally accepted, with work being undertaken by Aprea et al. (2016), Joybari et al. (2013) and Mohanraj (2013) to investigate replacements for R134a. Most refrigerants used in domestic refrigerators are azeotropes (they boil at a constant temperature) but it has been suggested that zeotropic refrigerants that have a wide temperature glide (they boil over a wide temperature range) could have advantages in domestic refrigerators, particularly in providing different temperatures in specific compartments. Mohanraj et al. (2009) showed a reduction of around 12% in electricity consumption when using a zeotropic mixture composed of R290 and R600a instead of R134a.

Research is also increasing into developing new refrigeration systems able to exploit the use of an ejector in a refrigeration cycle for domestic appliances, so as to improve cycle performance. The ejector is a component that expands a high-pressure primary substance to absorb a secondary substance at a pressure slightly above the low pressure reached by the primary substance. In refrigeration cycles, the two substances are identical, so both flows mix together leading to mixture pressure increase due to the change of the flows momentum. For example, Liu et al. (2015), Wang and Yu (2015) and Wang et al. (2014) have proposed a modified ejector-expansion refrigeration cycle for domestic appliances; the results showed that the new system could reduce the electricity consumption compared to the conventional domestic refrigerator-freezer by 5-7%.

Other important technical features of a domestic appliance that may impact the electricity consumption, are the evaporator defrosting cycle and the

design of the door gaskets. Automatic defrosting of domestic refrigerated appliances is normally fixed, for example after a certain number of on-cycles of the compressor. However, the need for defrosting can be predicted and initiated only when required, thus leading to the avoidance of excessive defrosting and electricity consumption associated with defrost cycles. For example, Modarres et al. (2016) showed that an adaptive defrost when compared to a fixed defrost cycle could reduce the electricity consumption by up to 12.5%. Door gaskets for refrigerators are generally based on magnetic strips encased in flexible plastics such as polyvinyl chloride (PVC). The magnetic strip is attracted to the metal outer case of the refrigerator and pulls the soft flexible plastic against it to form a seal. Inefficiencies include air gaps where the seal is not well formed, heat conduction through the plastic and metal, and over time damaged or stressed areas of the seals can fail. Also, Gao et al. (2017) investigated the total effective heat leakage at the refrigerator gasket with the average effective heat leakage at the door gasket region estimated to be 0.2 W/m.K, which corresponded to 14% and 17% of the total energy used by the fresh food and freezer compartments respectively.

1.2. Cold appliance operation

Real operating conditions of appliances are difficult to test in the laboratory as the behaviour of householders is quite varied. Limited information is available on the number of times appliance doors are opened, the types and temperature of the food placed in the appliance and the ambient temperature around the appliance (which does not remain constant over time). According to Gilbert et al. (2007) the temperature of food stored in refrigerators should be in the range of 1-5°C. Over the past 30 years there have been a large number of surveys on temperatures in domestic refrigerators. In some cases, it is very clear how temperatures were measured, which sensors were used, the position of the sensors and for how long the measurements were carried out. In other cases, insufficient information is available to adequately compare information. James et al. (2008) reviewed available information from 20 papers on temperatures in domestic refrigerators. They concluded that many refrigerators were running at higher than recommended temperatures.

Since 2008, there have been several papers published on temperatures in domestic refrigerators (James et al. (2017), Roccato et al. (2017), Hassan et al. (2015), Evans et al. (2014), Geppert (2011), Landfeld et al. (2011) and WRAP (2009)). These generally concur with the results from the James et al. (2008) review. An average temperature in UK refrigerators of 5.2°C was obtained in a survey reported by Geppert (2011). In the same survey the authors found higher mean refrigerator temperatures in France (6.7 °C) and Germany (6.2 °C) but lower mean refrigerator temperatures in Spain (4.1 °C). Roccato et al. (2017) presented data from previously published surveys but divided the data into northern and southern Europe. In southern Europe, the mean refrigerator temperature was 7°C whereas in southern Europe the mean refrigerator temperature was 6.1°C. Temperature measurements in domestic refrigerators and freezers were reported in the work of Evans et al. (2014). The overall mean refrigerators temperature was 4.4°C while the minimum and the maximum mean were -0.6°C and 10.4°C. Overall the refrigerators spent 58% of the time above the recommended temperature of 5°C. The overall mean temperature in the freezers was -20.1°C while the minimum and the maximum mean were -41.1°C and -11.1°C respectively, with 32% of the time spent over the recommended temperature of -18°C.

Higher temperatures in refrigerators may have an impact on food quality and safety. Surveys on the hygienic status of domestic fridges have found that 52% of refrigerators contained at least one pathogen (Kennedy et al. (2005)). A higher general incidence of pathogens and higher APCs (total aerobic plate counts) were found in the refrigerators of urban consumers than those of rural consumers, and consumers under 25 were more likely than older consumers to have one or more pathogens present in their refrigerators.

The internal compartment temperature of a domestic refrigerator not only affects the quality of the food stored in the appliance but also the electricity consumed by the appliance. Several regulations have been put into place over the last 25 years by the European Commission related to appliance electricity consumption (ecodesign and energy labelling Directives) but it is not known whether these translate energy savings in a laboratory environment into savings in the home.

There is very limited published information detailing comprehensive information on temperature control in appliances, and ambient temperature conditions combined with electricity consumption in real life conditions. In this paper, results from a recent survey in England are reported (Gemmell et al. (2017)). The survey involved 998 domestic refrigerators and freezer appliances and the following were monitored: (1) ambient temperature of the room where the appliance was installed; (2) internal appliance compartment temperature; (3) power consumption. Householders were also questioned about the management of their appliance with respect to door openings, quantity of food loaded in the appliance and shopping habits. Appliance models were also recorded in order to evaluate storage volume and surface area of the appliances. Using this detailed information, analysis was completed to assess the relationship between temperature control and electricity consumption, by investigating the impact of appliance features and occupant behaviour.

2. Materials and methods

2.1. Overview of field trial design

A large-scale survey was conducted across England in which 998 cold appliances were monitored in 766 properties. Data was collected over a period of 9 months, from March to November 2015. There were four waves of data collection, each lasting between three and five weeks: (1) Wave 1 - March; (2) Wave 2 - from April to June; (3) Wave 3 - from July to August and (4) Wave 4 - from October to November.

Simultaneous measurements of the temperature inside and outside of the cold appliances, as well as the electricity consumption were taken over a period of seven days. The cold appliances monitored in the work included: (1) Fridge-freezers; (2) Refrigerators with an ice-box; (3) Larder fridges; (4) Chest freezers and (5) Upright freezers. A diagram showing the types of cold appliance assessed is shown in Fig. 1. Table 1 presents the numbers of each type of cold appliance with valid monitoring data. In addition to data collection, an interview was conducted with the householders to collect information to understand how cold appliances were used and maintained.

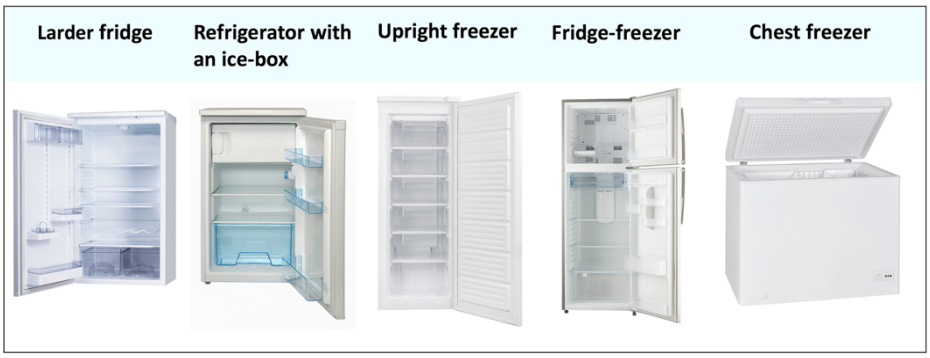

Fig. 1. Different types of cold appliance monitored in the survey.

2.2. Data collection method

The sampling frame used was formed from cases originally surveyed as part of the English Housing Survey (EHS). This replicates a well-established and successful procedure used for previous similar surveys, such as the Energy Follow-Up Survey conducted in 2011 (Hulme et al. (2014)).

Interview and monitoring data was collected by interviewers. On the first visit to each property the interviewers installed the monitoring equipment and conducted the householder interview. One week later they returned to remove the equipment and data was downloaded ready for analysis. The appliances were monitored for seven days to ensure the data reflected the performance of the cold appliances as accurately as possible.

Table 1. Numbers of cold appliances in each wave of the survey (percentage values in brackets).

Appliance type	**Wave 1**			**Wave 2**		
	Rf sec [a]	Fz sec [b]	El [c]	Rf sec [a]	Fz sec [b]	El [c]
Fridge-freezer	97 (77)	93 (60)	76 (56)	82 (67)	78 (55)	82 (51)
Refrigerator with an ice-box	11 (9)	5 (3)	6 (4)	12 (10)	8 (6)	13 (8)
Larder fridge	18 (14)	n/a	13 (9)	28 (23)	n/a	21 (13)
Chest freezer	n/a	18 (12)	12 (9)	n/a	19 (13)	15 (9)
Upright freezer	n/a	39 (25)	30 (22)	n/a	36 (26)	30 (19)
Total	126	155	137	122	141	161
Appliance type	**Wave 3**			**Wave 4**		
	Rf sec [a]	Fz sec [b]	El [c]	Rf sec [a]	Fz sec [b]	El [c]
Fridge-freezer	148 (74)	140 (69)	100 (60)	156 (70)	152 (62)	109 (55)

Refrigerator with an ice-box	18 (9)	11 (5)	11 (7)	11 (5)	7 (3)	6 (3)
Larder fridge	35 (17)	n/a	18 (11)	55 (25)	n/a	31 (15)
Chest freezer	n/a	18 (9)	12 (7)	n/a	27 (11)	18 (9)
Upright freezer	n/a	34 (17)	26 (15)	n/a	60 (24)	36 (18)
Total	201	203	167	222	246	200

[(a)] Refrigeration section temperature data
[(b)] Freezer section temperature data
[(c)] Electricity consumption data

2.2.1. Data monitoring equipment used: Temperature

The temperatures both inside and outside the appliance were monitored using TinyTag Transit 2 data loggers with a monitoring range of -40°C to 70°C, a reading resolution of 0.01°C and a reading accuracy of <0.8°C between -40-0°C, and <0.4°C between 0-50°C. One data logger was placed on the middle shelf of each appliance compartment in a plastic bag and one was attached to the outside of the door of the appliance. A photograph of one of these loggers is shown in Fig. 2a.

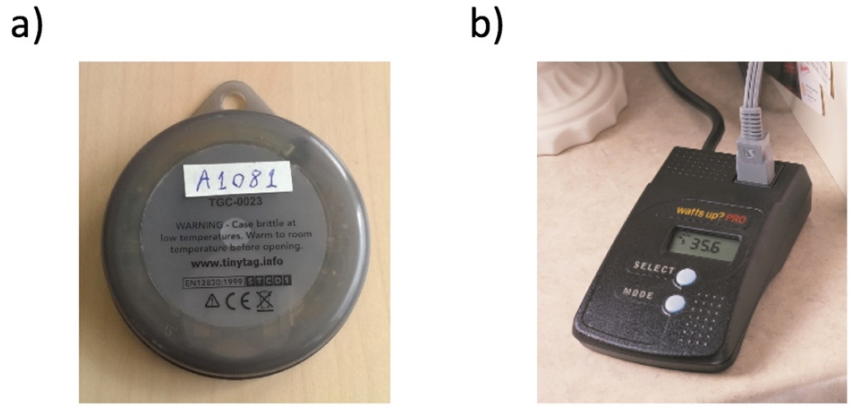

Fig. 2. TinyTag Transit 2 temperature data logger (a) and Watts Up PRO electricity consumption meter (b).

2.2.2. Data monitoring equipment used: Electricity consumption

The electricity consumption data of each cold appliance was collected using a Watts Up PRO monitor and data logger with an accuracy of +/- 1.5%. Each appliance was connected to the data logger, which itself was plugged into the wall socket. The electric power in Watts was monitored

every 30 seconds for the period the appliance was plugged in. A photograph of a Watts Up logger is shown in Fig. 2b.

2.2.3. Data monitoring: Cleaning phase

The data collected from the TinyTag and Watts Up logger for every appliance monitored were examined in detail and, where necessary, the data was cleaned to ensure that only valid and reliable data were included in the analysis. Any data which did not accurately reflect the performance of the appliance was removed prior to analysis. In addition, the data cleaning was always applied to give the longest possible period of continuous data within the profile. Only appliances for which there was at least 24 hours of continuous valid and reliable data were included in the analysis.

Cleaning of the temperature profiles was necessary where: (1) the appliances had been turned off and/or (2) the loggers had been removed from the appliances.

Cleaning of the consumption data recorded by the Watts Up monitors was required in some cases due to: (1) monitors being unplugged and plugged back in and/or (2) appliances being switched off and on by the occupant and (3) occasional faulty periods of monitoring. Faults in monitoring were evident in the data as periods where the consumption profiles recorded extreme values or zeros for portions of the data.

2.2.4. Householder interview

The householder interviews were conducted face-to-face and the occupant responses were collected on a tablet PC using a Computer Aided Personal Interviewing (CAPI) system. The interview collected data on: (1) number of occupants; (2) number, type, location and age of the cold appliances in the property; (3) how often the appliances were opened per day; (4) how full the appliances were kept; (5) how often occupants introduced warm food into the appliances; (6) how often the occupants maintained their appliance (if at all); (7) make and model of the appliances where possible; (8) energy label and size of the appliances where available. If the householders were not able to remember the exact age of the appliance an estimate was made to the nearest 5 years.

2.2.5. Participants

Data was collected at 766 households across England. Table 2 shows the sample breakdown by tenure, number of occupants, age of household reference person (HRP), and household type. It can be observed that the majority of households (56%) were owner occupied and 79% of them had 3 or less occupants with an average number of occupants per household of 2.43. The age of the householders was relatively well distributed across the age groups with an age range between 16 to over 65. The majority of participants were couples with no dependent children (34%), or couples with dependent children (20%).

2.2.6. Statistical analysis

Statistical analysis was conducted on temperature and electricity consumption data using IBM SPSS Statistics program (version 21). Data was tested for normality using a Kolmogorov-Smirnov test, and if normal parametric statistical analysis was performed by using Analysis of Variance (ANOVA). Where data was not normally distributed, non-parametric statistical analysis was used in the form of a Kruskal-Wallis test. Post-hoc tests were conducted using a Tukey test for parametric analysis, and a Mann-Whitney tests for non-parametric analysis. Significance was reported at the 95% confidence level (when $p<0.05$).

Table 2. Data about participants (percentage values in brackets).

Tenure	**N**
Owner occupied	370 (56)
Private rented	53 (8)
Local authority	107 (16)
RSL	130 (20)
Total	660 [(a)]
Number of occupants	**N**
1	216 (28)
2	266 (35)
3	122 (16)
4	101 (13)
5+	61 (8)
Total	766
Age of HRP	**N**
16-34	93 (14)
35-44	106 (16)
45-54	122 (19)
55-64	141 (21)
65 or over	198 (30)
Total	660 [(a)]
Household type	**N**
Couple, no dependent child(ren)	228 (34)
Couple with dependent child(ren)	130 (20)
Lone parent with dependent child(ren)	57 (9)
Other multi-person households	60 (9)
One person under 60	70 (11)
One person aged 60 or over	115 (17)
Total	660 [(a)]

[(a)] Only 660 households agreed to allow the information collected to be published

3. Results and discussion

3.1. Characteristics and use of monitored cold appliances

Monitoring data was collected from a total of 998 cold appliances, with valid temperature data for 938 cold appliances and valid consumption data for 665 cold appliances. Table 3 shows the breakdown of the monitored appliances monitored by: type; age; number of door openings; fill level; whether warm food was added to appliances; and the cleaning and maintenance of cold appliances.

3.1.1 Sample of monitored cold appliances

The majority of cold appliances monitored were fridge-freezers (52%), followed by upright freezers (19%) and larder fridges (14%). The vast majority of the cold appliances (75%) were located in the kitchen/kitchen-diner. Only 7% of appliances were located in the utility room and 6% in garages. In total, 89% of the appliances monitored were free standing and 11% were built-in. The majority of appliances were bought new (78%) while the remaining 22% includes appliances that were bought second-hand or received as a present or came with the property. Around 7% of the monitored cold appliances with a known age were less than 1-year-old while the majority had an age between 1 and 5 years (45%). Of the appliances that were greater than 5 years old, 27% were between 6 and 10 years and 19% were greater than 10 years old. The average age of the appliances in the survey was 7 years. This was lower than indicated by Cravioto et al. (2017) who found the average age of refrigerators in 5 developed countries to be 12.7 years. However, the age of appliances in the survey was quite similar to that presented by the NSW Food Authority (2009) who stated that 32% of appliances in a survey were 5 years or less, 34% were between 5 and 10 years old and 34% were older than 10 years. This compared to equivalent figures of 45% less than 5 years old, 27% between 5 and 10 years and 28% greater than 10 years old for the survey results.

Table 3. Characteristics and use of monitored cold appliances (percentage values in brackets).

Cold appliance type	**N**
Fridge-freezer	524 (52)
Refrigerator with an ice-box	57 (6)
Larder fridge	145 (14)
Chest freezer	86 (9)
Upright freezer	186 (19)
Total	998
Location of appliance	**N**
Kitchen/kitchen-diner	746 (75)
Utility room	69 (7)
Garage	57 (6)
Other	126 (12)
Total	998
Cold appliance age	**N**
< 1 yr	74 (7)
1 - 5 yrs	379 (38)
6 - 10 yrs	271 (27)
11 - 15 yrs	116 (12)
16 - 20 yrs	46 (5)
21 - 25 yrs	12 (1)
>25 yrs	11 (1)
n/a	89 (9)
Total	998
Number of door openings per day	**N**
< 1	163 (11)
1 - 4	619 (40)
5 - 9	275 (18)
10 - 14	255 (17)
15 - 20	88 (6)
20+	122 (8)
Total	1522 [(a)]
Fill level	**N**
0 - 25 %	86 (6)
26 - 50 %	290 (19)
51 - 75 %	539 (35)
76 - 100 %	607 (40)

Total	1522 [(a)]
Warm food added	**N**
Never	694 (91)
Occasionally	60 (8)
Often	10 (1)
Always	2 (<0.5)
Total	766

[(a)] This takes into account also the combined results from refrigerator, freezer and fridge-freezer openings

3.1.2. Use of cold appliances

Householders were also asked how often they opened their appliance, how full the appliance was kept and how frequently the temperature was adjusted. These three questions were asked for each of the monitored appliances in a household, as well as the individual compartments (fridge and freezer) in the case of a fridge-freezer. Householders reported that most appliances (40%) were opened 1-4 times a day while 11% of appliances were opened less than once a day. The majority of appliances that were opened less than once per day were freezers or the freezer section of fridge-freezers. The remainder of appliances were opened more than 5 times a day; these were generally fridges or the fridge section of fridge-freezers.

With regards to how full appliances were kept, 40% of appliances were kept completely full, 35% were kept three quarters or half full, 19% were kept half full while only 6% were kept a quarter or less full (Table 3). Usually, freezers were more commonly reported to be completely full and fridges, three quarters full. Concerning how often householders modify their appliances setting, the temperature setting was never adjusted for 68% of appliances, while it was adjusted occasionally in 24% of appliances and in 6% of appliances it was adjusted every six months. Only 1% of householders reported adjusting the temperature setting of their appliances weekly or monthly.

Householders were asked how frequently they put warm food in their cold appliances. The majority of householders (91%) said they ‘never’ added

hot food, 8% said they did occasionally and just 1% said they did often or always.

3.1.3. Cleaning and maintenance of cold appliances

Fig. 3 shows the frequency with which households cleaned and maintained their cold appliances. Over half the households (56%) said they regularly or occasionally defrosted their appliances, however, almost a third (32%) said they never carried out defrosting (most likely due to the appliance being frost-free). A large proportion (42%) of households said they regularly cleaned the door seals on their appliances, compared with 14% who regularly unblocked the drains and 7% who removed dust from the back of the appliance (where the condenser was located in the majority of cases). Almost half the households (45%) said they never unblocked the drains and about 60% of households said they never removed dust from the back of the appliance.

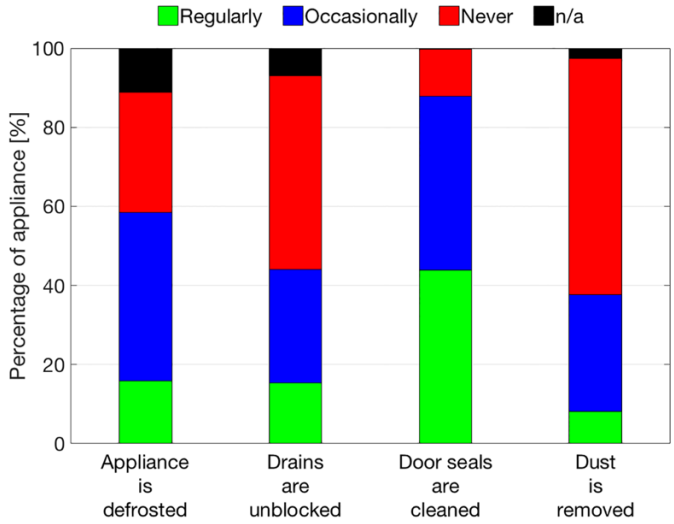

Fig. 3. Frequency of cleaning and maintenance of the cold appliances.

3.2. Ambient temperature

Based on 900 samples with valid ambient temperature data, the mean ambient temperature of the room in which the appliances were located was 18.5°C, the maximum mean temperature was 29.6°C and the minimum mean temperature was 5.6°C.

The ambient temperature was found to vary significantly according to the wave of the survey. The lowest mean temperatures were observed in wave

1 (16.1°C), higher mean temperatures were observed in wave 2 (18.5°C) and wave 4 (18.5°C) with the highest mean temperatures being observed in wave 3 (20.4°C). These differences were due to the waves being carried out at different times of the year (Table 4). Mean ambient temperature in wave 1 (early spring time) was significantly lower than in waves 2 (late spring to summer time), 3 (summer time) and 4 (autumn/winter time). The mean temperatures in wave 3 were significantly higher than in all the other waves. There was no significant difference between mean temperatures in waves 2 and 4.

Table 4. Statistical analysis results: Mean ambient temperature [°C] and waves.

	N	**Mean temperature [°C]**	***σ***	***se***
Wave 1	175	16.1 [a]	4.0	0.3
Wave 2	181	18.5 [b]	2.9	0.2
Wave 3	248	20.4 [c]	2.4	0.2
Wave 4	296	18.5 [b]	3.1	0.2
Total	900	18.5	3.4	0.1

The frequency distributions of the time spent at 2°C mean ambient temperature intervals are shown in Fig. 4. Overall the mean ambient temperatures in the survey were between 18 and 22°C for 35% of the monitoring time in wave 1, 52% in wave 2 and 4 and 65% in wave 3. A low mean ambient temperature (<16°C) was registered for 38% of the time in wave 1, 18% in wave 2 and 4 and only 4% in wave 3. It should be noted that, during spring and summer seasons, the low ambient temperatures were primarily related to chest freezers and upright freezers which were often installed in the garage or in the cellar where there was no heating.

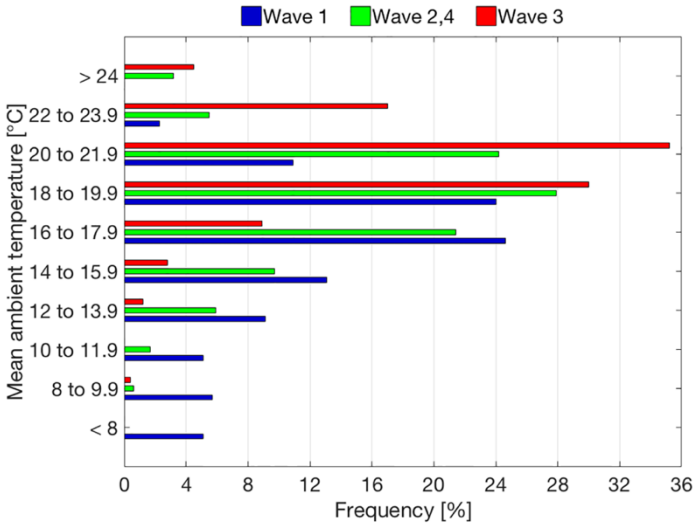

Fig. 4. Frequency distribution for time and mean ambient temperature [°C] during the survey.

3.3. Cold appliance temperature data

3.3.1. Refrigerator temperature

The overall mean internal temperature of all refrigerators (671 appliances) measured in the survey was 5.3°C. The maximum overall mean temperature in a single refrigerator was 14.3°C and the overall minimum mean temperature was -4.1°C.

Based on the 671 appliances, the mean internal refrigerator temperature was not found to vary according to the study wave. However, the appliance type was found to have a significant effect on the refrigerator temperature. The refrigerator sections in fridge-freezers were found to be significantly lower in mean temperature than refrigerators with an ice-box and larder fridges. Statistically significant differences are shown in Table 5.

Table 5. Statistical analysis results: Refrigerator temperature [°C] and appliance type.

	N	**Mean temperature [°C]**	***σ***	***se***
Fridge-freezer	483	5.0 [a]	2.4	0.1
Refrigerator with an ice-box	52	5.7 [b]	3.3	0.5
Larder fridge	136	5.8 [b]	2.5	0.2
Total	671	5.3	2.5	0.1

The mean temperature of each refrigerator type was ranked in order of increasing temperature as presented in Fig. 5. This shows clearly that there was a trend for temperatures in larder fridges and refrigerators with an ice box to be higher than the temperature in fridge-freezers. The frequency distribution at 1°C intervals based on absolute values for temperature over the survey period is shown in Fig. 6.

Overall the fridge-freezers in the survey operated between 0 and 5°C (recommended zone) for 45% of the time, while 51% of the time was spent at temperatures above 5°C. In the case of refrigerators with an ice-box and larder fridges 32% of the time was spent between 0 and 5°C and 64% of the time was spent above 5°C. It can be noted in Fig. 6 that within the range of temperatures 0-6°C, the temperature frequency distribution of fridge-freezers was always higher than that of refrigerators with an ice-box and larder fridges. When the temperature was above 6°C the fridge-freezer temperature frequency distribution was always lower than that one of the other refrigerators. Overall, 108 fridge-freezers, 18 refrigerators with an ice-box and 48 larder fridges operated for 100% of the time at a temperature higher than 5°C. Only 30 fridge-freezers, 3 refrigerators with an ice-box and 4 larder fridges operated for 100% of the survey period within the recommended temperature of 5°C.

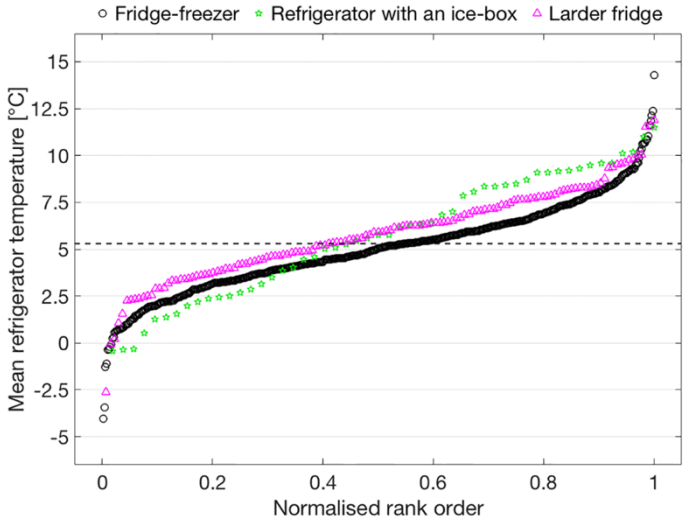

Fig. 5. Mean refrigerator temperature [°C] of each appliance. Overall mean refrigerators temperature [°C] in the survey is reported with a dashed line.

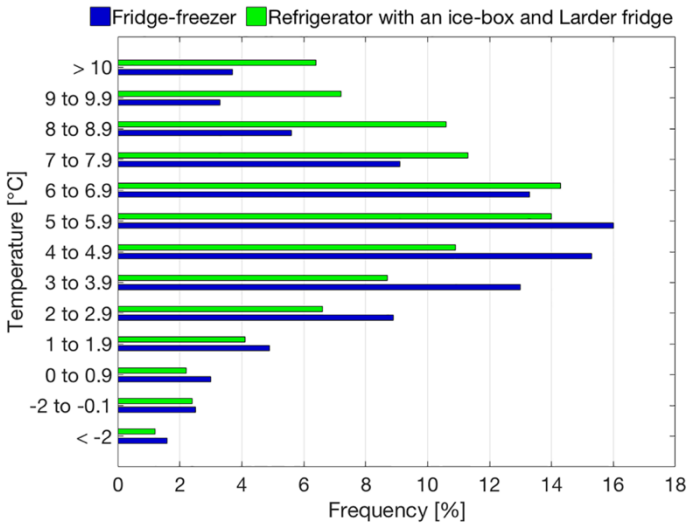

Fig. 6. Frequency distribution of time and temperature [°C] for refrigerators in the survey.

3.3.2. Freezer temperature

The overall mean temperature of freezers in the survey (745 appliances) was -20.3°C. The maximum mean temperature was -5.6°C and the minimum mean temperature was -37.0°C.

The mean temperature of freezers was found to be significantly different according to the wave of the survey, with the lowest mean temperature being observed in wave 3, the highest mean temperature in wave 1 and intermediate mean temperatures observed in wave 2 and 4. Statistically significant differences are shown in Table 6. The mean freezer temperature in the different waves shown by rank order is presented in Fig. 7.

As the survey waves were carried out at different times of the year it was possible that the differences in freezer temperature could be related to ambient temperature. Fig. 8 shows a graph of mean freezer temperature plotted against mean ambient temperature. No clear relation between freezer and ambient temperature was demonstrated apart from in the case of chest freezers where the correlation coefficient (Pearson's coefficient) was found to be -0.265, thus showing a slight reverse correlation. This was because there was a larger range in ambient temperature for these appliances. For most appliances, the range in ambient temperature was probably not large enough to show any influence on performance.

Table 6. Statistical analysis results: Freezer temperature [°C] and waves.

	N	Mean temperature [°C]	σ	*se*
Wave 1	155	-19.3 [a]	4.4	0.4
Wave 2	141	-20.1 [a,c]	4.6	0.4
Wave 3	203	-21.1 [b]	4.4	0.3
Wave 4	246	-20.5 [b,c]	4.2	0.3
Total	745	-20.3	4.4	0.2

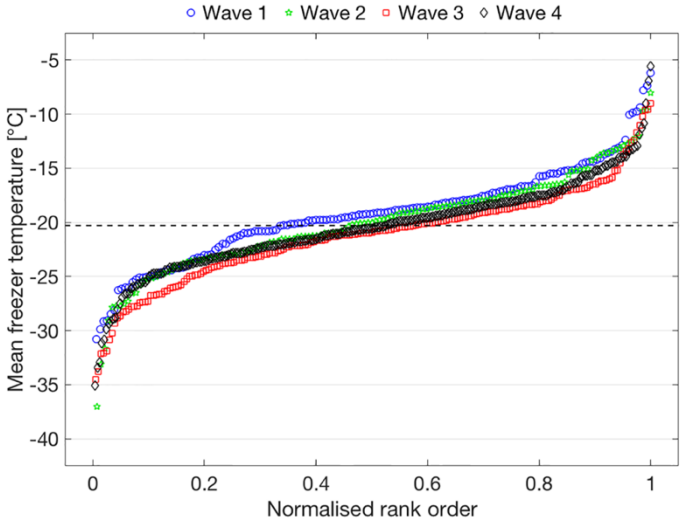

Fig. 7. Mean freezer temperature [°C] divided into waves. Overall mean freezers temperature [°C] in the survey is reported with a dashed line.

Freezer temperature was found to also depend on the appliance type. The main difference in freezer temperature between appliances was observed between refrigerators with an ice-box and all other types of appliance (Table 7). The overall mean freezer temperature of refrigerators with an ice-box was higher than the recommended temperature of -18°C, whereas all other freezer appliances operated at a mean temperature below -18°C. This was most likely due to the ice-box appliances being rated as 2 star appliances whereas other appliances were most likely rated as 3 or 4 star appliances. The number of stars indicates the operating temperature of the appliance; 3 or 4 stars is normally referred to as operation below -18°C while 2 stars is operation below -12°C.

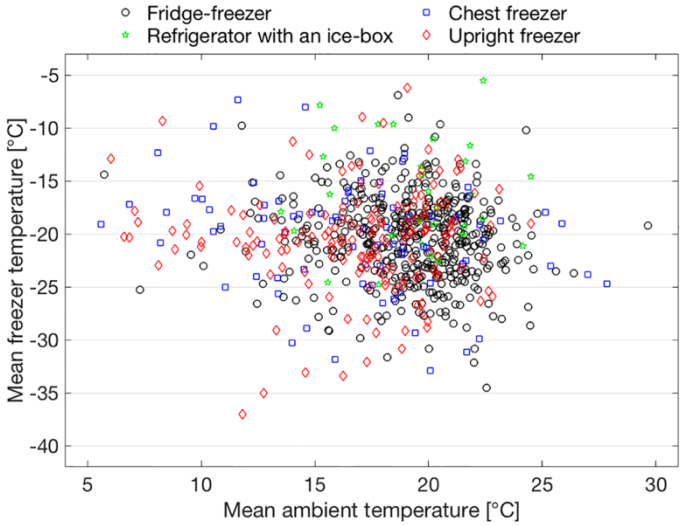

Fig. 8. Mean freezer temperature [°C] against mean ambient temperature [°C].

Table 7. Statistical analysis results: Freezer temperature [°C] and appliance type.

	N	Mean temperature [°C]	σ	se
Fridge-freezer	463	-20.5 [a]	3.9	0.2
Refrigerator with an ice-box	31	-16.5 [b]	5.1	0.9
Chest freezer	82	-20.3 [a]	5.3	0.6
Upright freezer	169	-20.6 [a]	4.8	0.4
Total	745	-20.3	4.4	0.2

The mean freezer temperature within the different types of appliance shown by rank order is presented in Fig. 9. The frequency distribution based on absolute values of time and temperature for fridge-freezers, refrigerators with an ice-box, chest freezers and upright freezers in the survey is shown in Fig. 10. In the case of fridge-freezers, chest freezers and upright freezers, 73% of the survey time was spent at a freezer temperature lower than -18°C (recommended zone) whilst in ice-box freezers 54% of the time was spent at a temperature higher than -18°C. It can be noted in Fig. 10 that the frequency for refrigerators with an ice-box at higher temperatures was greater than those for fridge-freezers, chest freezers and upright freezers. In total, 99 fridge-freezers, 28 chest freezers and 67 upright freezers always operated at a freezer temperature lower than the recommended zone, however no ice-box freezers were found to be in this category. In total, 39 fridge-freezers, 12 refrigerators with an ice-box,

15 chest freezers and 23 upright freezers always operated at a temperature higher than -18°C.

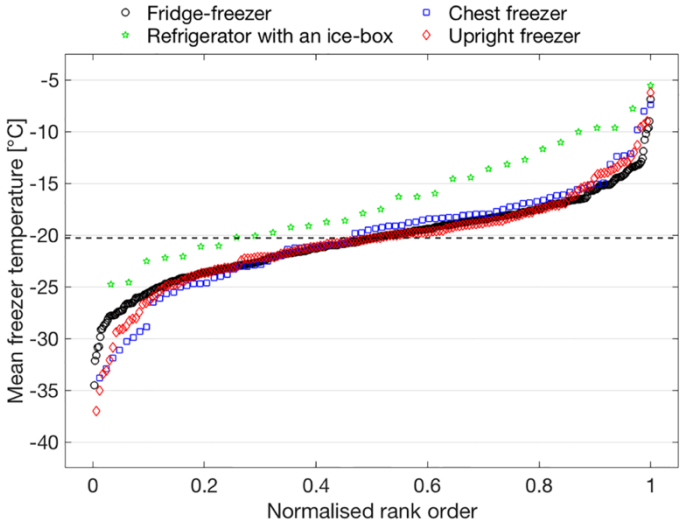

Fig. 9. Mean freezer temperature [°C] of each appliance. Overall mean freezers temperature [°C] in the survey is reported with a dashed line.

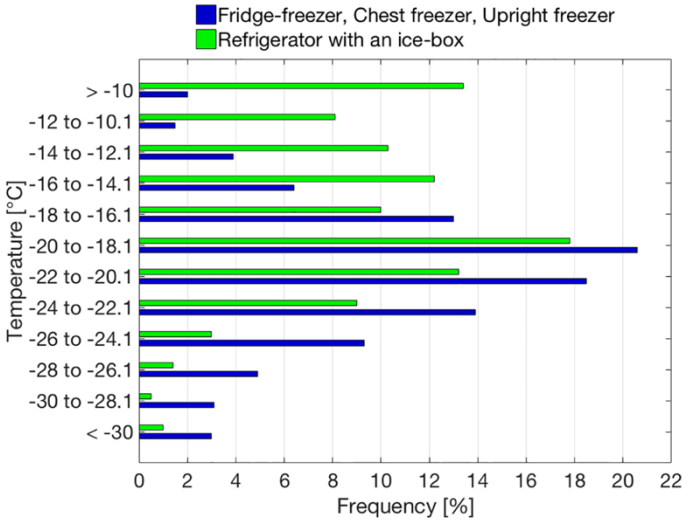

Fig. 10. Frequency distribution of time and temperature [°C] for freezers in the survey.

3.4. Electricity consumption

Electricity consumption data was collected from 665 cold appliances. Overall mean annual consumption was 354 kWh per year, based on the entire monitored period.

The average consumption was found to vary significantly according to the period when the survey was carried out. Table 8 illustrates that the lowest mean electricity consumption was monitored in wave 1 (310 kWh per year), intermediate electricity consumptions were observed in wave 2 (343 kWh per year) and 4 (349 kWh per year) whilst the highest consumption was registered in wave 3 (403 kWh per year). Mean electricity consumption divided into waves and plotted in rank order is shown in Fig. 11.

Warmer temperatures in the summer period may explain the higher energy consumption in wave 3; moreover, higher levels of electricity consumption match with colder freezer temperatures in wave 3 (Table 7). Fig. 12 shows a graph of mean electricity consumption plotted against mean ambient temperature. No marked relation between electricity consumption and ambient temperature was demonstrated. Only in the case of chest freezers and larder fridges the correlation coefficient (Pearson's coefficient) accounted for 0.287 and 0.497 of the variability respectively. The differences found did not appear to be related to the appliance types and appeared to be primarily due to the random nature of the appliance selection process where high or low energy using appliances were included by chance in certain waves.

Table 8. Statistical analysis results: Energy consumption [kWh per year] and waves.

	N	**Energy consumption**	***σ***	***se***
Wave 1	137	310 [a]	193	16.5
Wave 2	161	343 [a,b]	215	16.9
Wave 3	167	403 [c]	223	17.3
Wave 4	200	349 [b]	201	14.2
Total	665	354	211	8.2

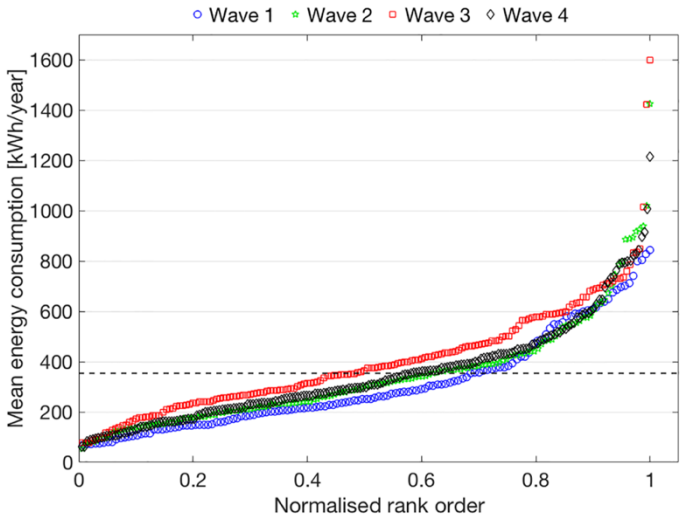

Fig. 11. Electricity consumption [kWh per year] of each cold appliance divided into waves. Overall mean energy consumption [kWh per year] in the survey is reported with a dashed line.

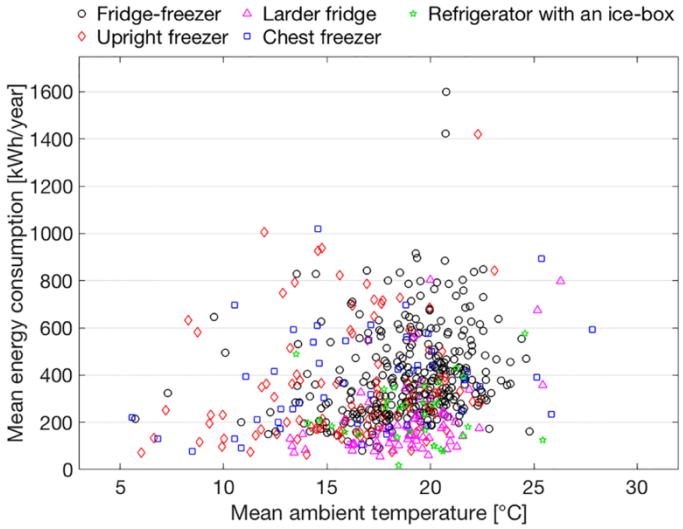

Fig. 12. Electricity consumption [kWh per year] against mean ambient temperature [°C].

Electricity consumption was also found to vary based on the appliance type (Table 9 and Fig. 13). Larder fridges had the lowest consumption (201 kWh per year) with chest freezers (420 kWh per year) and fridge-freezers (390 kWh per year) having the highest electricity consumption. The

electricity consumption of larder fridges was significantly lower than other cold appliances. This is related to the thermodynamic cycle of larder fridges, which is more efficient since the appliance is designed to operate at a temperature above 0°C (whereas all other appliances need to operate at least one compartment as a freezer).

The frequency distribution for electrical power, based on absolute values, split by cold appliance type is shown in Fig. 14. The compressor cycled on and off during the operation of most appliances, however in a small number of appliances, the compressor operated constantly throughout the survey period. This state was observed in 3 fridge-freezers, 5 larder fridges, 12 chest freezers and 7 upright freezers. No refrigerators with an ice box operated continually in the survey. The appliances that operated for 100% of the time consumed on average, 81% more energy than the mean energy consumption of all cold appliances in the survey.

Table 9. Statistical analysis results: Energy consumption [kWh per year] and cold appliance type.

	N	**Energy consumption**	***σ***	***se***
Fridge-freezer	367	390 [a]	190	9.9
Refrigerator with an ice-box	36	274 [b]	159	26.5
Larder fridge	83	201 [c]	163	17.9
Chest freezer	57	420 [a]	249	33.0
Upright freezer	122	342 [b]	236	21.4
Total	665	354	211	8.2

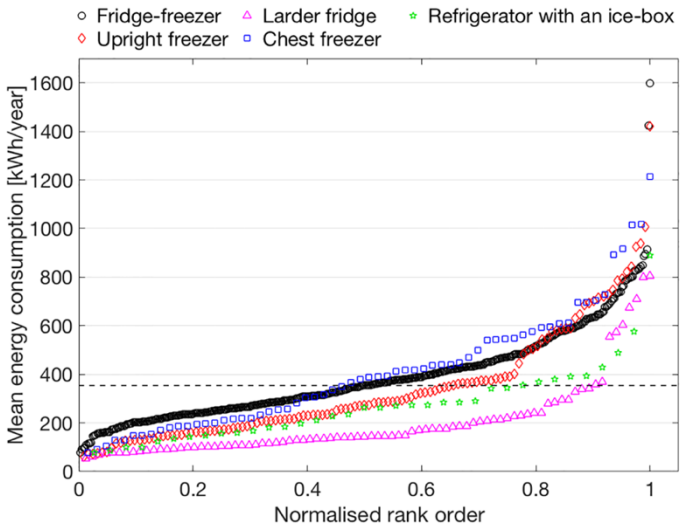

Fig. 13. Electricity consumption [kWh per year] of each cold appliance. Overall mean energy consumption [kwh per year] in the survey is reported with dashed line.

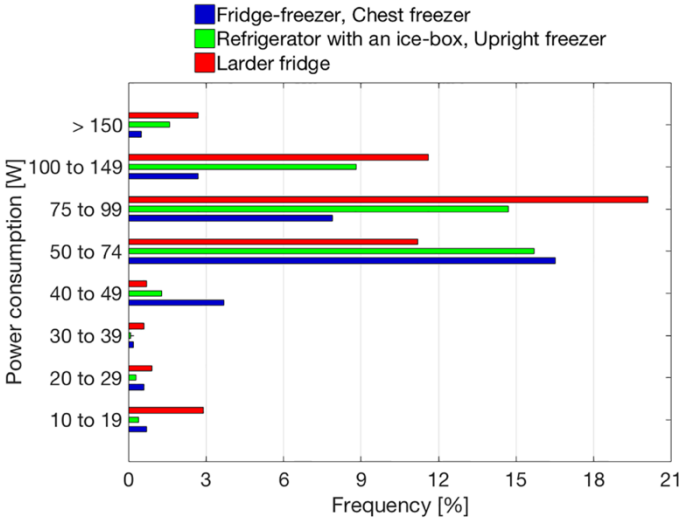

Fig. 14. Frequency distribution of time and power consumption [W] for cold appliances in the survey.

3.4.1 Specific energy consumption (SEC) of appliances

The internal volume of the appliances studied in the survey varied and this may contribute to the variation in electricity consumption. The electricity data was therefore analysed according to the electricity used per unit of net volume and per unit of external surface area. Accurate data on volume and

surface area was not available for all appliances. Refrigerators with an ice-box were not considered in the statistical analysis since the SEC data that was available was not considered sufficient to conduct the analysis.

Results from the statistical analysis are shown in Tables 10 (for volume) and 11 (for surface area). Chest freezers were found to have the highest mean SEC value, both in the case of volume and of external area. Upright freezers also had a high mean SEC volume value while the mean SEC volume for fridge-freezers and larder fridges was significantly lower than those for chest freezers and upright freezers (Table 10). Considering the results reported in Table 11, fridge-freezers and upright freezers had similar SEC values in terms of electricity use per unit of external area. The lowest SEC per surface area was obtained in the case of larder fridges.

Table 10. Statistical analysis results: Specific energy consumption [kWh/m^3.year] and appliance type.

	N	**SEC (volume)**	***σ***	***se***
Fridge-freezer	126	1575 [a]	965	86.0
Refrigerator with an ice-box	5	1585 [-]	722	322.9
Larder fridge	29	1257 [b]	971	180.3
Chest freezer	21	2997 [c]	2126	463.9
Upright freezer	40	2648 [c]	1772	280.2
Total	221	1863	1400	94.2

Table 11. Statistical analysis results: Specific energy consumption [kWh/m^2.year] and appliance type.

	N	**SEC (area)**	***σ***	***se***
Fridge-freezer	111	82 [a]	43	4.1
Refrigerator with an ice-box	5	63 [-]	8	3.6
Larder fridge	24	64 [b]	49	10.0
Chest freezer	12	109 [c]	57	16.5
Upright freezer	27	72 [a]	24	4.6
Total	179	79	43	3.2

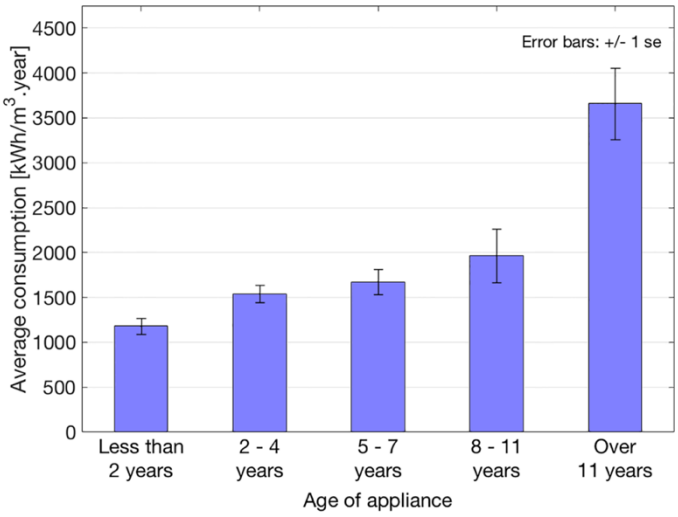

Fig. 15. Average specific energy consumption [kWh/m^3.year] by appliance age.

4. Conclusions

This paper presents the results of a large-scale survey of domestic cold appliances in households in England. Simultaneous measurements of the temperature inside and outside of the cold appliances, as well as the electricity consumption, were obtained over a period of seven days for 998 cold appliances. Data was collected from March to November 2015. Moreover, an interview was conducted with the householders to collect information about how the cold appliances were used and maintained.

Results from statistical analysis have shown that temperatures and electricity consumption in cold appliances significantly varied according to the time of year and appliance type. The mean temperature in domestic refrigerators was found to be 5.3°C, slightly higher than the recommended range of 0 to 5°C. In particular, 174 refrigerators operated for 100% of the time at a temperature higher than 5°C, in contrast only 37 refrigerators were found to operate for 100% of the survey period within the recommended range of 0 to 5°C. The mean temperature in domestic freezers was found to be -20.3°C, lower than the recommended temperature of -18°C. In total, 194 freezers always operated at a freezer temperature lower than the recommended value (-18°C), while a temperature higher than -18°C was monitored in 89 freezers. Overall, the mean electricity consumption was 354 kWh per year. The compressor

operated continually in 27 cold appliances and, on average, these appliances used 81% more energy than the mean energy consumption of all cold appliances in the survey. Such information could potentially be used to target the replacement of high consuming appliances.

The most common cold appliances that were monitored were fridge-freezers which were found to operate within recommended temperature levels more commonly than other appliance types. Mean temperatures in fridge-freezers were between 0°C and 5°C in 48% of cases whereas in other types of refrigerator this figure was 35%. In fridge-freezers, the freezer compartment temperature was on average above -18°C in 24% of cases whereas in other appliances this figure was 30%.

Acknowledgements

The authors would like to acknowledge the funding from the UK Department of Energy and Climate Change (now Department for Business, Energy & Industrial Strategy) for the work reported in this publication.

References

Amara SB, Laguerre O, Mojtabi MCC, Lartigue B, Flick D. PIV measurement of the flow field in a domestic refrigerator model: comparison with 3D simulations. *Int J Refrig* 31 (2008) pp. 1328-1340.

Aprea C, Greco A, Maiorino A. An experimental investigation on the substitution of HFC134a with HFO1234YF in a domestic refrigerator *Appl Therm Eng* 106 (2016) pp. 959-967.

Avci H, Kumlutaş D, Özer Ö, Özşen M. Optimisation of the design parameters of a domestic refrigerator using CFD and artificial neural networks. *Int J Refrig* 67 (2016) pp. 227-238.

Belman-Flores JM, Gallegos-Muñoz A, Puente-Delgado A. Analysis of the temperature stratification of a no-frost domestic refrigerator with bottom mount configuration. *Appl Therm Eng* 65 (2014) pp. 299-307.

Cravioto J, Yasunaga R, Yamasue E. Comparative analysis of average time of use of home appliances. *Procedia CIRP* 61 (2017) pp. 657-662.

European Parliament and Council. No 517/2014 of the European parliament and of the council of 16 April 2014 on fluorinated greenhouse gases and repealing regulation (EC) No 842/2006 text with EEA relevance. *O J L* 150 (2014) pp. 195-230.

Evans JA, Foster AM, Brown T. Temperature Control in Domestic Refrigerators and Freezers (third ed.). *IIR IRC*, Twickenham, UK (2014).

Gao F, Naini SS, Wagner J, Miller R. An experimental and numerical study of refrigerator heat leakage at the gasket region. *Int J Refrig* 73 (2017) pp. 99-110.

Gemmell AJ, Foster HJ, Siyanbola B, Evans JA. Study of Over-Consuming HouseHold Cold Appliances. Building Research Establishment Ltd (BRE) (2017).

Geppert J. Modelling of Domestic Refrigerators' Energy Consumption under Real Life Conditions in Europe. Ph.D. thesis; Diss. University of Bonn, Shaker Verlag, Aachen, (2011) pp. 146.

Gilbert SE, Whyte R, Bayne G, Lake R, Van der Logt P. Survey of internal temperatures of New Zealand domestic refrigerators. *Br Food J* 109 (2007) pp. 323-329.

Gupta JK, Gopal MR, Chakraborty S. Modeling of a domestic frost-free refrigerator. *Int J Refrig* 30 (2007) pp. 311-322.

Hammond EC, Evans JA. Application of Vacuum Insulation Panels in the cold chain – Analysis of viability. *Int J Refrig* 47 (2014) pp. 58-65.

Hassan HF, Dimassi H, El Amin R. Survey and analysis of internal temperatures of Lebanese domestic refrigerators. *Int J Refrig* 50 (2015) pp. 165-171.

Hulme J, Beaumont A, Summers C. The Energy Follow-Up Survey (EFUS): 2011. https://www.gov.uk/government/statistics/energy-follow-up-survey-efus-2011 (2014).

C. James C, B.A. Onarinde BA, S.J. James SJ. The use and performance of household refrigerators: a review. *Compr Rev Food Sci Food Saf* 16 (2017) pp. 160-179.

James SJ, Evans J, James C. A review of the performance of domestic refrigerators. *J Food Eng* 87 (2008) pp. 2-10.

Joybari MM, Hatamipour MS, Rahimi A, Modarres FG. Exergy analysis and optimization of R600a as a replacement of R134a in domestic refrigerator system. *Int J Refrig* 36 (2013) pp. 1233-1242.

Kennedy J, Jackson V, Blair IS, McDowell DA, Cowan C, Bolton DJ. Food safety knowledge of consumers and the microbiological and temperature status of their refrigerators. *J Food Prot* 68 (2005) pp. 1421-1430.

Kumlutaş D, Karadeniz HK, Avci H, Özşen M. Investigation of design parameters of a domestic refrigerator by artificial neural networks and numerical simulations. *Int J Refrig* 35 (2012) pp. 1678-1689.

Laguerre O, Amara SB, Moureh J, Flick D. Numerical simulation of air flow and heat transfer in domestic refrigerators. *J Food Eng* 81 (2007) pp. 144-156.

Laguerre O, Benamara S, Flick D. Numerical simulation of simultaneous heat and moisture transfer in a domestic refrigerator. *Int J Refrig* 33 (2010) pp. 1425-1433.

Landfeld A, Kazilova L, Houska M. Time Temperature Histories of Perishable Foods during Shopping, Transport and Home Refrigerated Storage. *IIR IRC*, Prague (2011).

Liu X, Yu J, Yan G. Theoretical investigation on an ejector–expansion refrigeration cycle using zeotropic mixture R290/R600a for applications in domestic refrigerator/freezers. *Appl Therm Eng* 90 (2015) pp. 703-710.

Modarres FG, Rasti M, Joybari AA, Nasrabadi MRF, Nematollahi O. Experimental investigation of energy consumption and environmental impact of adaptive defrost in domestic refrigerators. *Measurement* 92 (2016) pp. 391-399.

Mohanraj M. Energy performance assessment of R430A as a possible alternative refrigerant to R134a in domestic refrigerators. *Energy Sustain Dev* 17 (2013) pp. 471-476.

Mohanraj M, Jayaraj S, Muraleedharan C, Chandrasekar P. Experimental investigation of R290/R600a mixture as an alternative to R134a in a domestic refrigerator. *Int J Therm Sci* 48 (2009) pp. 1036-1042.

NSW Food Authority. Domestic Fridge Survey, NSW/FA/CP039/0912. http://www.foodauthority.nsw.gov.au/_Documents/scienceandtechnical/Domestic_Fridge_Survey.pdf (2009).

Roccato A, Uyttendaele M, Membré J-M. Analysis of domestic refrigerator temperatures and home storage time distributions for shelf-life studies and food safety risk assessment. *Food Res Int* 96 (2017) pp. 171-181.

Wang X, Yu J. An experimental investigation on a novel ejector enhanced refrigeration cycle applied in the domestic refrigerator-freezer. *Energy* 93 (2015) pp. 202-209.

Wang X, Yu J, Zhou M, Lv X. Comparative studies of ejector-expansion vapor compression refrigeration cycles for applications in domestic refrigerator-freezers. *Energy* 70 (2014) pp. 635-642.

WRAP. Reducing food waste through the chill chain. Part 1: insights around the domestic refrigerator. Project code: RSC007-003 (2009).

Yang M, Jung CW, Kang YT. Development of high efficiency cycles for domestic refrigerator-freezer application. *Energy* 93 (2015) pp. 2258-2266.

Yoon WJ, Seo K, Kim Y. Development of an optimization strategy for insulation thickness of a domestic refrigerator freezer. *Int J Refrig* 36 (2013) pp. 1162-1172.

6.2. Fifth paper

Energy Procedia 82 (2015) pp. 540-545

DOI: 10.1016/j.egypro.2015.11.867

Performance assessment of a multi-energy system for a food industry

Alessandro Biglia [a], Enrico Fabrizio [b,*], Maria Ferrara [b], Paolo Gay [a,c], Davide Ricauda Aimonino [a]

[a] DiSAFA – Universitá degli Studi di Torino, 2 Largo Paolo Braccini, Grugliasco (TO) 10095, Italy

[b] DENERG – Politecnico di Torino, 24 Corso Duca degli Abruzzi, Torino 10129, Italy

[c] CNR-IEIIT – 24 Corso Duca degli Abruzzi, Torino 10129, Italy

* Corresponding author: Tel. +39 011 090 4465
e-mail address: enrico.fabrizio@polito.it

Abstract

The energy saving is becoming an important topic also in the food industry. For this reason, it is important to use multi-energy systems to produce hot water for processes and space heating. The application considered in this paper, which concerns a chocolate factory, focuses on the hot water production through a multi-source storage tank. The water inside the tank is heated by four solar panels when there is enough solar radiation and by a gas back-up boiler. The cold aqueduct water, which it is going to be heated in the accumulator, is first preheated recovering waste heat from the condenser of the chiller. The system was equipped with an energy monitoring and recording device. The thermal model was used to analyse the hot water production system during the summer season considering the options of the heat recovery and of the solar thermal exploitation. The performance analysis was developed in order to establish energy savings that may be achieved.

Keywords: Food industry, Multi-energy systems, TRNSYS modelling, Solar thermal, Heat recovery.

1. Introduction

Industrial energy savings play an important role in process industries because of various factors (IEA; IPCC). First of all, the rising cost of both electricity and fossil fuels involves an increase of cost of bills and consequently the percentage of energy costs are becoming not negligible in the global financial balance of the industries. Another aspect is related to the energy certificates that industries can obtain in order to gain economic benefits and for being more competitive in the market sector.

The food industry is not considered an energy intensive industry because energy costs are a small part of the total profit and loss account. However, the energy consumptions in food industry may be not negligible whenever all direct and indirect energy drivers (i.e. gas burned in the boiler or gasoline used for food transportation) are considered. Fossil fuels are the most common energy sources for thermal processes, in particular natural gas, while the electric energy is mainly used for cooling processes, refrigeration and machine drive. Around half of all energy inputs are used to process raw materials into final products (Wang, 2014). The energy efficiency measures able to reduce energy consumption that may be adopted are for example:

- increase in the efficiency of energy production by installation of new energy converters (several examples are presented in (Wang, 2014));
- reduction of the final energy demand by a better process scheduling, avoiding whenever possible temporal concurrence of high energy demanding tasks (Comba et al., 2010; Comba et al., 2011);
- waste heat recovery;
- use of different energy sources, fossil and renewable ones, in multi-energy integrated systems in order to produce the energy carriers (Fabrizio et al., 2009; Fabrizio, 2011).

In literature, several works about strategies for energy savings in food industry can be found. For example, in order to define road maps towards energy efficiency measures, Muller et al. (2007) have proposed an energy management method based on both top-down and bottom-up approaches. It is very important to emphasize that one method is not preferable to the other one because only starting from the global energy consumption of the

factory (e.g. analysing energy bills, top-down approach) it is possible to develop and implement thermal models for the specific process operations that require more energy (bottom-up approach). Another case study (Seck et al., 2013) shows that a detailed bottom-up approach can be used in order to study heat pump systems for recovering waste heat in the French food & drink industry. Also, the potential for low-grade heat recovery in the UK food and drink processing industry (Law et al., 2013) was studied. Others possible solutions to recover waste heat are, for example, pinch analysis method (Kemp, 2007) and low temperature organic Rankine cycles (Handayani et al., 2011).

In this paper, a thermal model of a multi-energy system for a chocolate industry was developed within the TRNSYS® software tool and was used to study and optimize the global energy performance of the system during the summer season. The thermal model was calibrated against measured data obtained by a monitoring system installed in the existing plant. The scope of this paper is to analyse from the numerical point of view the effectiveness of the installed heat recovery system and sketch possible scenarios that may be adopted to increase the fraction of RES. The paper is structured as follows: Section 2 gives a description of the case study; Section 3 describes the TRNSYS model and Section 4 presents the results.

2. The case study

A chocolate industry located in Turin, in the north of Italy, is the case study presented in the paper. The building is composed by the main floor at the ground level of around 800 m^2, a basement and a first floor used as office space. The chocolate processing takes place in the laboratory, located at the ground floor, where cocoa beans are roasted, debacterised and finally shattered in order to obtain cocoa butter. During these operating stages, steam and hot water are used for debacterisation process and for cleaning machinery and equipment used for the processing of cocoa butter in praline.

2.1. The energy system

The plant scheme of the industry is shown in Fig. 1. Steam and hot water (DHW) used in the laboratory are produced in the boiler room.

The steam from the boiler is always available and in summer season it is used only for thermal processes in the laboratory, while in winter season it is also used to heat water for space heating. As regards the DHW production, a 1,500 l multi-source water storage tank (HW) is connected to the water supply network. The water inside the tank is heated by four flat plate solar collectors and by an auxiliary gas heater when the temperature of the water, at the top of the tank, is lower than 65 °C. The pump of the solar circuit is regulated by a differential thermostat which acquires the temperatures of the coldest point inside the tank and of the outlet of the solar panels. The efficiency of the DHW production is improved by a recovery system installed on the condenser of the chiller. Indeed, the condenser is cooled transferring thermal energy to a 200 l heat recovery water storage (HR) that pre-heats the water from the supply network. The possible excess heat is dissipated into the ambient air.

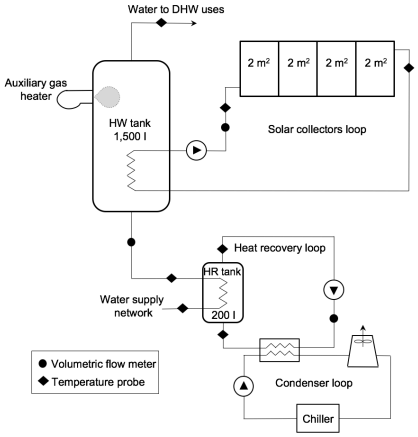

Fig. 1. Energy system scheme.

2.2. The monitoring system

The plant was equipped with an energy monitoring system. In Fig. 1 volumetric flow meters (circle) and temperature probes (diamond) are indicated. Thereby, it is possible to assess supply and return temperature levels, volumetric flow rate, thermal energy and instantaneous thermal power of the following parts of the plant:

- multi-source water storage tank (HW) + water supply network;
- solar collectors loop;
- heat recovery loop;

- heating energy to the building.

3. The system modelling

The model of the system was developed within the TRNSYS® simulation environment. The graphical representation of the whole model is shown in Fig. 2. The building model is located in the upper part of the diagram while the multi-source system is located in the lower part of the diagram.

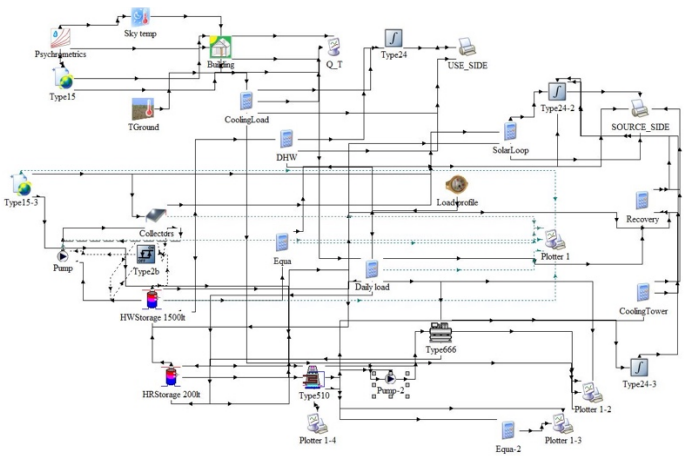

Fig. 2. The model in the TRNSYS interface.

3.1. Use-side modelling

Using the TRNSYS Type 56 and the TRNBuild interface, the ground floor of the building, occupied by the food laboratory, was modelled as a unique thermal zone, whose net floor area is equal to 792 m^2. It is adjacent to the non-conditioned basement and to the conditioned office zone located on the first floor. Part of the ceiling corresponds to the flat roof where solar panels are located. The building opaque external envelope is composed by 0.50 m thick massive walls made of bricks, while the transparent envelope is made of double-glass windows (with a WWR around 30%). The cooling set point temperature in the laboratory was set to 22 °C from Monday to Friday, between 6 am and 7 pm. The laboratory zone occupancy was set to 10 working people from Monday to Friday between 8 am and 6 pm, while other internal gains due to light and appliances were set to 30 W m^{-2}. The natural ventilation rate was set to 1 vol h^{-1} during occupancy.

The typical daily load profile of the DHW use is shown in Fig. 3a. The daily hot water demand was assumed equal to 6,445 l day^{-1}.

3.2. Source-side modelling

The modelling of the subsystem that supplies space cooling and DHW production is presented in this section. Many TRNSYS types were used to model the system and in particular:

- Type 1 for the performance of multiple flat plate solar collectors that are linked in series. The area of each solar collector is 2.0 m^2 with $\eta_0 = 0.8$, $a_1 = 3.927$ W/(m^{2}K), $a_2 = 0.0138$ W/(m^{2}K^2). The fluid of the solar loop is a mixture of water and glycol (55 %).
- Type 2b (differential temperatures controller) for regulation of the solar loop. The pump of the solar loop is running whenever the difference between the temperatures in the HW tank and at the outlet of solar collectors is greater than 10 °C, it stops if temperature difference reaches 2 °C.
- Type 60 for stratified fluid storage tanks with internal heat exchangers. This type was used to model the HW tank (Fig. 1), which is a 1,500 l puffer with a temperature set point for DHW equal to 65 °C, and for modelling the HR tank, a 200 l puffer.
- Type 666, for the water cooled chiller. The type is based on manufacturer performance data provided as external text files. The rated capacity was set to 90 kW and the rated CoP to 3.28.
- Type 510 for a closed circuit cooling tower connected to the condenser loop. The water of the condenser loop goes from the condenser of the chiller to the HR tank before going into the cooling tower. In this way, part of the wasted heat can be recovered for tempering the DHW from the water supply network.

The simulation time-step was set to 5 minutes.

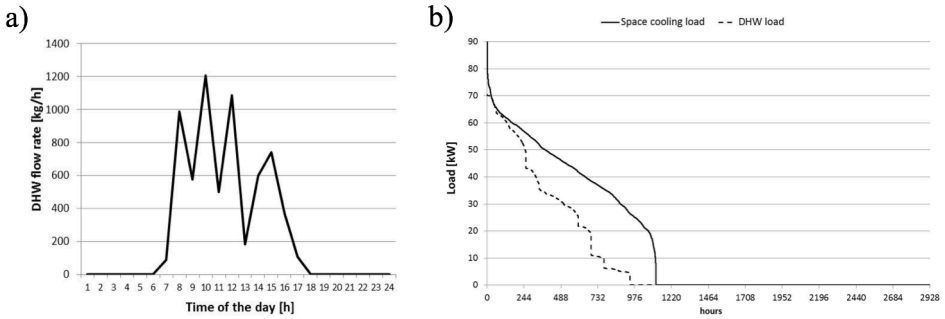

Fig. 3. Daily load profile for DHW (a) and cumulative frequency of the space cooling and DHW loads (b).

4. Results

Simulations were run for a complete summer period (1st June - 30th September, corresponding to 2,928 hours). The cumulative frequency curves of the DHW heating load and the space cooling load of the laboratory are reported in Fig. 3b. The cooling energy required for the space cooling over the whole considered period was equal to 48,645 kWh, which corresponds to 61.4 kWh m^{-2} per year. The heating energy required for the hot water production is equal to 30,812 kWh (38.9 kWh m^{-2}).

The simulations were organized as follows. A first simulation run (System Configuration SC 0) was carried out without heat recovery from the chiller condenser in order to fix a baseline condition. Then, the simulation of the complete system was performed (SC 1).

Simulations results are reported in Table 1 in terms of solar radiation available on the panels surface (Rsol), useful solar energy collected (Qsol), mean seasonal solar collectors efficiency (η), heat recovery from the chiller condenser (Qhr), heating energy from the gas auxiliary heater (Qgas), heat waste from the cooling tower (Qct).

In SC 0, on a seasonal basis, the seasonal efficiency of the hot water production is equal to 0.96 (and obtained not considering the efficiency of the gas heater). Results in Table 1 show that the solar system accounts for 6.9% of energy required for the hot water production.

In the case of the system of Fig. 1 (SC 1), the hot water production seasonal efficiency slightly decreases to 0.95 (again not considering the efficiency of the gas heater), and the DHW production is obtained for the 6.3% from the solar thermal, showing a slight decrease with respect to SC 0, for the

16.3% from the heat recovery, while the remaining part is provided by the auxiliary heater. In order to study the time-correspondence between the DHW load and the availability of the heat recovery, the correlation coefficient between the DHW load and the cooling load time series was computed and was equal to 0.72, which means a quite good correlation.
In order to reduce the gas energy consumption and increase the system efficiency, a sensitivity analysis on the solar collector area (SC 2) and on the heat recovery tank volume and heat exchanger (SC 3) was carried out. Some results are reported in Table 1. In the SC 2 case, the solar panels area was assumed doubled while in the SC 3 case the volume of the heat recover tank was doubled. It can be seen that large solar collector area increases the solar fraction while it leads to a small decrease of the solar system efficiency. In the last case, a larger HR tank increases the heat recovery, even if it is hard to go beyond 20%. For all cases, it can be seen that the heat recovered fraction on the total dissipated heat is very small (from 7.6 % to 9.1 %).

Table 1. Simulation results in the various system configurations (SC 0 - SC 3).

SC	Rsol [kWh]	Qsol [kWh]	η [-]	Qhr [kWh]	Qgas [kWh]	Qct [kWh]
SC 0	5,715	2,201	0.385	-	29,891	69,419
SC 1	5,715	2,043	0.357	5,296	25,073	64,039
SC 2	11,431	3,680	0.322	5,297	24,303	64,080
SC 3	5,715	2,204	0.386	6,298	23,805	63,079

5. Conclusions

A multi-energy system for a food industry was studied by transient simulations. In particular, the performance of the storage system for the heat recovery of the condenser of the factory chiller, and its integration with a solar system, was assessed. Results show that solar integration becomes profitable, from the energy point of view, only if the collector's area is increased. However, this would lead to high investment costs that is not sure to be compensated by savings due to the reduction of energy requirement.

On the other hand, the heat recovery system results to be more profitable in reducing the amount of energy required by the gas heater, even if an amount of energy is still dissipated in the cooling tower.
The real system is under monitoring so the model of the system may be calibrated against measured data allowing the future optimization of the design variables (storage volumes, storage temperatures, etc.) to maximize the overall efficiency of the system. Further development of the work should also include techno-economic analysis for optimizing the system from both points of view, checking economic feasibility.

Acknowledgements

The authors would like to thank the owner of the chocolate factory for supporting this research.

References

Comba L, Gay P, Piccarolo P, Ricauda Aimonimo D. Thermal processes in the candy process of chestnuts. Acta Horticulturae 866 (2010) pp. 587-594.

Comba L, Belforte G, Gay P. Modeling techniques for the control of thermal exchanges in mixed continuous-discontinuous flow food plants. *J Food Eng* 106 (2011) pp. 177-187.

Fabrizio E, Filippi M, Virgone J. Trade-off between environmental and economic objectives in the optimization of multi-energy systems. *Build Simul* 2 (2009) pp. 29-40.

Fabrizio E. Feasibility of polygeneration in energy supply systems for health-care facilities under the Italian climate and boundary conditions. *Energy Sustain Dev* 15 (2011) pp. 92-103.

Handayani TP, Law R, Reay DA, Harvey AP. Organic Rankine Cycle Opportunities in the Proces Industry. Proc. SusTEM Conference (2011) Newcaste-upon-Tyne, UK.

International Energy Agency (iea).
[Online] - www.iea.org/topics/energyefficiency/subtopics/industry/.

International Panel on Climate Change (IPCC). Fifth Assessment report (AR5).
[Online] - www.ipcc.ch/report/ar5/.

Kemp IC. Pinch Analysis and Process Integration – A User Guide, second ed. Elsevier (2007).

Law R, Harvey A, Reay D. Opportunities for low-grade heat recovery in the UK food processing industry. *Appl Therm Eng* 53 (2013) pp. 188-196.

Muller DCA, Marechal FMA, Wolewinski T, Roux PJ. An energy management method for the food industry. *Appl Therm Eng* 27 (2007) pp. 2677-2686.

Seck GS, Guerassimoff G, Maïzi N. Heat recovery with heat pumps in non-energy intensive industry: A detailed bottom-up model analysis in the French food & drink industry. *Appl Energ* 111 (2013) pp. 489-504.

Wang L. Energy efficiency technologies for sustainable food processing. *Energ Effic* 7 (2014) pp. 791-810.

7. Conclusions

The role of food and beverage industry will be extremely important to supply food to more than seven billion of people by 2050. In this context, the design and development of food processing systems play a key role to: (1) minimise capital and/or running costs, (2) minimise energy consumption, water use and food waste (3) improve quality of final food product.

This thesis has provided original research works on matters of:

- steam batch thermal processes in unsteady state conditions (1st paper);
- food freezing at very low temperatures (2nd and 3rd papers);
- energy consumption and temperature monitoring (4th and 5th papers).

In the case of the steam batch processes in unsteady state conditions, a numerical model describing a three-stage steam plant (steam boiler, steam accumulator and food processing tank) was developed to be effective as design tool and/or to verify the operating conditions of a given plant. Indeed, the model allows the sizing of the steam boiler and of the steam accumulator volume as a function of the steam demand (mass flow rate and pressure) for food processing. The model was applied to a real case study. According to the real available data concerning the steam user, the analysed real steam plant was found to be oversized in terms of steam accumulator volume and of maximum pressure of the steam boiler.

With respect to the food freezing at very low temperatures, an innovative plant configuration, based on a reversed Brayton cycle, was here studied. No published research works to date analyse the plant configuration here proposed. The innovative system can achieve temperatures lower than -100 °C, which are favourable for very fast freezing processes. The results of the numerical model showed as the performance of the cycle increases when the cycle operates at minimum pressure higher than the atmospheric pressure. Moreover, when one kW of cooling load is produced, four kW of heat can be recovered at medium-low temperatures. Useful charts to design a freezing plant as a function of various design parameters (freezing time, cooling capacity, medium temperature, food production rate and type

of food product) were also developed. Future research activities concerning food freezing at low temperatures will be carried out working on a real prototype of the plant.
Regarding the research activities in energy and temperature monitoring, results from statistical analysis of electricity consumption and temperature measurements in domestic cold appliances have shown that electricity consumption and temperature significantly varied according to the time of year and appliance type. Such information could potentially be used to target the replacement of high consuming appliances. The most common cold appliances that were monitored were fridge-freezers.
Energy monitoring was also performed in a chocolate industry where demand of domestic hot water and heat production from solar panels were registered. A model of the plant was developed by using TRYNSIS® and calibrated with the monitored data. Results of the model showed that solar integration could be more profitable increasing collector's area.

This thesis has been focused on thermal and freezing processes and energy monitoring. Future research activities could be:

1) It could be interesting to monitor the steam accumulator and the debacterisation tank. This is not a simple task as the installation of steam flow rate meters and temperature probes would require the entire steam plant and the cocoa beans processing to be stopped. However, the collaboration between the owner of chocolate industry and DiSAFA is still ongoing as both partners have interest in performing research activities to further improve energy efficiency and food processing efficacy. Indeed, the installed energy monitoring system installed in the chocolate industry is still operating.
2) The prototype of the innovative freezing plant described in § 5. is under construction (CRYOFOOD project – PORFERS 2014/2020). The prototype will be operated by 2018. Many research activities will be carried out: (a) the energy performance of the prototype will be tested and comperared to numerical simulations; (b) the freezing time of several food products (e.g. slices of meet, peas, etc.) will be monitored and (c) the final quality of frozen foods will be analysed

and compared with quality of foods frozen by using standard freezing plants.

3) A monitoring campaign to test professional cabinets, installed in supermarkets, and domestic cold appliances in terms of satisfaction of recommended temperatures will be carried out in collaboration with ASL TO 1.

Publications list

Articles on ISI International Journals

Biglia A, Gemmell AJ, Foster HJ, Evans JA. Temperature and energy performance of domestic cold appliances in households in England. *Int J Refrig* (Article in press).

Biglia A, Comba L, Fabrizio E, Gay P, Mannini A, Mussinatto A, Ricauda Aimonino D. Reversed Brayton cycle for food freezing at very low temperatures: Energy performance and optimisation. *Int J Refrig* 81 (2017) pp. 82-95.

Biglia A, Caredda FV, Fabrizio E, Filippi M, Mandas N. Technical-economic feasibility of CHP systems in large hospitals through the Energy Hub method: The case of Cagliari AOB. *Energ Buildings* 147 (2017) pp. 101-112.

Biglia A, Comba L, Fabrizio E, Gay P, Ricauda Aimonino D. Steam batch thermal processes in unsteady state conditions: Modelling and application to a case study in the food industry. *Appl Therm Eng* 118 (2017) pp. 638-651.

Articles on Scopus indexed Journals

Barge P, Biglia A, Comba L, Fabrizio E, Gay P, Ricauda Aimonino D, Tortia C. Temperature and position effect on readability of passive UHF RFID labels for beverage packaging. *Chemical Engineering Transactions* 58 (2017) pp. 169-174.

Fabrizio E, Biglia A, Branciforti V, Filippi M, Barbero S, Tecco G, Mollo P, Molino A. Monitoring of a micro-smart grid: Power consumption data of some machineries of an agro-industrial test site. *Data in Brief* 10 (2017) pp. 564-568.

Biglia A, Comba L, Fabrizio E, Gay P, Ricauda Aimonino D. Case Studies in Food Freezing at Very Low Temperature. *Energy Procedia* 101 (2016) pp. 305-312.

Costantino A, Fabrizio E, Biglia A, Cornale P, Battaglini L. Energy Use for Climate Control of Animal Houses: The State of the Art in Europe. *Energy Procedia* 101 (2016) pp. 184-191.

Biglia A, Ferrara M, Fabrizio E, Gay P, Ricauda Aimonino D. Performance assessment of a multi-energy system for a food industry. *Energy Procedia* 82 (2015) pp. 540-545.

Conference proceedings

Barge P, Biglia A, Comba L, Gay P, Guidoni S, Tortia C, Ricauda Aimonino D. Features extraction from vineyard 3D dense point-cloud model for precision agriculture. International AIIA Conference. Bari, Italy. July 5-8, 2017.

Biglia A, Comba L, Fabrizio E, Gay P, Ricauda Aimonino D. Dynamic simulation of steam storage systems for industry plants. Agricultural Engineering CIGR – AgEng. Aarhus, Denmark. June 26-29, 2016.

Costantino A, Fabrizio E, Biglia A, Cornale P, Battaglini L. Benchmarks of energy performance for the indoor climate control of livestock houses. Agricultural Engineering CIGR – AgEng. Aarhus, Denmark. June 26-29, 2016.

Fabrizio E, Ghiggini A, Bariani M, Biglia A, Costantino A. Climate and energy use in broiler houses: comparison between numerical and experimental results. Agricultural Engineering CIGR – AgEng. Aarhus, Denmark. June 26-29, 2016.

Barge P, Biglia A, Comba L, Gay P, Primicerio J, Tortia C, Ricauda Aimonino D. Features extraction from UAV imagery for precision viticulture. Agricultural Engineering CIGR – AgEng. Aarhus, Denmark. June 26-29, 2016.

Biglia A, Fabrizio E, Ferrara M, Gay P, Ricauda Aimonino D. Modelling and calibration of a multi-energy system in a chocolate industry. AIIA International Mid-Term Conference. Naples, Italy. June 22-23, 2015. (Best Poster Award).

Biglia A, Caredda FV, Fabrizio E, Filippi M, Mandas N. Modelling of the energy system of the AOB hospital with the energy hub approach. ASME-ATI-UIT Conference. Naples, Italy. May 17-20, 2015.